Midwest States' Regional Pooled Fund Research Program
Fiscal Year 2000-2001 (Year 11)
Research Project Number SPR-3 (017)
NDOR Sponsoring Agency Code RPFP-01-02

Phase II Development of a Short-Radius Guardrail for Intersecting Roadways

Submitted by

Bob W. Bielenberg, M.S.M.E., E.I.T.
Research Associate Engineer

Ronald K. Faller, Ph.D., P.E.
Research Assistant Professor

James C. Holloway, M.S.C.E., E.I.T.
Research Associate Engineer

John D. Reid, Ph.D.
Associate Professor

John R. Rohde, Ph.D., P.E.
Associate Professor

Dean L. Sicking, Ph.D., P.E.
Professor and MwRSF Director

MIDWEST ROADSIDE SAFETY FACILITY
University of Nebraska-Lincoln
527 Nebraska Hall
Lincoln, Nebraska 68588-0529
(402) 472-6864

Submitted to

Midwest States' Regional Pooled Fund Program

Nebraska Department of Roads
1500 Nebraska Highway 2
Lincoln, Nebraska 68502

MwRSF Research Report No. TRP-03-137-03

September 9, 2003

Technical Report Documentation Page

1. Report No.	2.	3. Recipient's Accession No.
TRP-03-137-03		

4. Title and Subtitle	5. Report Date
Phase II Development of a Short-Radius Guardrail for Intersecting Roadways	September 9, 2003
	6.

7. Author(s)	8. Performing Organization Report No.
Bielenberg, B.W., Faller, R.K., Holloway, J.C., Reid, J.D., Rohde, J.R., and Sicking, D.L.	TRP-03-137-03

9. Performing Organization Name and Address	10. Project/Task/Work Unit No.
Midwest Roadside Safety Facility (MwRSF) University of Nebraska-Lincoln 527 Nebraska Hall Lincoln, NE 68588-0529	11. Contract © or Grant (G) No. SPR-3(017)

12. Sponsoring Organization Name and Address	13. Type of Report and Period Covered
Midwest States Regional Pooled Fund Program Nebraska Department of Roads 1500 Nebraska Highway 2 Lincoln, Nebraska 68502	Final Report 2003
	14. Sponsoring Agency Code RPFP-01-02

15. Supplementary Notes

16. Abstract (Limit: 200 words)

This research study consisted of the development and testing of a short-radius guardrail system for protection of hazards near intersecting roadways and capable of meeting the Test Level 3 (TL-3) impact conditions of the NCHRP Report No. 350 criteria. A short-radius system was designed and consisted of a curved and slotted thrie beam nose section with two adjacent slotted thrie beam sections supported by breakaway posts. One side of the system was attached to a TL-3 steel post transition while the other attached to a TL-2 end terminal.

A series of four full-scale crash tests were conducted on the short-radius guardrail system. The first two tests were conducted according to NCHRP Report No. 350 Test Designation 3-33. Test nos. SR-1 and SR-2 consisted of target impact conditions of a 2,000-kg pickup truck impacting the center of the nose of the short-radius at a speed of 100 km/hr and at an angle of 15 degrees. Test nos. SR-1 and SR-2 were judged unacceptable according to NCHRP Report No. 350 criteria due to rollover of the test vehicle. The third and fourth tests on the short-radius system were conducted as a modified version of NCHRP Report No. 350 Test Designation 3-31. As such, both impacts were oriented at an angle of 0 degrees to the roadway, but the impact point was altered to force the vehicle to move directly down the primary side of the system. This was believed to be a more critical impact condition than provided by the standard test 3-31. In test SR-3, a 2,036-kg pickup truck impacted the short-radius aligned with post no. 1P at an speed of 102.9 km/hr and at an angle of 0.9 degrees. Test SR-3 was judged unacceptable due to rollover of the test vehicle. Prior to running test SR-4, the short-radius was modified by adding a parabolic flare to the primary side of the system, raising the system height 51 mm, and increasing the capacity of the nose cable plates. In test SR-4, the 2,005-kg pickup truck impacted the short-radius guardrail at a speed of 106.3 km/hr and at an angle of 1.8 degrees. This test was judged unacceptable according to NCHRP Report No. 350 criteria due to intrusion of thrie beam into the wheel well of the pickup truck, rapid deceleration, and significant penetration into the interior occupant compartment.

After review of the four full-scale tests, it was evident that the short-radius guardrail system showed potential but further development was required.

17. Document Analysis/Descriptors	18. Availability Statement
Highway Safety, Guardrail Longitudinal Barrier, Short-Radius Barrier, Intersection Protection, Roadside Appurtenances, Crash Test, Compliance Test	No restrictions. Document available from: National Technical Information Services, Springfield, Virginia 22161

19. Security Class (this report)	20. Security Class (this page)	21. No. of Pages	22. Price
Unclassified	Unclassified	187	

DISCLAIMER STATEMENT

The contents of this report reflect the views of the authors who are responsible for the facts and the accuracy of the data presented herein. The contents do not necessarily reflect the official views or policies of the state highway departments participating in the Midwest State's Regional Pooled Fund Program nor the Federal Highway Administration. This report does not constitute a standard, specification, or regulation.

ACKNOWLEDGMENTS

The authors wish to acknowledge several sources that made a contribution to this project: (1) the Midwest States Regional Pooled Fund Program funded by the Connecticut Department of Transportation, Iowa Department of Transportation, Kansas Department of Transportation, Minnesota Department of Transportation, Missouri Department of Transportation, Montana Department of Transportation, Nebraska Department of Roads, Ohio Department of Transportation, South Dakota Department of Transportation, Texas Department of Transportation, and Wisconsin Department of Transportation for sponsoring this project; (2) Martin Snow and Universal Steel for donating the slotted nose section of guardrail; and (3) MwRSF personnel for constructing the barriers and conducting the crash tests.

A special thanks is also given to the following individuals who made a contribution to the completion of this research project.

Midwest Roadside Safety Facility

K.A. Polivka, Research Associate Engineer
A.T. Russell, Laboratory Mechanic II
M.L. Hanau, Laboratory Mechanic I
G.L. Schmutte, Laboratory Mechanic I
Undergraduate and Graduate Assistants

Connecticut Department of Transportation

Dionysia Oliveira, Transportation Engineer 3

Iowa Department of Transportation

David Little, P.E., Assistant District Engineer
Will Stein, P.E., Design Methods Engineer

Kansas Department of Transportation

Ron Seitz, P.E., Assistant Bureau Chief
Rod Lacy, P.E., Road Design Leader

Minnesota Department of Transportation

Jim Klessig, Implementation Liaison
Mohammad Dehdashti, P.E., Design Standards Engineer
Ron Cassellius, Former Research Program Coordinator
Andrew Halverson, P.E., Former Assistant Design Standards Engineer

Missouri Department of Transportation

Daniel Smith, P.E., Research and Development Engineer

Montana Department of Transportation

Susan Sillick, Research Bureau Chief

Nebraska Department of Roads

Leona Kolbet, former Research Coordinator
Amy Starr, Research Engineer
Phil Tenhulzen, P.E., Design Standards Engineer

Ohio Department of Transportation

Monique Evans, P.E., Administrator
Dean Focke, Roadway Safety Engineer

South Dakota Department of Transportation

David Huft, Research Engineer
Bernie Clocksin, Lead Project Engineer

Texas Department of Transportation

Mark Bloschock, P.E., Supervising Design Engineer
Mark Marek, P.E., Design Engineer

Wisconsin Department of Transportation

Peter Amakobe, Standards Development Engineer
Beth Cannestra, P.E., Chief in Roadway Development

Federal Highway Administration

John Perry, P.E., Nebraska Division Office
Danny Briggs, Nebraska Division Office

Dunlap Photography

James Dunlap, President and Owner

TABLE OF CONTENTS

Page

List of Figures

Page

List of Tables

Page

1 INTRODUCTION

1.1 Problem Statement

A short-radius guardrail is a common safety treatment for situations where driveways or secondary roadways intersect a high-speed roadway near a bridge. Short-radius guardrail systems involve a curved section of guardrail placed around the corner of the intersecting roadway with tangent sections on each end that parallel the respective roadways. The tangent sections of guardrail found along the primary roadway are generally attached to an approach guardrail transition and then anchored to a bridge rail, while the sections found along the secondary roadway are generally attached to a guardrail end terminal. A short-radius guardrail system is intended to perform in a similar manner to a bullnose median barrier or a crash cushion. For example, when a high-angle impact occurs in the curved portion of the system, the vehicle is to be captured and brought to a controlled stop. In addition, the system must be capable of redirecting impacting vehicles along the tangent sections of the guardrail installation.

Recently, the members of the Midwest States' Regional Pooled Fund Program contracted with the Midwest Roadside Safety Facility (MwRSF) to develop a new short-radius guardrail design that would meet the Test Level 3 (TL-3) criteria set forth in NCHRP Report No.350 (1). Previously, MwRSF conducted a review of past NCHRP Report No. 230 (2) short-radius designs, identified the important design considerations for such a system, and developed an initial design concept for a TL-3 short-radius system (3). Phase II of this research, described herein, consisted of further analysis, design, and full-scale testing of the short-radius system.

1.2 Objective

The objective of this research study was to evaluate the safety performance of the short-

radius guardrail system through full-scale crash testing and modify the design, as necessary, in order to improve its safety performance. The system's safety performance was evaluated according to the TL-3 criteria set forth in NCHRP Report No. 350.

1.3 Scope

Four full-scale crash tests of the short-radius guardrail system were conducted in order to reach the research objective. All four tests utilized 3/4-ton pickup trucks weighing approximately 2,000 kg. The target impact conditions for the first two tests, NCHRP Report No. 350 test designation 3-33, were at a speed of 100 km/h and at an angle of 15 degrees on the center of the curved nose of the system. The third test, a modification of NCHRP Report No. 350 test designation 3-31, was performed at a target impact speed of 100 km/h and at an angle of 0 degrees aligned with the center of the first post on the primary roadway side of the system. The fourth test, a modification of NCHRP Report No. 350 test designation 3-31, impacted the primary roadway side of the system at a target impact speed of 100 km/h and at an angle of 0 degrees. The test results were analyzed, evaluated, and documented. Conclusions and recommendations were then made that pertain to the safety performance of the short-radius guardrail design.

2 SHORT-RADIUS DESIGN DETAILS

The design of the short-radius guardrail system for test no. SR-1 was based on previous research conducted on short-radius systems discussed during Phase I of this research (4-10). Full details on the considerations and parameters that shaped the design of the short-radius guardrail system can be found in that report. Experience gained by the MwRSF researchers during the development of the bullnose median barrier system (11-15) was also applied.

2.1 Design Details

After reviewing the Midwest Regional Pooled Fund member states' standards and the previously tested short-radius systems, a 2,426-mm radius design was selected for use in the current study. The small radius reduced the overall size of the system and allowed for easier application of the design to a variety of intersections. The nose section was formed using one 3,810-mm long, curved section of thrie beam guardrail. The size of the radius was based on the constraint that the nose bend would form a 90-degree angle between the leg ends.

The front-end section of the short-radius system was designed without a post at the centerline of the nose since the end post typically rotates backwards after impact, thus creating a potential for the vehicle to vault over the rail. It was determined that a nose section without the centerline post would have sufficient structural strength to maintain the shape of the rail without rail sagging while also reducing the vaulting hazard.

The layout of the initial design concept for the short-radius guardrail system is shown in Figures 1 through 3. For the short-radius system, the nose section consists of a 2,426-mm radius nose section bent to form a 90-degree arc with two tangential sides. The primary roadway side is 11,430-mm long, while the side along the secondary roadway is 13,335-mm long. After post no. 9P

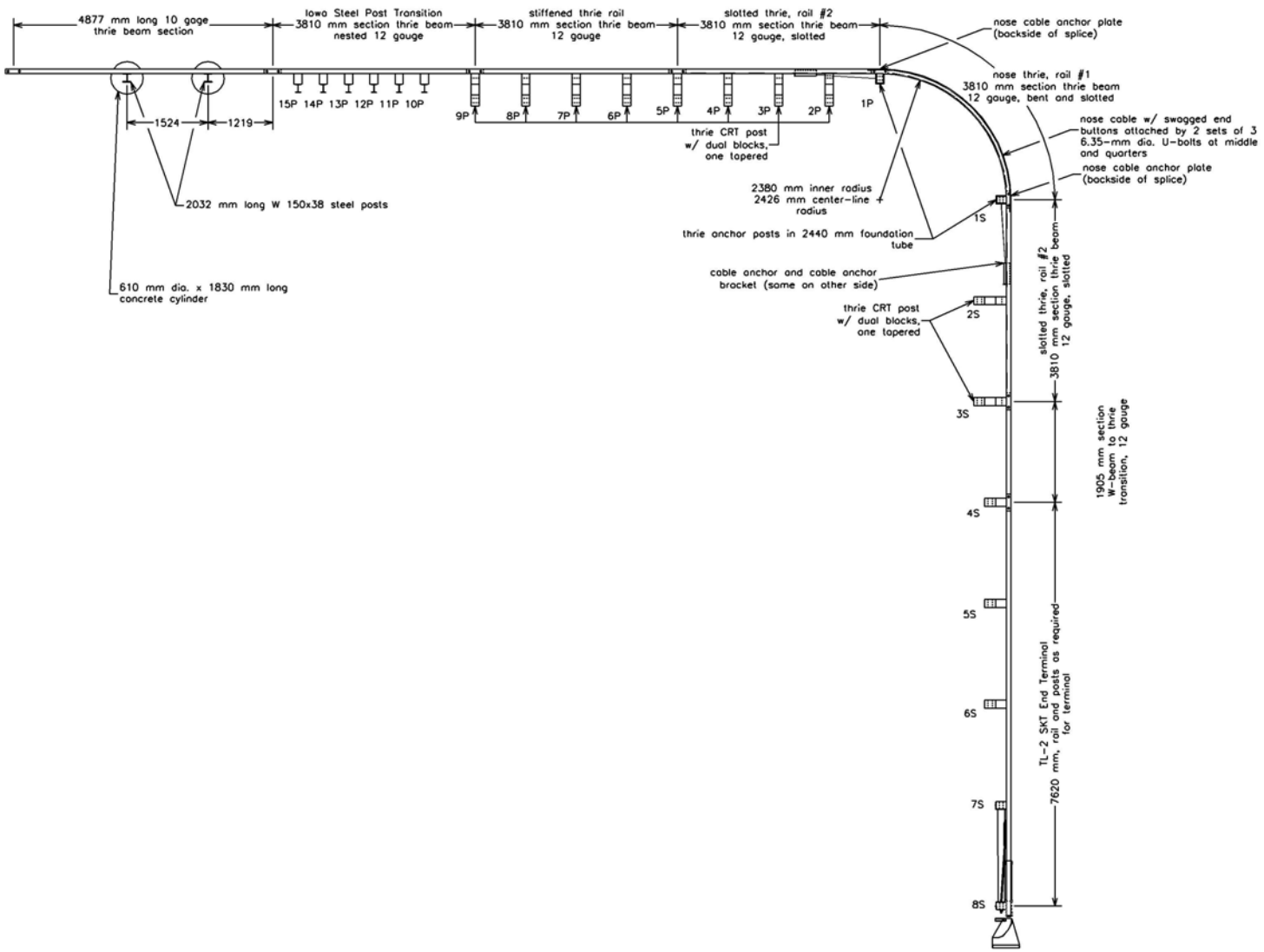

Figure 1. Overall System Layout, Test SR-1

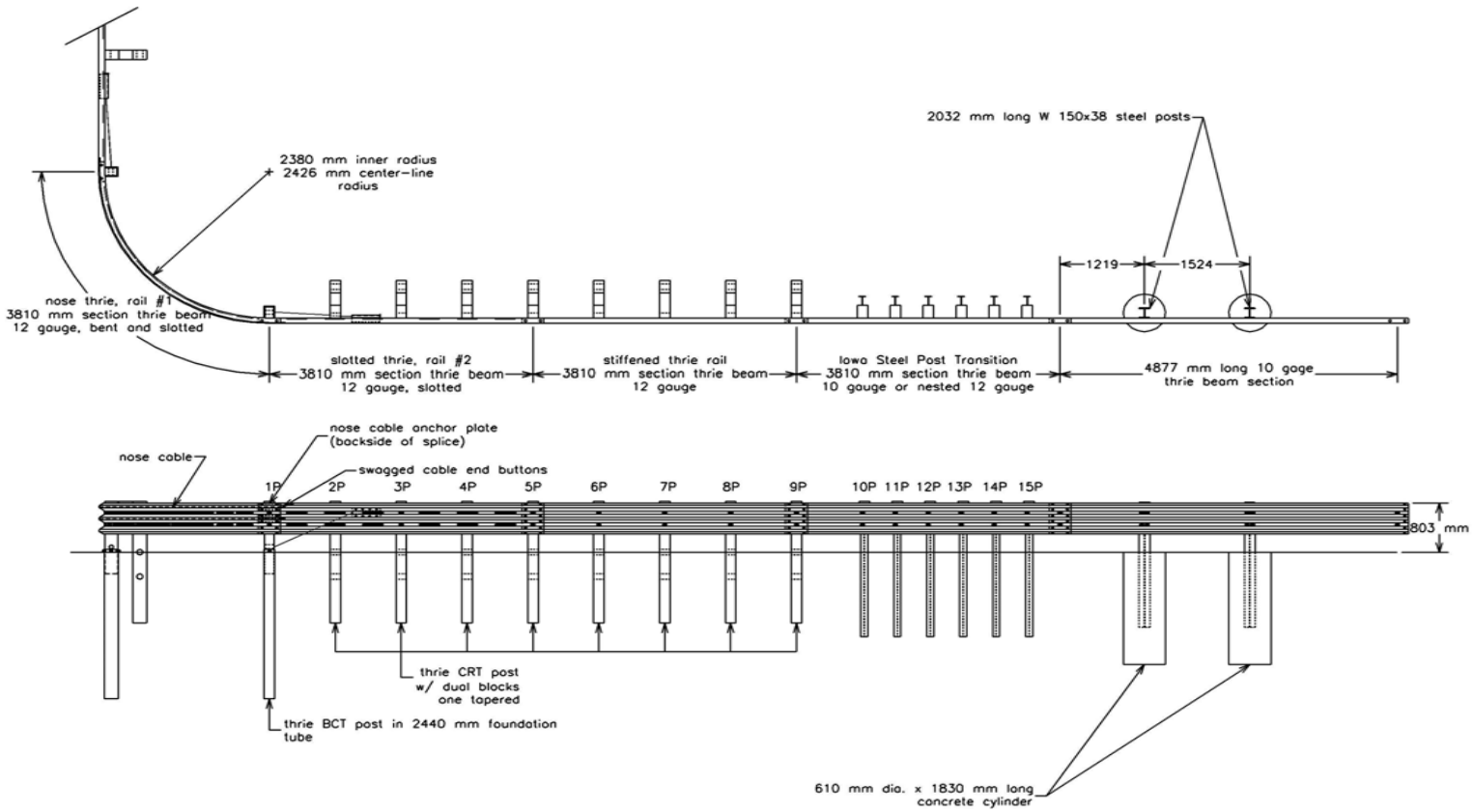

Figure 2. Primary Side System Layout, Test SR-1

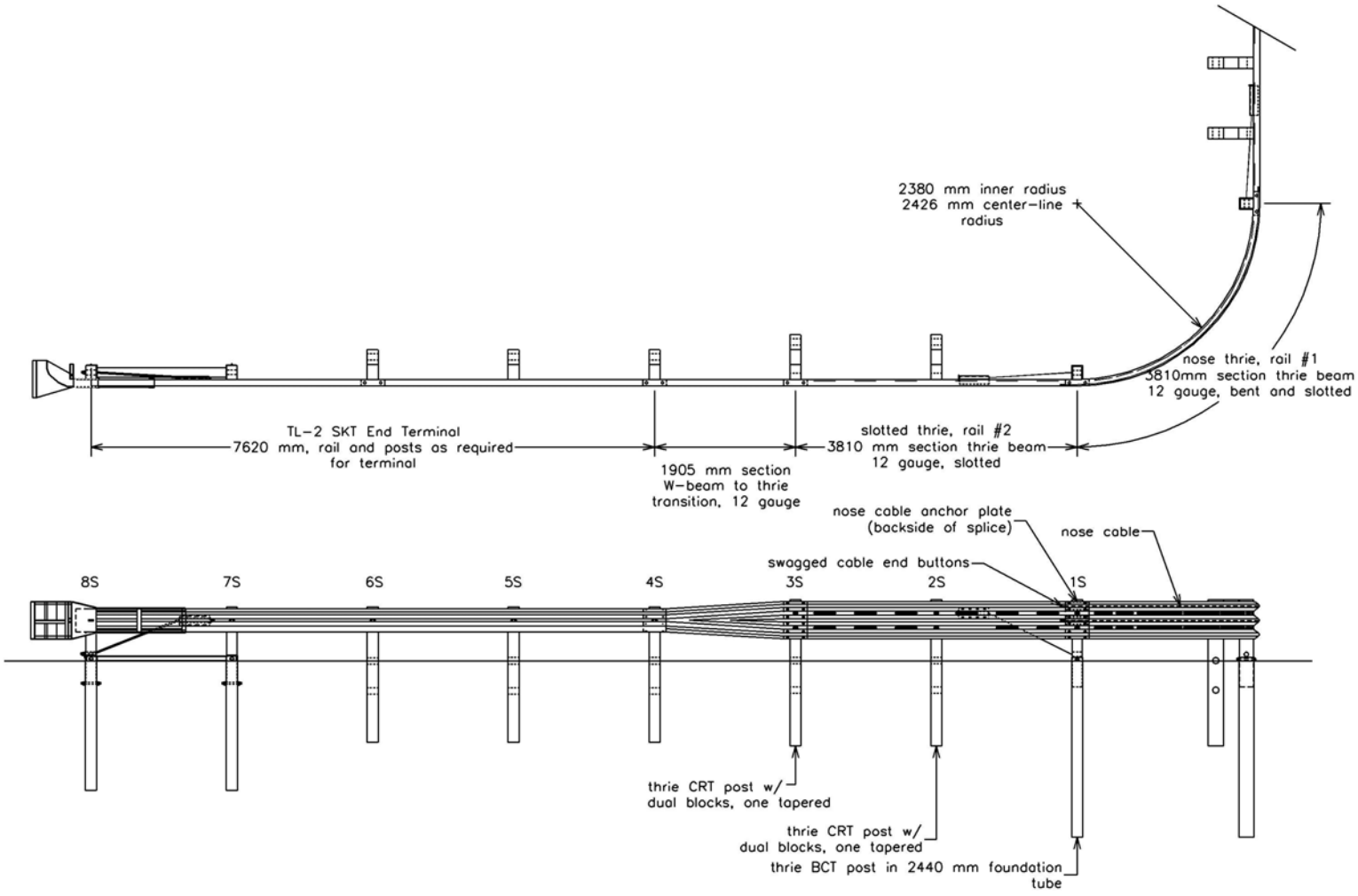

Figure 3. Secondary Side System Layout, Test SR-1

on the primary roadway side of the system, a 3,810-mm long approach guardrail transition system was used to adapt the short-radius system to a thrie beam bridge rail. Details on the approach guardrail transition, used in combination with a safety shape bridge rail, can be found in previous publications by MwRSF (16-17). Actual installations of the short-radius guardrail system could use any NCHRP Report No. 350 approved approach guardrail transition. On the secondary roadway, a 7,620-mm long Test Level 2 (TL-2) SKT end terminal was attached at post no. 4S in order to terminate that side of the system. Details on the SKT can be found in the Transportation Research Record No. 1647 (18). A TL-2 end terminal was chosen for the design based on expectations of lower speeds along the secondary roadway and the desire to keep the length of the secondary side to a minimum. In the following sections, barrier details are given for the remainder of the short-radius system, excluding these end connections.

The system was configured with thirteen wood posts - nine positioned along the primary roadway prior to the transition section and four placed along the secondary roadway prior to the end terminal. Starting from the radius, the first post on each side of the system was a 140-mm wide by 190.5-mm deep by 1,178-mm long Breakaway Cable Terminal (BCT) post set in 2,440-mm long foundation tubes. No blockout was used at post no. 1 on either side of the radius. Post nos. 2P through 9P along the primary roadway and post nos. 2S and 3S along the secondary roadway were 1,980-mm long CRT posts. Each of these posts included double 150-mm wide by 200-mm deep by 360-mm long wood blockouts to space the rail away from the post. The front blockouts on the double blockout posts were chamfered at a 25-degree angle from the middle of the front face of the blockout to the bottom. Post spacing for all of the posts up to post no. 9P along the primary roadway was 952.5 mm. Post spacing for all post up to post no. 4S along the secondary roadway was 1,905

mm. The top mounting height of the rail was 804 mm, as measured from the ground surface. Post nos. 2P through 9P along the primary roadway and post nos. 2S through 4S along the secondary roadway had a soil embedment depth of 1,153 mm. Details of these posts are shown in Figure 4 through Figure 5.

A cable anchor system was attached between the thrie beam and post no. 1 on each side of the system in order to develop the tensile strength of the thrie beam guardrail downstream from the nose section. Details of the anchor system are shown in Figure 6.

The four guardrail sections used in the short-radius system consisted of 12-gauge steel thrie beam. The 3,810-mm long sections were spliced together using a standard, bolted lap splice on each interior end. The nose section and rail section no. 2 on each side were cut with slots in the valleys. The nose section of the rail (rail section no. 1) consisted of a 3,810-mm long beam bent into a 2,426-mm radius. The nose section was cut with slots in the valleys to aid in vehicle capture, as shown in Figure 7. There were six primary 700-mm long slots centered about the mid span of the rail, three in each valley. The primary slots were divided from one another by 25-mm wide slot tabs. Eight additional smaller 230-mm long slots, four on each end of the rail section, were also cut with a 50-mm wide slot tab between them. All slots were 25-mm wide. Rail section no. 2 on each side was straight section of thrie beam guardrail. These sections were cut with a different pattern of slots, as shown in Figure 8. The slot pattern for this section consisted of two sets of six 300-mm long slots centered between the post slots. The slots were separated by 250-mm wide slot tabs, which provided three slots per valley between posts. The remaining section of thrie beam guardrail along the primary roadway was not slotted.

A 12-gauge thrie beam to W-beam transition section was placed between post nos. 3S and

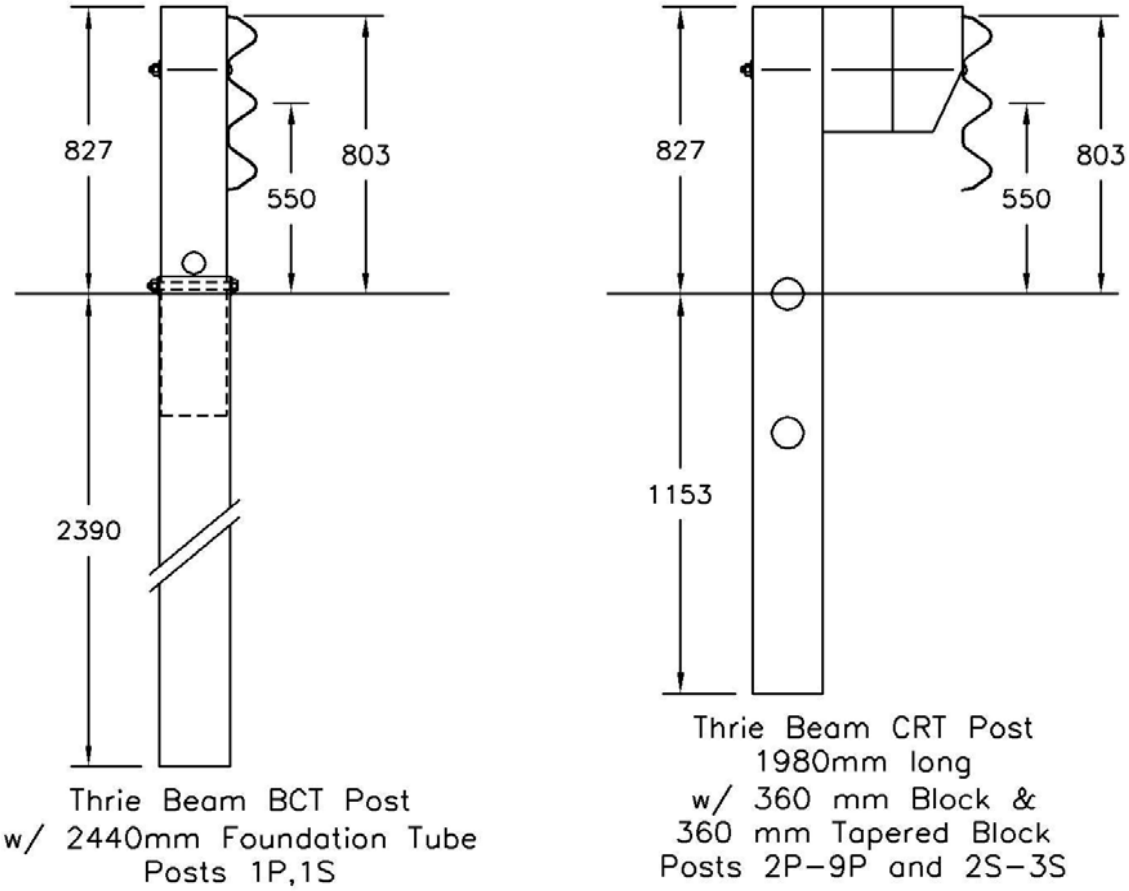

Figure 4. System Details, Test SR-1

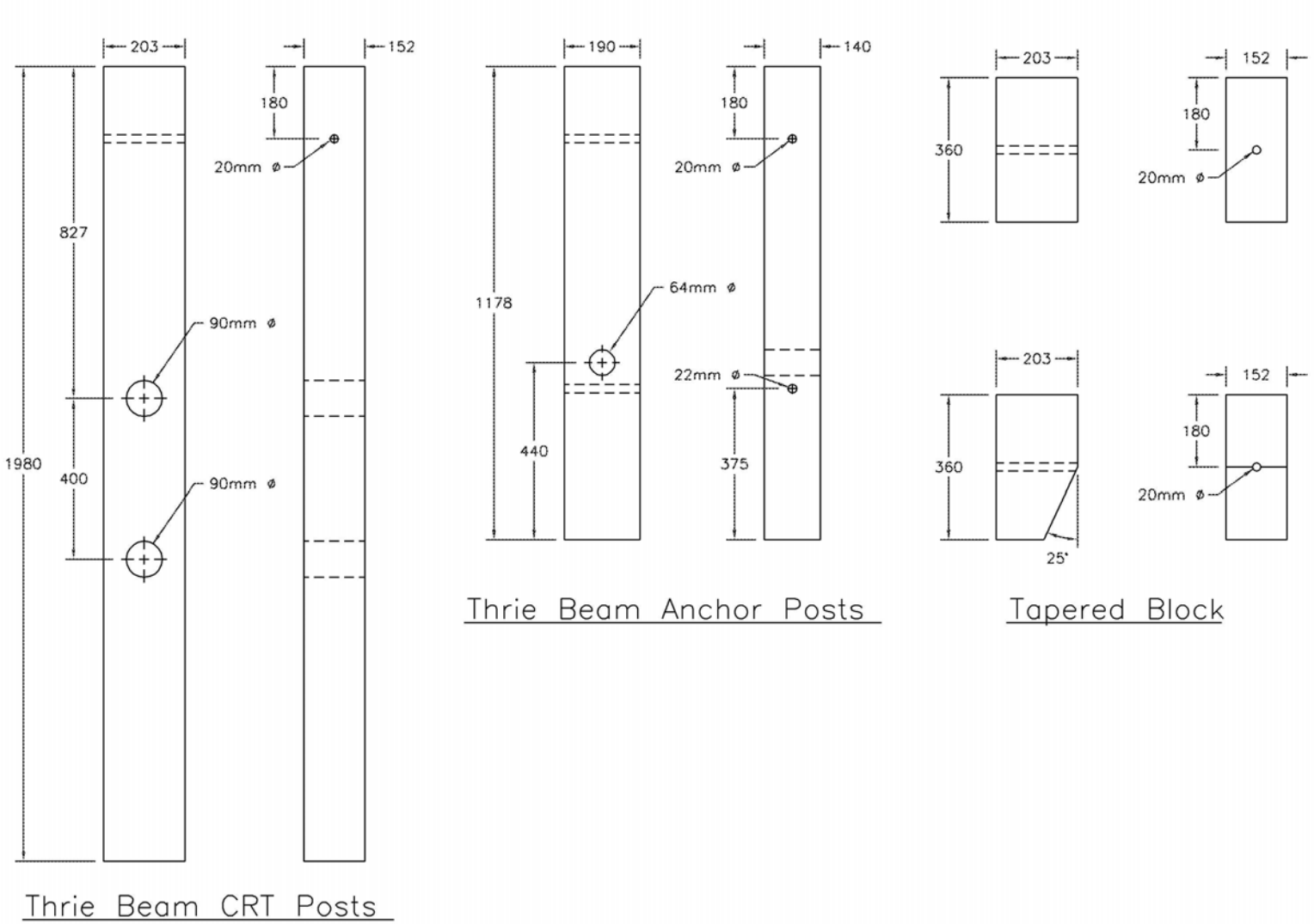

Figure 5. System Details, Test SR-1

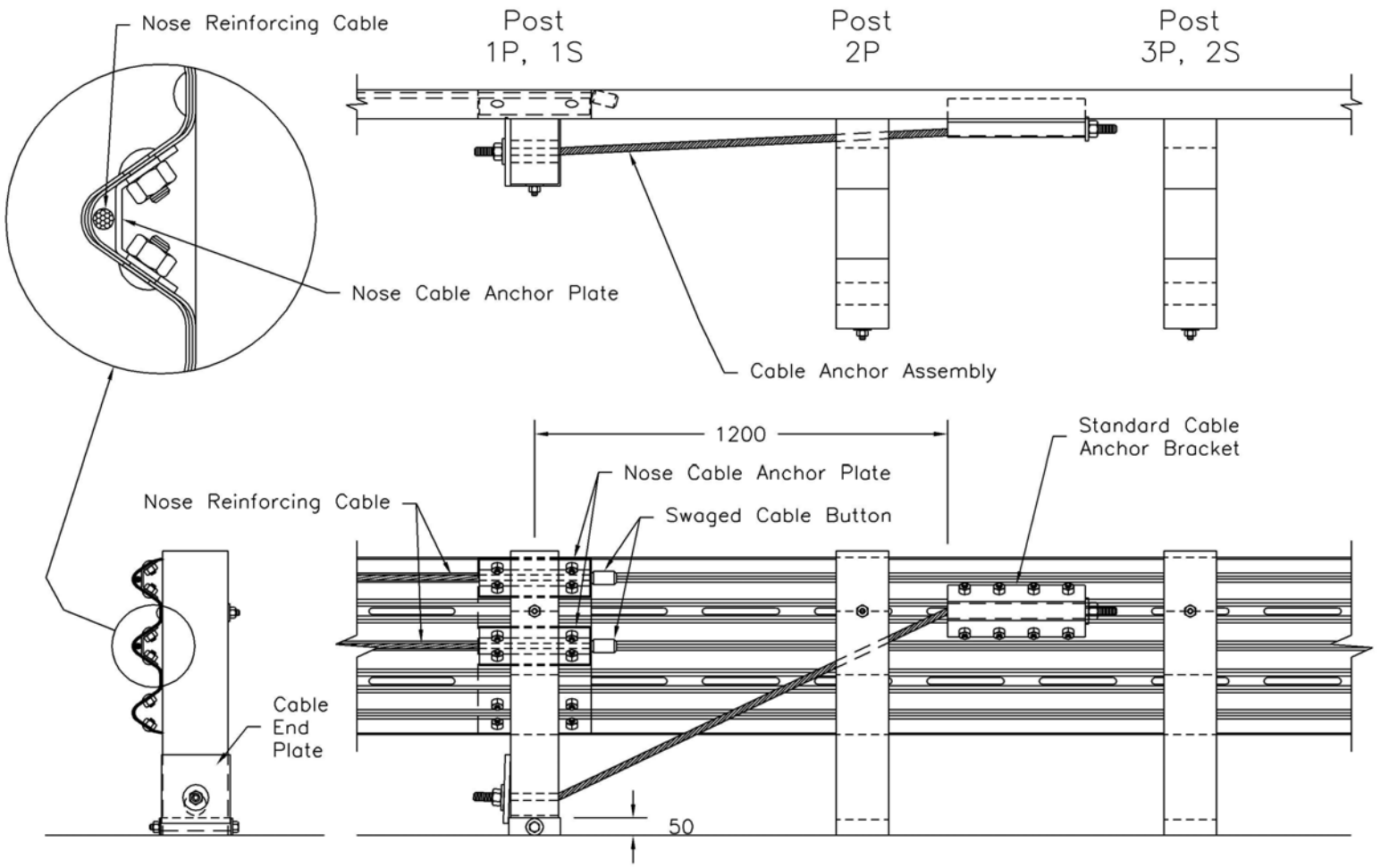

Figure 6. System Details, Test SR-1

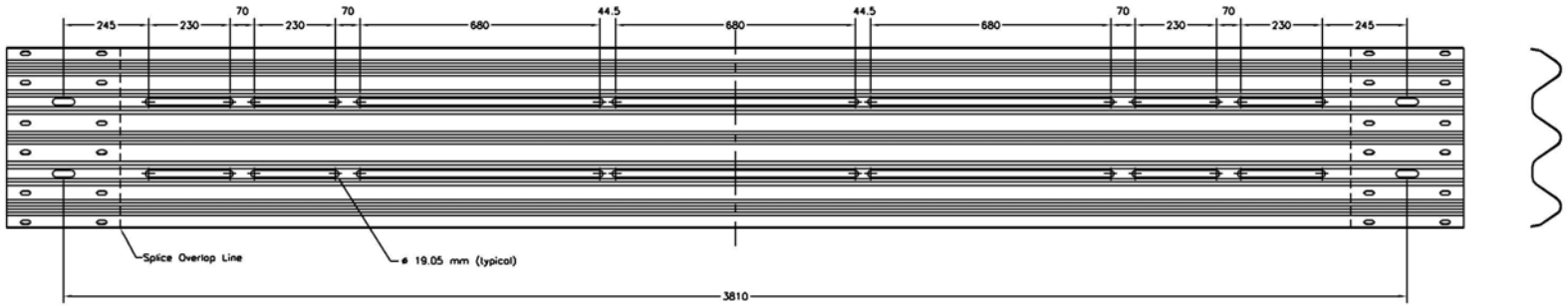

Rail Section 1 ("Nose" Section)

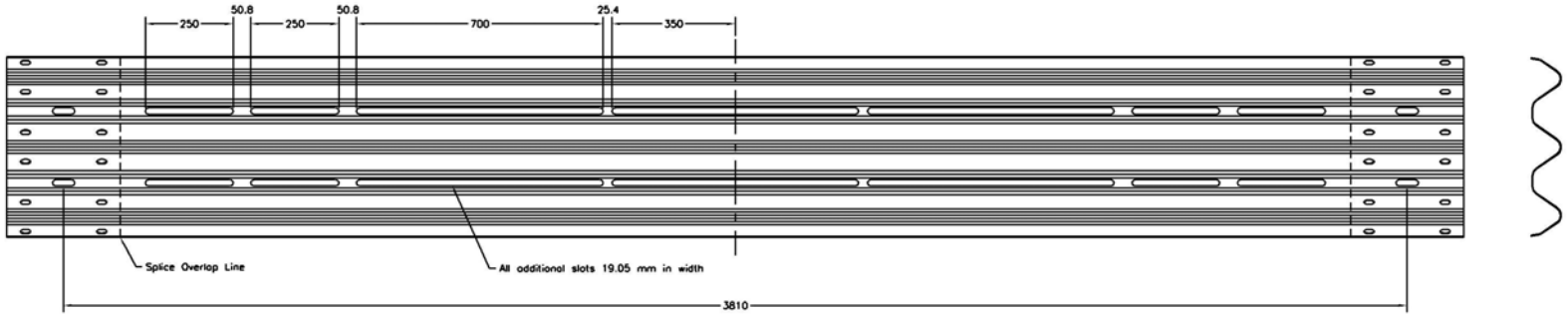

Rail Section 1 ("Nose" Section)

Note: All units are in mm unless specifed otherwise

Figure 7. System Details, Test SR-1

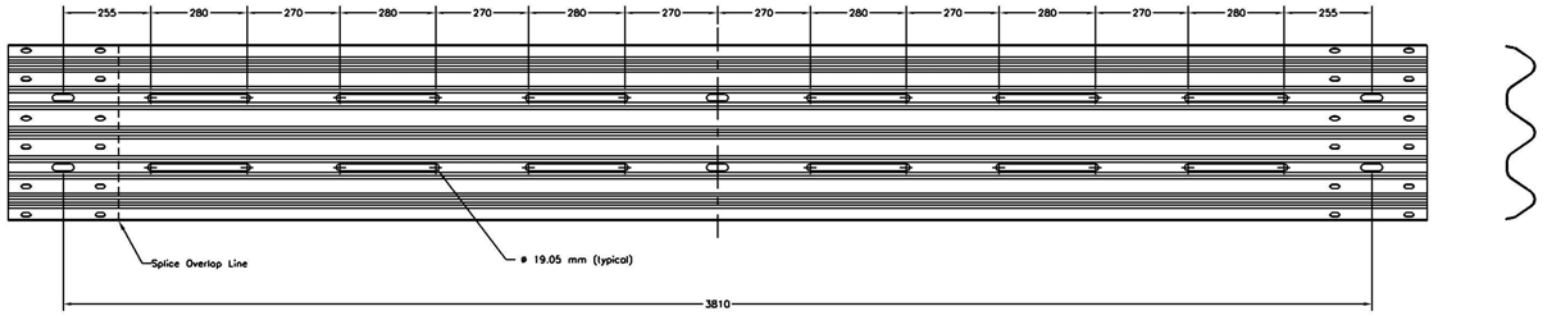

Rail Section 2

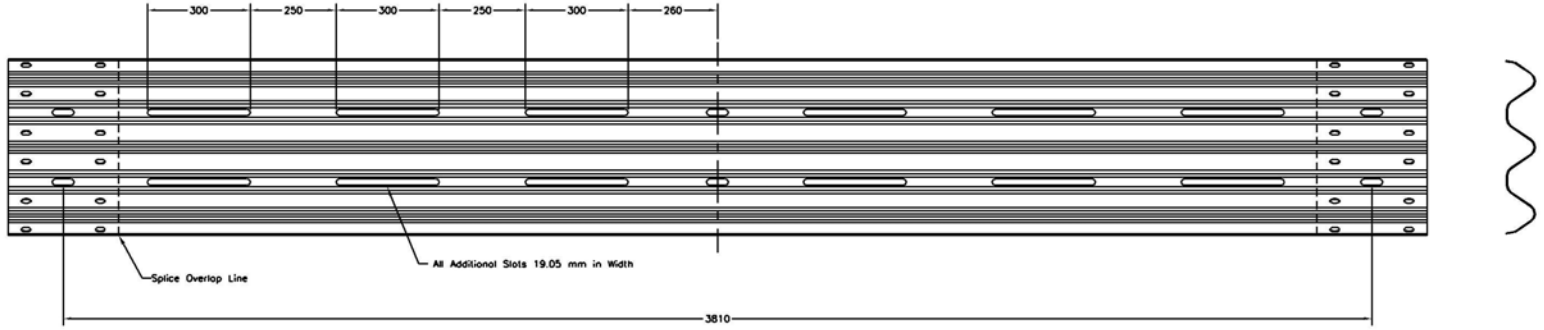

Rail Section 2

Note: All units are in mm unless specified otherwise

Figure 8. System Details, Test SR-1

4S along the secondary roadway. The transition section was necessary in order to end the guardrail with an approved W-beam guardrail end terminal, such as the SKT.

A set of steel retention cables were attached to the back of the nose section to contain impacting vehicles in the event of rail rupture. A 4.38-m long by 15.9-mm diameter cable was added behind the top and middle humps of the nose section of thrie beam rail. A 6 x 25 cable was chosen with the intent that one of the two cables would be capable of containing the impacting vehicle. It is noted that the steel cables were only placed behind rail section no. 1. This was done because it was believed that the rail sections beyond the nose section would remain active and intact throughout the impact event. Therefore, the use of longer cable lengths was not deemed necessary. The cables were attached to the guardrail using three 6.35-mm diameter U-bolts per cable to fix the cables behind the top and middle humps of the thrie beam. The ends of each cable were fitted with "Cold Tuff" buttons and clamped between formed steel plates located at the guardrail splice at post no. 1 on each side. The "Cold Tuff" buttons are swaged-grip button ferrules. As such, any similarly sized swaged-grip button ferrule could be substituted into the design. The cable plate and the cable detail are shown in Figure 9, while the assembly details are shown in Figure 6.

An end anchorage was developed for the primary roadway side of the short-radius system in order to simulate the anchorage provided by the bridge rail in an actual installation, as shown in Figure 10. This anchorage was for test purposes only. The anchorage consisted of a pair of 2032-mm long, W150x28 steel posts embedded 1,219 mm into a reinforced concrete base. The reinforced concrete bases consisted of 1,830-mm long by 610-mm diameter concrete cylinders set in the ground. Reinforcement of the cylinders was done using a pre-formed, circular, 559-mm diameter welded wire mesh cage. A 10-gauge section of thrie beam was mounted on the posts and spliced to the end of the

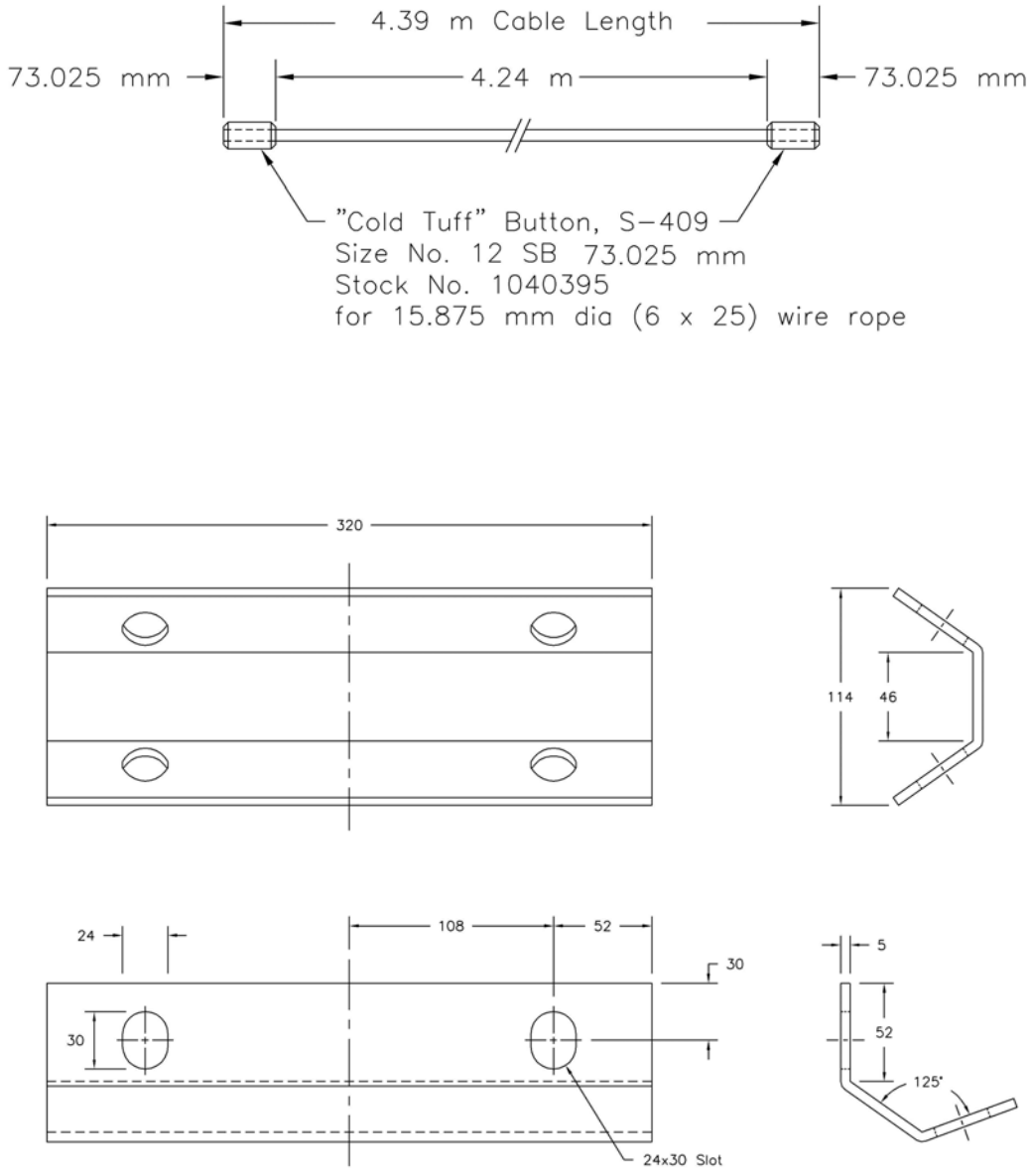

Figure 9. System Details, Test SR-1

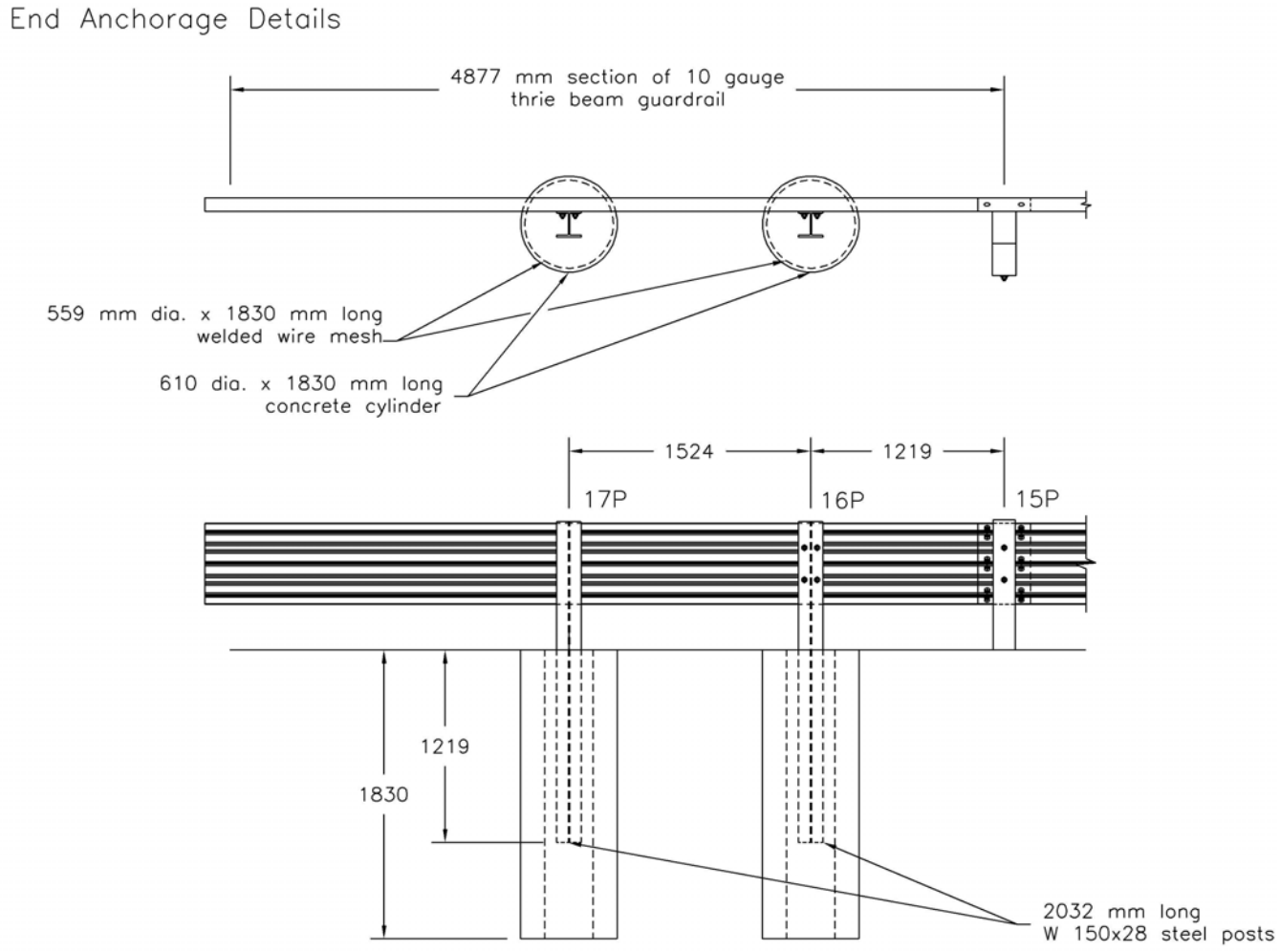

Figure 10. Primary Side End Anchorage Details, Test SR-1

bridge transition to complete the anchorage.

Finally, it should be noted that previous testing of short-radius guardrail systems at the Texas Transportation Institute (TTI) and the Southwest Research Institute (SwRI) utilized a moat behind the system in order to simulate the steep grading typically present at actual field installations. As such, it was decided to create a moat behind the installation of the short-radius guardrail system in test SR-1. The moat consisted of a 1,829-mm deep pit placed 610-mm behind the perpendicular sides of the system and 3,324-mm behind the nose. The front faces of the moat were sloped at 2:1 while the backside was sloped at 1:1. A diagram of the moat is shown in Figure 11.

Photographs of the short-radius guardrail system used in test SR-1 are shown in Figures 12 through 14.

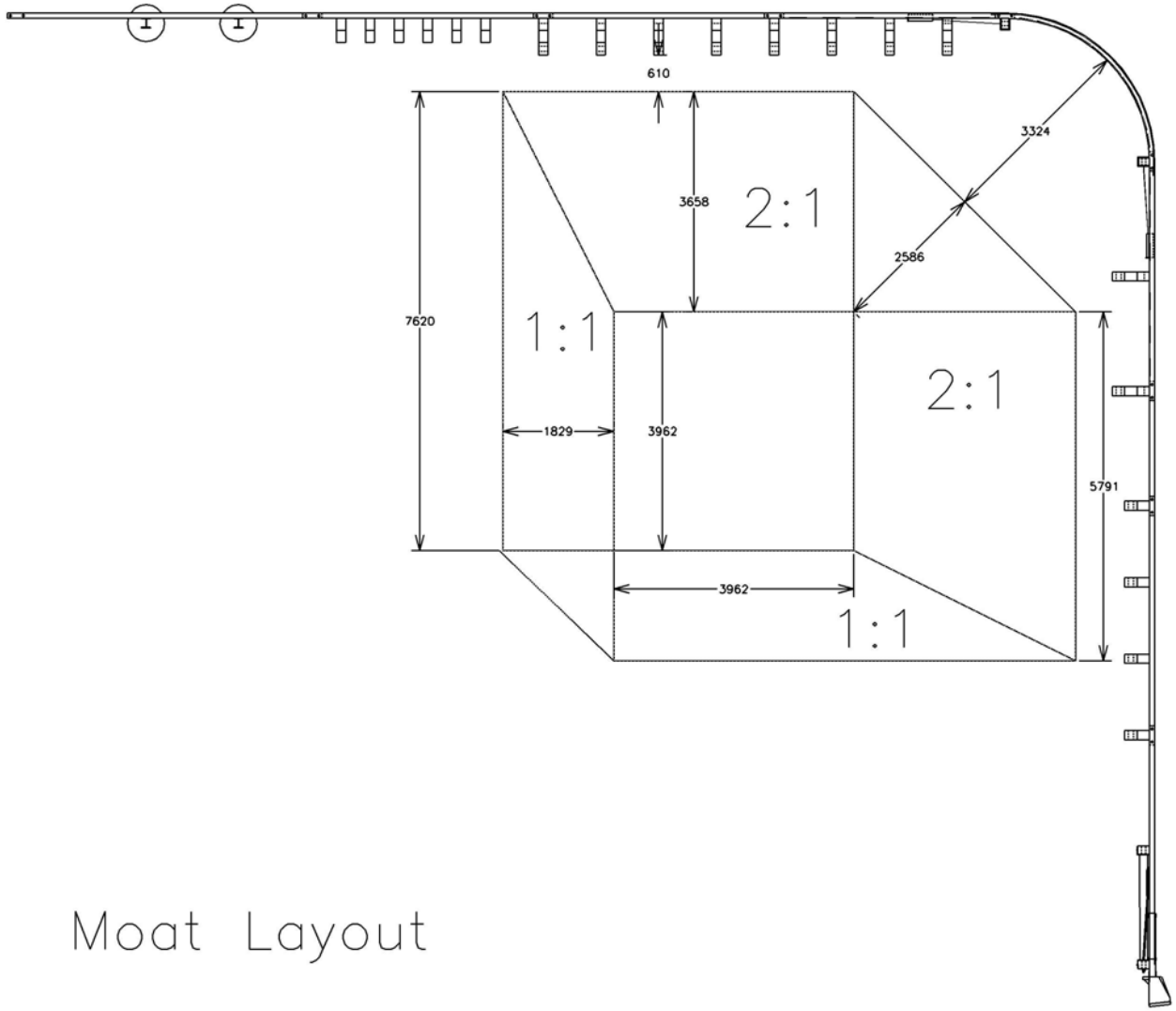

Figure 11. Moat Layout, Test SR-1

Figure 12. Short-Radius System, Test SR-1

Figure 13. Short-Radius System, Test SR-1

Figure 14. Short-Radius System, Test SR-1

3 NCHRP 350 TESTING AND EVALUATION CRITERIA

3.1 Test Requirements

Due to the nature of potential impacts into the curved section of a short-radius guardrail system, it was believed necessary to classify the system as either a terminal or crash cushion in order to determine the appropriate NCHRP Report No. 350 crash tests and evaluation criteria. A short-radius guardrail should be defined as a non-gating device and must fulfill the requirements for non-gating terminals and crash cushions. A non-gating device is designed to contain and redirect a vehicle when impacted downstream from the end of the device. According to NCHRP Report No. 350, non-gating end terminals and crash cushions must be subjected to eight full-scale vehicle crash tests, five using a 2000-kg pickup truck and three using an 820-kg small car. The required 2000-kg pickup truck crash tests for a Test Level 3 (TL-3) device are:

(1) Test 3-31, a 100 km/h impact at a nominal angle of 0 degrees on the tip of the barrier nose,
(2) Test 3-33, a 100 km/h impact at a nominal angle of 15 degrees on the tip of the barrier nose,
(3) Test 3-37, a 100 km/h impact at a nominal angle of 20 degrees on the beginning of the Length-of-Need (LON),
(4) Test 3-38, a 100 km/h impact at a nominal angle of 20 degrees on the Critical Impact Point (CIP), and
(5) Test 3-39, a 100km/h reverse direction impact at an angle of 20 degrees one half of the LON from the end of the terminal.

The required 820-kg small car crash tests for a TL-3 device are:

(1) Test 3-30, a 100 km/h impact at a nominal angle of 0 degrees on the tip of the barrier nose with a ¼-point offset,
(2) Test 3-32, a 100 km/h impact at a nominal angle of 15 degrees on the tip of the barrier nose, and
(3) Test 3-36, a 100 km/h impact at a nominal impact angle of 15 degrees on the beginning of the LON.

Of the eight recommended NCHRP Report 350 compliance tests, it was deemed that only five crash

tests were necessary for evaluating the short-radius system's safety performance. Two length of need tests, 3-36 and 3-37, were not conducted because previous testing has shown that thrie beam guardrail is capable of meeting the length of need requirements found in the safety standards. Similarly, the reverse direction impact test was not tested. Test 3-39 calls for a reverse direction impact of a 2000-kg pickup truck on a point at the length of the terminal divided by two. Thus, based on previous experience with straight thrie beam guardrail testing, it was believed that test 3-39 was unnecessary. A diagram showing the impact location for the seven of the eight crash tests is shown in Figure 15. Test no. 3-39 is not shown because the LON for the system was unknown at this time. In addition, the critical impact point is defined for non-gating terminals as the point along the installation where it is unknown whether the guardrail will capture or redirect the impacting vehicle.

3.2 Evaluation Criteria

Evaluation criteria for full-scale vehicle crash testing are based on three appraisal areas: (1) structural adequacy; (2) occupant risk; and (3) vehicle trajectory after collision. Criteria for structural adequacy are intended to evaluate the ability of the barrier to contain, redirect, or allow controlled vehicle penetration in a predictable manner. Occupant risk evaluates the degree of hazard to occupants in the impacting vehicle. Vehicle trajectory after collision is a measure of the potential for the post-impact trajectory of the vehicle to cause subsequent multi-vehicle accidents. This criterion also indicates the potential safety hazard for the occupants of other vehicles or the occupants of the impacting vehicle when subjected to secondary collisions with other fixed objects. These three evaluation criteria are defined in Table 1. The full-scale vehicle crash test was conducted and reported in accordance with the procedures provided in NCHRP Report No. 350.

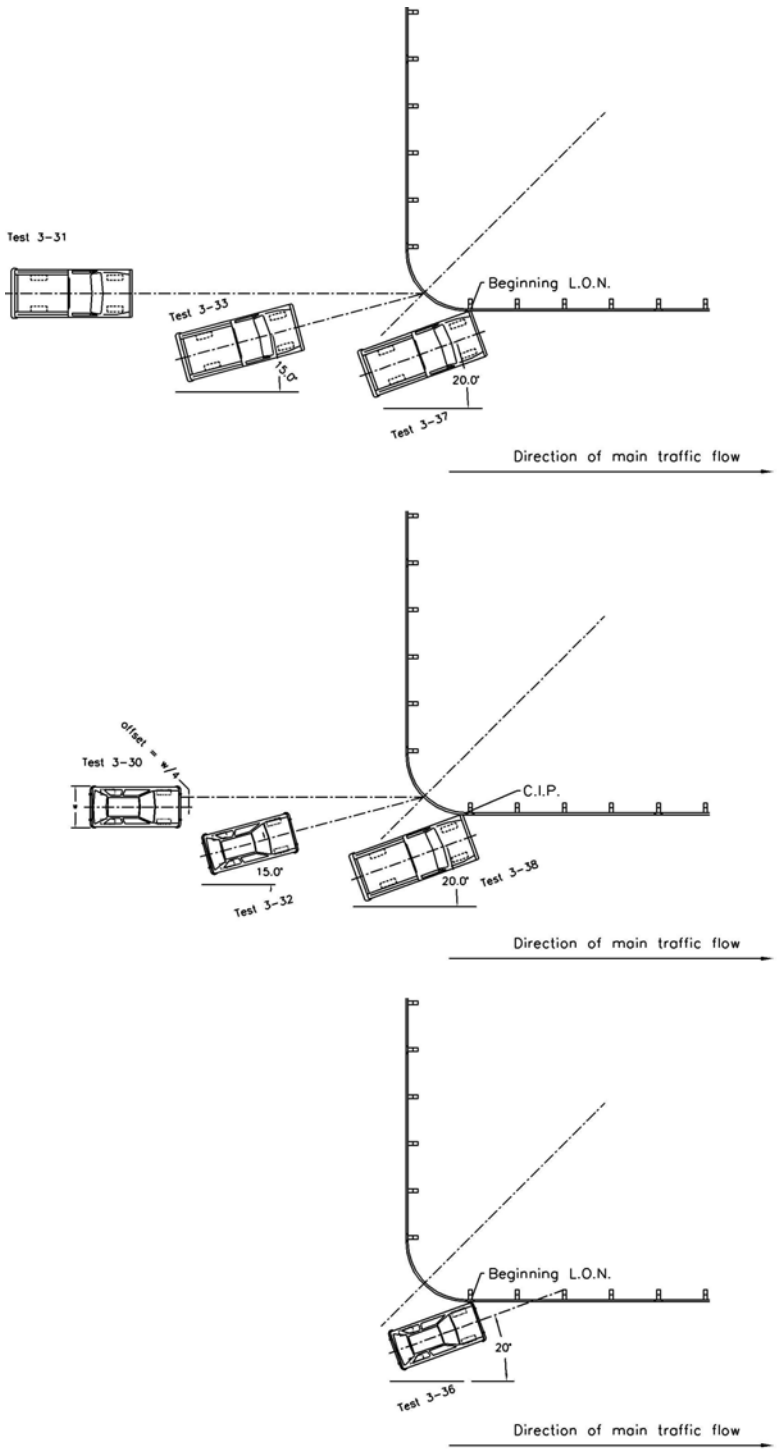

Figure 15. Full-Scale Crash Test Matrix

Table 1. NCHRP Report 350 Evaluation Criteria for 2000P Pickup Truck and 820C Small Car Tests

Evaluation Factors		Evaluation Criteria	Applicable Tests
Structural Adequacy	A.	Test article should contain and redirect the vehicle; the vehicle should not penetrate, underride, or override the installation although controlled lateral deflection of the test article is acceptable.	3-37 3-38
	C.	Acceptable test article performance may be by redirection, controlled penetration, or controlled stopping of the vehicle.	3-30 3-31 3-32 3-33 3-39
Occupant Risk	D.	Detached elements, fragments or other debris from the test article should not penetrate or show potential for penetrating the occupant compartment, or present an undue hazard to other traffic, pedestrians, or personnel in a work zone. Deformations of, or intrusions into, the occupant compartment that could cause serious injuries should not be permitted.	ALL
	F.	The vehicle should remain upright during and after collision although moderate roll, pitching, and yawing are acceptable.	ALL
	H.	Occupant impact velocities should satisfy the following: **Occupant Impact Velocity Limits (m/s)** Component — Preferred — Maximum Longitudinal and Lateral — 9 — 12	3-30 3-31 3-32 3-33 3-36
	I.	Occupant ridedown accelerations should satisfy the following: **Occupant Ridedown Acceleration Limits (G's)** Component — Preferred — Maximum Longitudinal and Lateral — 15 — 20	3-30 3-31 3-32 3-33 3-36
Vehicle Trajectory	K.	After collision it is preferable that the vehicle's trajectory not intrude into adjacent traffic lanes.	ALL
	L.	The occupant impact velocity in the longitudinal direction should not exceed 12 m/sec and the occupant ridedown acceleration in the longitudinal direction should not exceed 20 G's.	3-37 3-38 3-39
	M.	The exit angle from the test article preferably should be less than 60 percent of the test impact angle, measured at the time the vehicle lost contact with the device.	3-36 3-37 3-38 3-39
	N.	Vehicle trajectory behind the test article is acceptable.	3-30 3-31 3-32 3-33 3-39

4 TEST CONDITIONS

4.1 Test Facility

The testing facility is located at the Lincoln Air-Park on the northwest (NW) side of the Lincoln Municipal Airport and is approximately 8.0 km NW of the University of Nebraska-Lincoln.

4.2 Vehicle Tow and Guidance System

A reverse cable tow system with a 1:2 mechanical advantage was used to propel the test vehicle. The distance traveled and the speed of the tow vehicle were one-half that of the test vehicle. The test vehicle was released from the tow cable before impact with the short-radius system. A digital speedometer was located on the tow vehicle to increase the accuracy of the test vehicle impact speed.

A vehicle guidance system developed by Hinch (19) was used to steer the test vehicle. A guide-flag, attached to the front-left wheel and the guide cable, was sheared off before impact with the longitudinal barrier. The 9.5-mm diameter guide cable was tensioned to approximately 13.3 kN, and supported laterally and vertically every 30.48 m by hinged stanchions. The hinged stanchions stood upright while holding up the guide cable, but as the vehicle was towed down the line, the guide-flag struck and knocked each stanchion to the ground. The vehicle guidance system was approximately 304.8-m long.

4.3 Test Vehicles

For test no. SR-1, a 1995 GMC 2500 pickup truck was used as the test vehicle. The test inertial and gross static weights were 2,029 kg and 2,029 kg, respectively. The test vehicle dimensions are shown in Figure 16.

For test no. SR-2, a 1994 Chevrolet 2500 pickup truck was used as the test vehicle. The test

Date: 11/10/00 Test Number: SR-1 Model: 2000P

Make: GMC Vehicle I.D.#: 1GCGC24K4SZ558439

Tire Size: LT 245/75 R16 Year: 1995 Odometer: 228494

*(All Measurements Refer to Impacting Side)

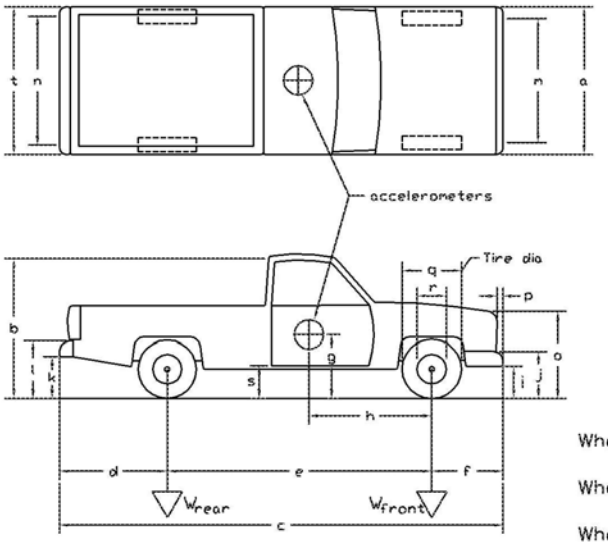

Vehicle Geometry – mm

a	1887	b	1861
c	5544	d	1303
e	3327	f	914
g	667	h	1389
i	457	j	673
k	597	l	787
m	1582	n	1621
o	1046	p	89
q	757	r	445
s	483	t	1867

Wheel Center Height Front 368

Wheel Center Height Rear 368

Wheel Well Clearance (FR) NA

Wheel Well Clearance (RR) NA

Engine Type 8 CYL. GAS

Engine Size 5.7 L 350 CID

Transmission Type:

(Automatic) or Manual

FWD or (RWD) or 4WD

Weights – kg	Curb	Test Inertial	Gross Static
W_{front}	1178	1182	1182
W_{rear}	846	847	847
W_{total}	2024	2029	2029

Note any damage prior to test: _____

Figure 16. Vehicle Dimensions, Test SR-1

inertial and gross static weights were 2,014 kg and 2,014 kg, respectively. The test vehicle dimensions are shown in Figure 17.

For test no. SR-3, a 1995 Ford 250 pickup truck was used as the test vehicle. The test inertial and gross static weights were 2,036 kg and 2,036 kg, respectively. The test vehicle dimensions are shown in Figure 18.

For test no. SR-4, a 1997 GMC 2500 pickup truck was used as the test vehicle. The test inertial and gross static weights were 2,005 kg and 2,005 kg, respectively. The test vehicle dimensions are shown in Figure 19.

The longitudinal component of the center of gravity was determined using the measured axle weights. The location of the final centers of gravity are shown in Figures 16 through 23.

Square, black and white-checkered targets were placed on the vehicle to aid in the analysis of the high-speed film and E/cam video, as shown in Figures 20 through 23. Round, checkered targets were placed on the center of gravity on the driver's side door, the passenger's side door, and on the roof of the vehicle. The remaining targets were located for reference so that they could be viewed from the high-speed cameras for film analysis.

The front wheels of the test vehicle were aligned for camber, caster, and toe-in values of zero so that the vehicle would track properly along the guide cable. Two 5B flash bulbs were mounted on both the hood and roof of the vehicle to pinpoint the time of impact with the barrier system on the high-speed film and E/cam video. The flash bulbs were fired by a pressure tape switch mounted on the front face of the bumper. A remote controlled brake system was installed in the test vehicle so the vehicle could be brought safely to a stop after the test.

Date: 5/1/01 Test Number: SR-2 Model: 2000P/2500 PU

Make: Chevrolet Vehicle I.D.#: 1GCGC24K3RE285001

Tire Size: LT 245/75 R16 Year: 1994 Odometer: 164994

*(All Measurements Refer to Impacting Side)

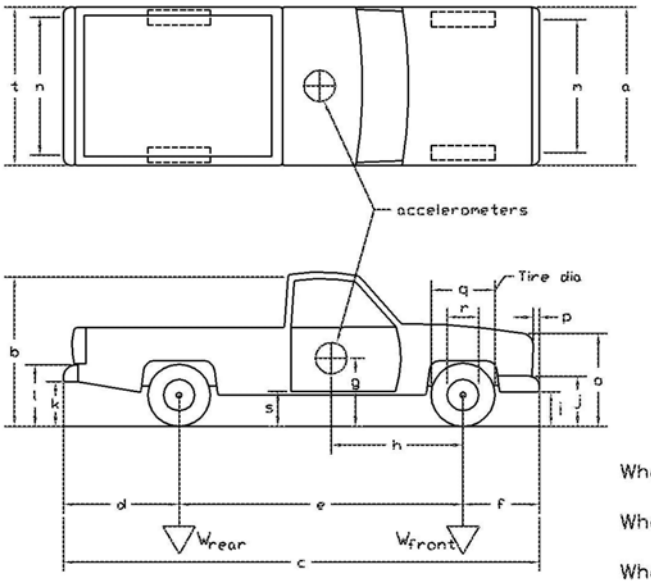

Vehicle Geometry – mm

a	1867	b	1854
c	5537	d	1295
e	3327	f	914
g	667	h	1445
i	425	j	635
k	584	l	781
m	1600	n	1613
o	1003	p	102
q	629	r	445
s	476	t	1867

Wheel Center Height Front 359

Wheel Center Height Rear 365

Wheel Well Clearance (FR) 886

Wheel Well Clearance (RR) 953

Engine Type 8 CYL. GAS

Engine Size 5.7 L 350 CID

Transmission Type:

Automatic or (Manual)

FWD or (RWD) or 4WD

Weights – kg

	Curb	Test Inertial	Gross Static
W_{front}	1134	1139	1139
W_{rear}	874	874	874
W_{total}	2009	2014	2014

Note any damage prior to test: Passenger Front Fender Dent

Figure 17. Vehicle Dimensions, Test SR-2

Date: 10/24/01 Test Number: SR-3 Model: 2000P/F250

Make: Ford Vehicle I.D.#: 2FTHF25H85CA35408

Tire Size: LT 235/85 R16 Year: 1995 Odometer: 365000

*(All Measurements Refer to Impacting Side)

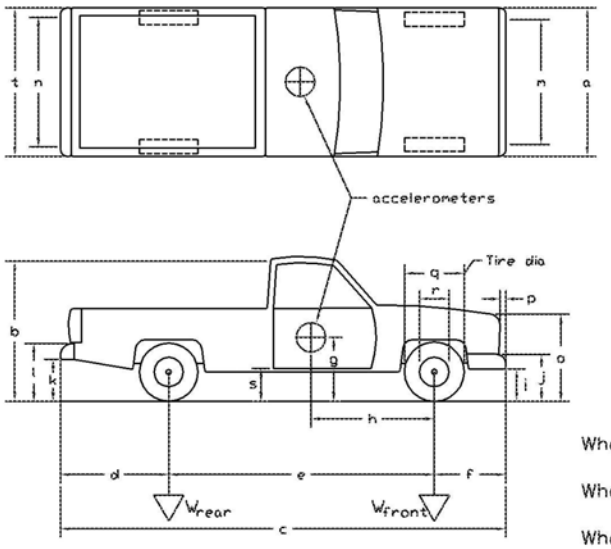

Vehicle Geometry – mm

a	1938	b	
c	5525	d	1295
e	3378	f	851
g	737	h	1426
i	476	j	711
k	546	l	730
m	1689	n	1651
o	1111	p	95
q	787	r	445
s	552	t	1943

Wheel Center Height Front 378

Wheel Center Height Rear 381

Wheel Well Clearance (FR) 899

Wheel Well Clearance (RR) 959

Engine Type 8 CYL. GAS

Engine Size 5.8 L 351 CID

Transmission Type:

Automatic or (Manual)

FWD or (RWD) or 4WD

Weights – kg	Curb	Test Inertial	Gross Static
W_{front}	1124	1177	1177
W_{rear}	876	859	859
W_{total}	2000	2036	2036

Note any damage prior to test: SMALL DENTS–VARIOUS BODY/SMALL FRAME DAMAGE

Figure 18. Vehicle Dimensions, Test SR-3

Date: 9/19/02 Test Number: SR-4 Model: 2000P/F250

Make: GMC Vehicle I.D.#: 1GDGC24R6V2536203

Tire Size: LT 245/75 R16 Year: 1997 Odometer: 261838

*(All Measurements Refer to Impacting Side)

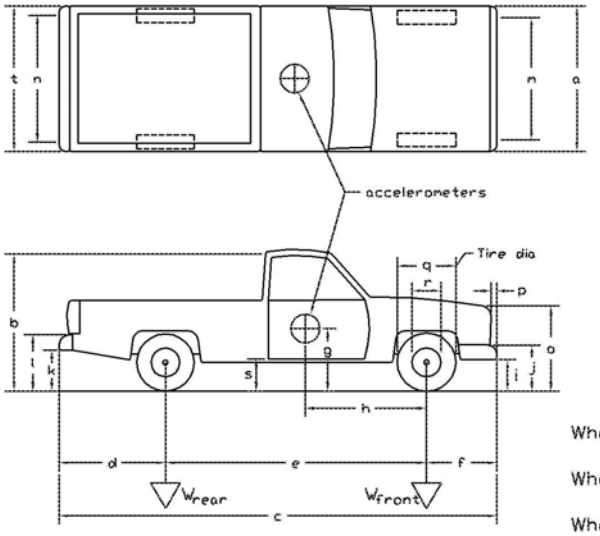

Vehicle Geometry – mm

a	1886	b	1854
c	5537	d	1308
e	3327	f	902
g	667	h	1381
i	445	j	660
k	603	l	781
m	1600	n	1619
o	1016	p	89
q	762	r	445
s	470	t	1867

Wheel Center Height Front 365

Wheel Center Height Rear 368

Wheel Well Clearance (FR) 914

Wheel Well Clearance (RR) 956

Engine Type 8 CYL. GAS

Engine Size 5.8 L 351 CID

Transmission Type:

(Automatic) or Manual

FWD or (RWD) or 4WD

Weights – kg	Curb	Test Inertial	Gross Static
W_{front}	1142	1173	1173
W_{rear}	844	832	832
W_{total}	1986	2005	2005

Note any damage prior to test: NONE– CRACKED WINDSHEILD

Figure 19. Vehicle Dimensions, Test SR-4

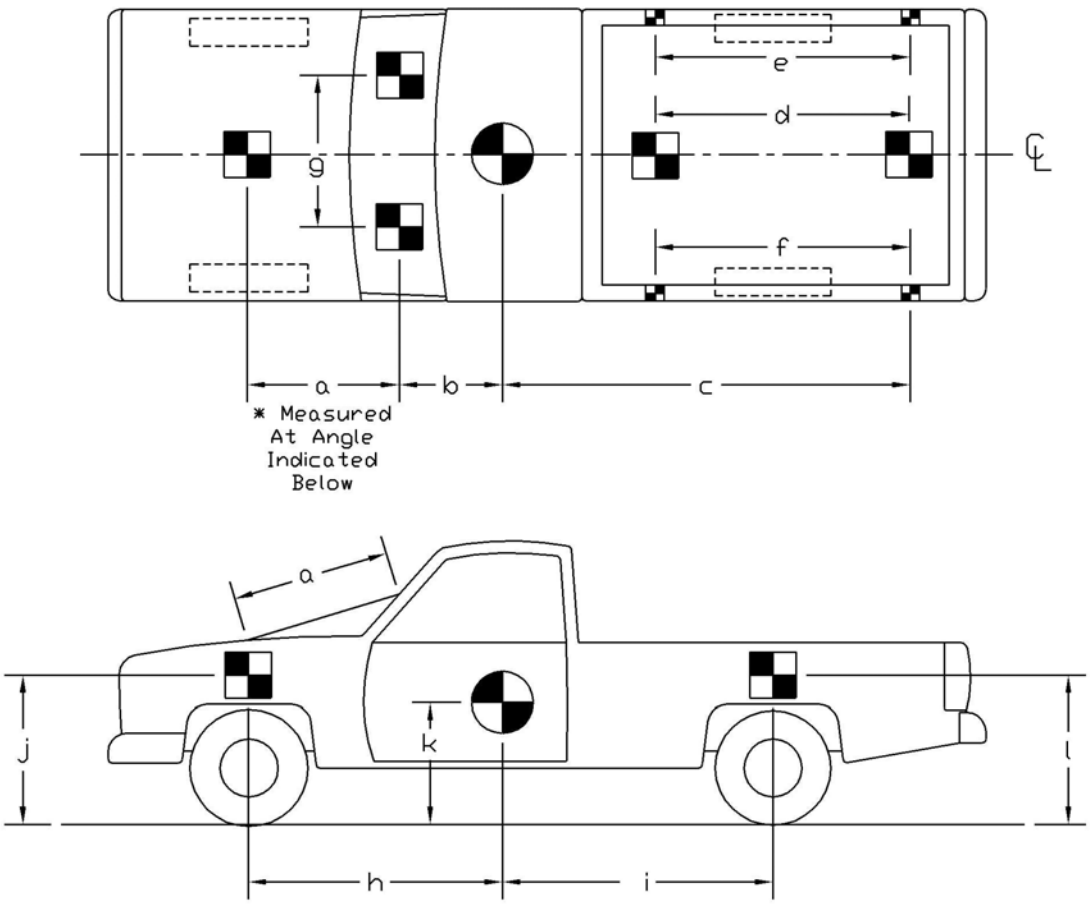

TEST #: SR-1

TARGET GEOMETRY (mm)

a	864	d	1697	g	919	j	1016
b	737	e	2153	h	1388	k	667
c	2892	f	2153	i	1939	l	1062

Figure 20. Vehicle Target Locations, Test SR-1

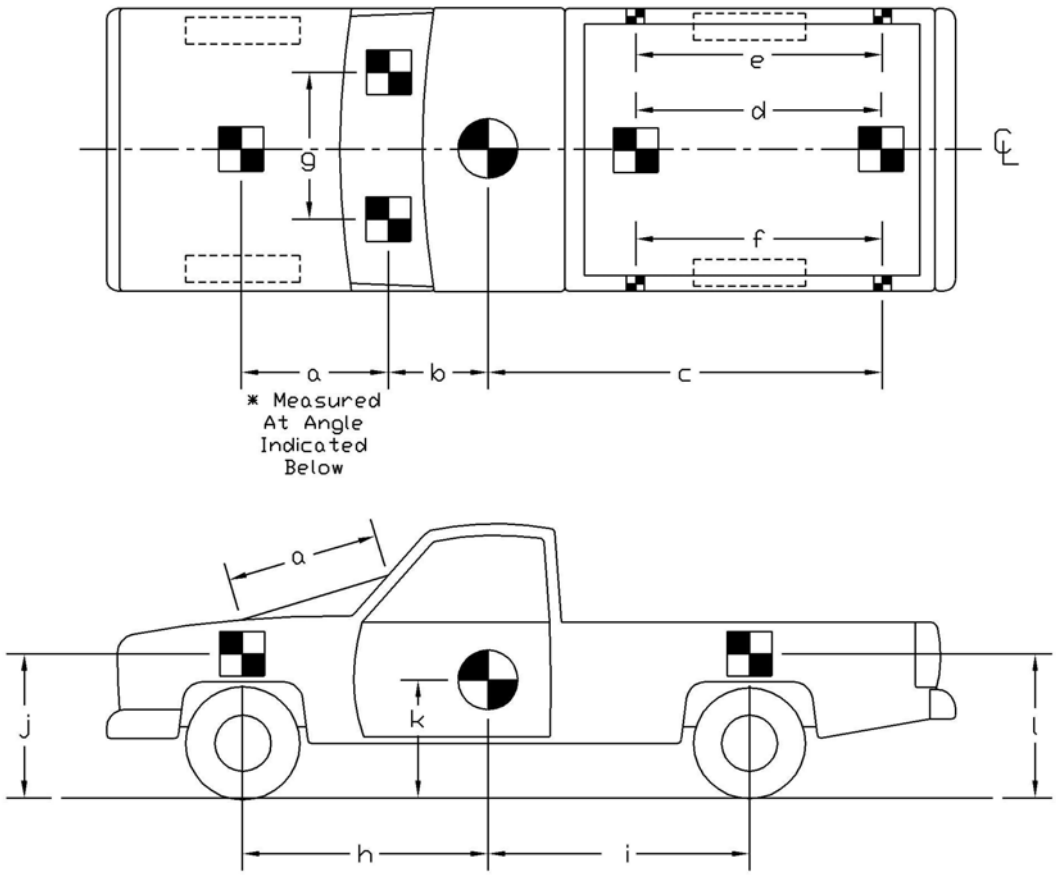

TEST #: SR-2

TARGET GEOMETRY (mm)

a 829	d 1838	g 1099	j 991
b 765	e 2153	h 1445	k 667
c 2715	f 2153	i 1883	l 1054

Figure 21. Vehicle Target Locations, Test SR-2

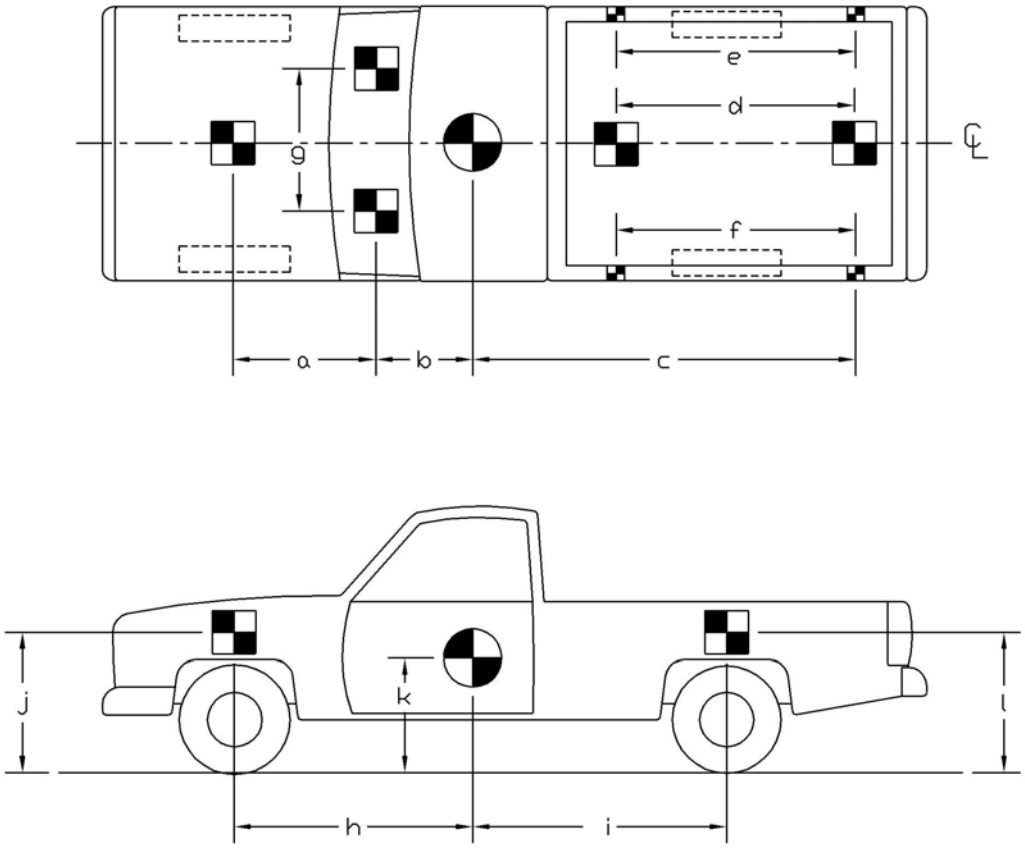

TEST #: SR-3

TARGET GEOMETRY (mm)

a	867	d	1810	g	1105	j	1000
b	718	e	2200	h	1426	k	737
c	2661	f	2200	i	1953	l	1000

Figure 22. Vehicle Target Locations, Test SR-3

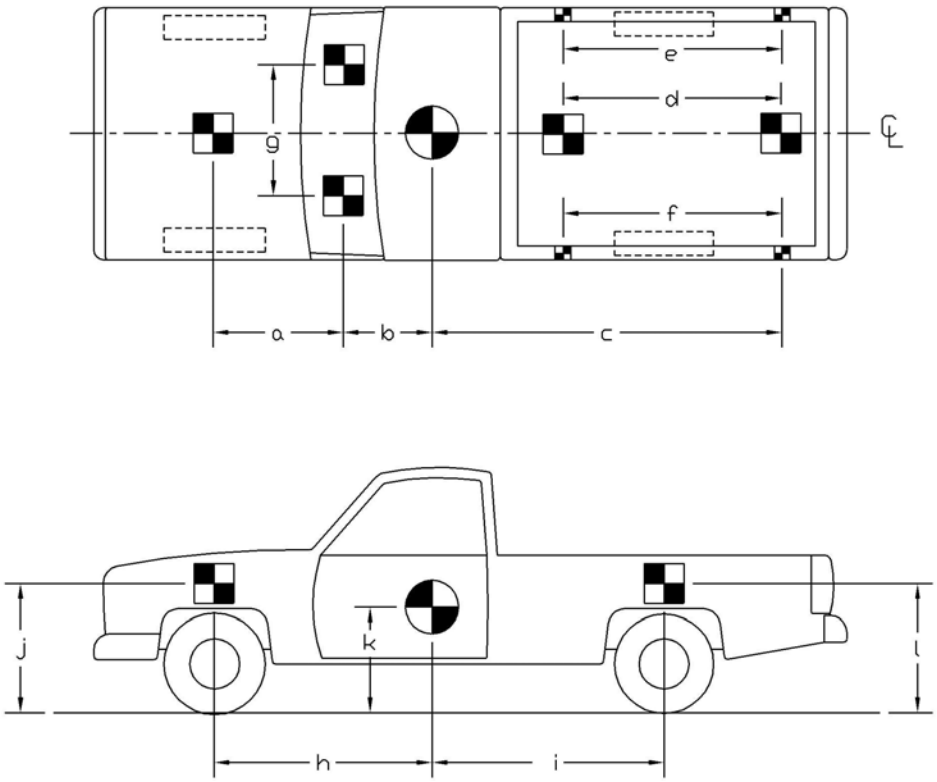

TEST #: SR-4

TARGET GEOMETRY (mm)

a	889	d	1765	g	1130	j	1010
b	699	e	2153	h	1381	k	667
c	2680	f	2153	i	1927	l	1175

Figure 23. Vehicle Target Locations, Test SR-4

4.4 Data Acquisition Systems

4.4.1 Accelerometers

One triaxial piezoresistive accelerometer system with a range of ±200 G's was used to measure the acceleration in the longitudinal, lateral, and vertical directions at a sample rate of 10,000 Hz. The environmental shock and vibration sensor/recorder system, Model EDR-4M6, was developed by Instrumented Sensor Technology (IST) of Okemos, Michigan and includes three differential channels as well as three single-ended channels. The EDR-4 was configured with 6 Mb of RAM memory and a 1,500 Hz lowpass filter. Computer software, "DynaMax 1 (DM-1)" and "DADiSP" were used to analyze and plot the accelerometer data.

A backup triaxial piezoresistive accelerometer system with a range of ±200 G's was also used to measure the acceleration in the longitudinal, lateral, and vertical directions at a sample rate of 3,200 Hz. The environmental shock and vibration sensor/recorder system, Model EDR-3, was developed by Instrumental Sensor Technology (IST) of Okemos, Michigan. The EDR-3 was configured with 256 Kb of RAM memory and a 1,120 Hz lowpass filter. Computer software, "DynaMax 1 (DM-1)" and "DADiSP" were used to analyze and plot the accelerometer data.

4.4.2 Rate Transducers

A Humphrey 3-axis rate transducer with a range of 360 deg/sec in each of the three directions (pitch, roll, and yaw) was used to measure the rates of motion of the test vehicle. The rate transducer was rigidly attached to the vehicle near the center of gravity of the test vehicle. Rate transducer signals, excited by a 28 volt DC power source, were received through the three single-ended channels located externally on the EDR-4M6 and stored in the internal memory. The raw data measurements were then downloaded for analysis and plotted. Computer software, "DynaMax 1 (DM-1)" and

"DADiSP" were used to analyze and plot the rate transducer data.

4.4.3 High-Speed Photography

For test no. SR-1, five high-speed Red Lake E/cam video cameras, with operating speeds of 500 frames/sec, and one16-mm Red Lake Locam camera, with an operating speed of approximately 500 frames/sec, were used to film the crash test. Three Canon digital video cameras, with a standard operating speed of 28.97 frames/sec, were also used to film the crash test. One E/cam high-speed video camera and a Locam with a wide angle 12.5-mm lens were placed above the installation to provide a field of view perpendicular to the ground. An additional E/cam high-speed video camera and a Canon digital video camera were placed downstream of the impact point to provide a field of view downstream of the impact point. Another E/cam high- speed video camera and a Canon digital video camera were placed upstream and offset to the left of the impact point and had an angled view of the impacts. An E/cam high-speed video camera and a Canon digital video camera were placed upstream and to the right of the impact point to provide a second angled view of the impact. An E/cam high-speed video camera was placed to the left of the impact point to provide a view perpendicular to the impact. A final E/cam digital video camera was placed upstream of the impact point to provide an upstream view. A schematic of all of the camera locations for tests SR-1 is shown in Figure 24.

For test no. SR-2, five high-speed Red Lake E/cam video cameras, with operating speeds of 500 frames/sec, and three16-mm Red Lake Locam cameras, with operating speeds of approximately 500 frames/sec, were used to film the crash test. Three Canon digital video cameras, with a standard operating speed of 28.97 frames/sec, and two SVHS video cameras were also used to film the crash test. Two E/cam high-speed video cameras and a Locam with a wide angle 12.5-mm lens were

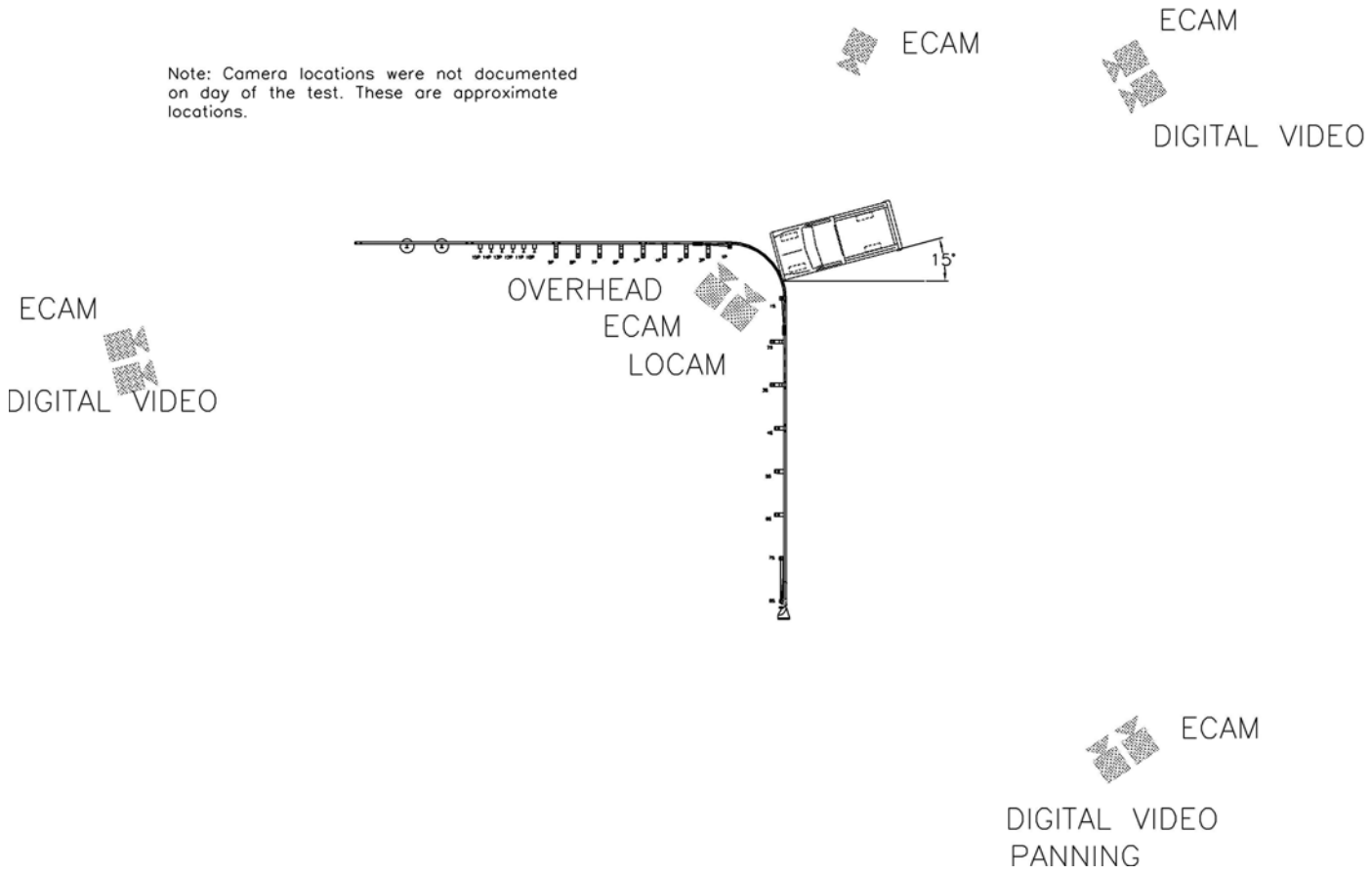

Figure 24. Location of High-Speed Cameras, Test SR-1

placed 12.4-m above the installation to provide a field of view perpendicular to the ground. A Locam camera, a Nikon F5 camera, and a SVHS camera were placed downstream of the impact point to provide a field of view downstream of the impact point. Two E/cam high-speed video cameras and a Canon digital video camera were placed downstream and offset to the right of the impact point and had an angled view of the impacts. An E/cam high-speed video camera and a Canon digital video camera were placed upstream and to the right of the impact point to provide a second angled view of the impact. A Canon digital video camera was placed farther upstream of the impact point to provide a tracking view of the impact. A final SVHS video camera was placed to the left of the impact point to provide a panning view. A schematic of all of the camera locations for tests SR-2 is shown in Figure 25.

For test no. SR-3, five high-speed Red Lake E/cam video cameras, with operating speeds of 500 frames/sec, and one16-mm Red Lake Locam camera, with an operating speed of approximately 500 frames/sec, were used to film the crash test. Four Canon digital video cameras, with a standard operating speed of 28.97 frames/sec were also used to film the crash test. Two E/cam high-speed video cameras and a Locam with a wide angle 12.5-mm lens were placed 15.85-m above the installation to provide a field of view perpendicular to the ground. A Nikon F5 camera was placed downstream and to the left of the impact point to provide an angled view of the impact. One E/cam high-speed video camera and a Canon digital video camera were placed downstream to provide a downstream view of the impact. An E/cam high-speed video camera and a Canon digital video camera were placed downstream and to the left of the impact point to provide an angled view of the impact. Another E/cam high-speed video camera and a Canon digital video camera were placed directly to the left of the impact point to provide a perpendicular view of the impact. A Canon

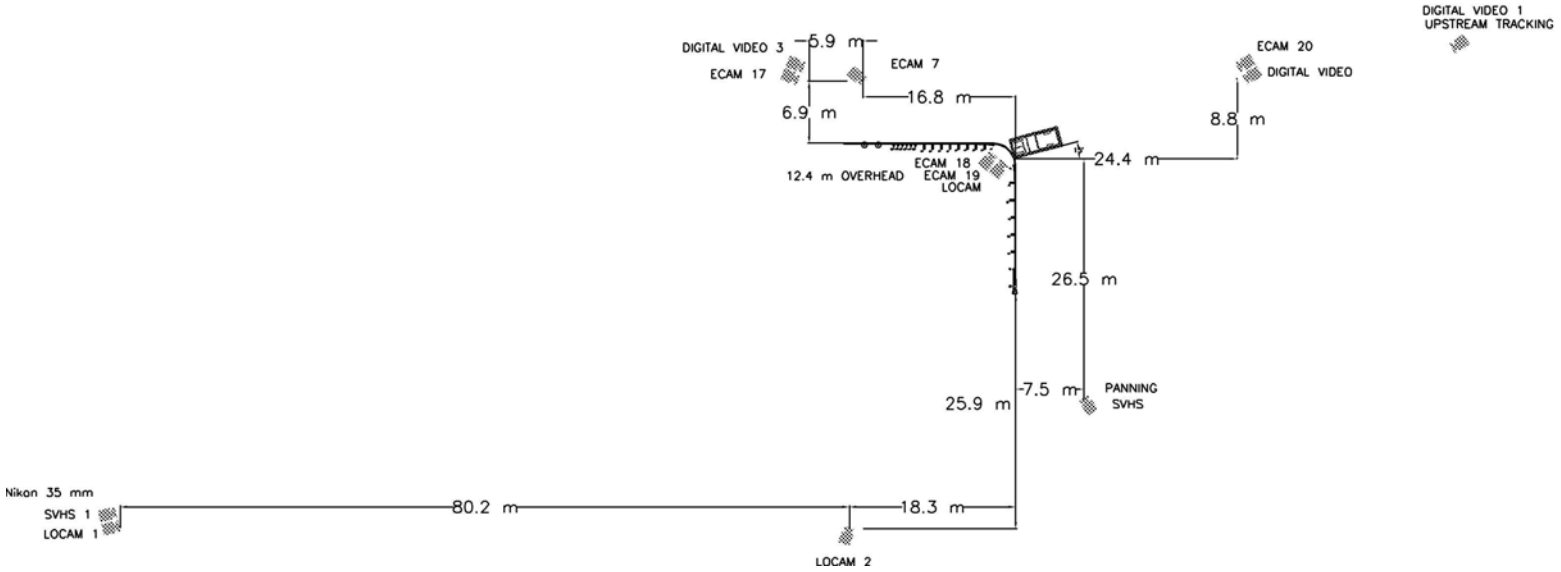

Figure 25. Location of High-Speed Cameras, Test SR-2

digital video camera was placed upstream of the impact point to provide an upstream view of the impact. A final Canon digital video camera was placed to the downstream and to the right of the impact point to provide an additional angled view. A schematic of all of the camera locations for tests SR-3 is shown in Figure 26.

For test no. SR-4, five high-speed Red Lake E/cam video cameras, with operating speeds of 500 frames/sec, and one16-mm Red Lake Locam camera, with an operating speed of approximately 500 frames/sec, were used to film the crash test. Five Canon digital video cameras, with a standard operating speed of 28.97 frames/sec were also used to film the crash test. Two E/cam high-speed video cameras and a Locam with a wide angle 12.5-mm lens were placed 17.22-m above the installation to provide a field of view perpendicular to the ground. One E/cam high-speed video camera and a Canon digital video camera were placed downstream to provide a downstream view of the impact. An E/cam high-speed video camera and a Canon digital video camera were placed downstream and to the left of the impact point to provide an angled view of the impact. Another Canon digital video camera was placed directly to the left of the impact point to provide a perpendicular view of the impact. A Canon digital video camera was placed downstream and to the right of the impact point to provide an angled view of the impact. A final E/cam high-speed video camera and a Canon digital video camera were placed to the downstream and to the right of the impact point to provide an additional angled view. A schematic of all of the camera locations for tests SR-4 is shown in Figure 27.

The Locam films and E/cam videos were analyzed using the Vanguard Motion Analyzer and the Redlake Motion Scope software, respectively. Actual camera speed and camera divergence factors were considered in the analysis of the high-speed film.

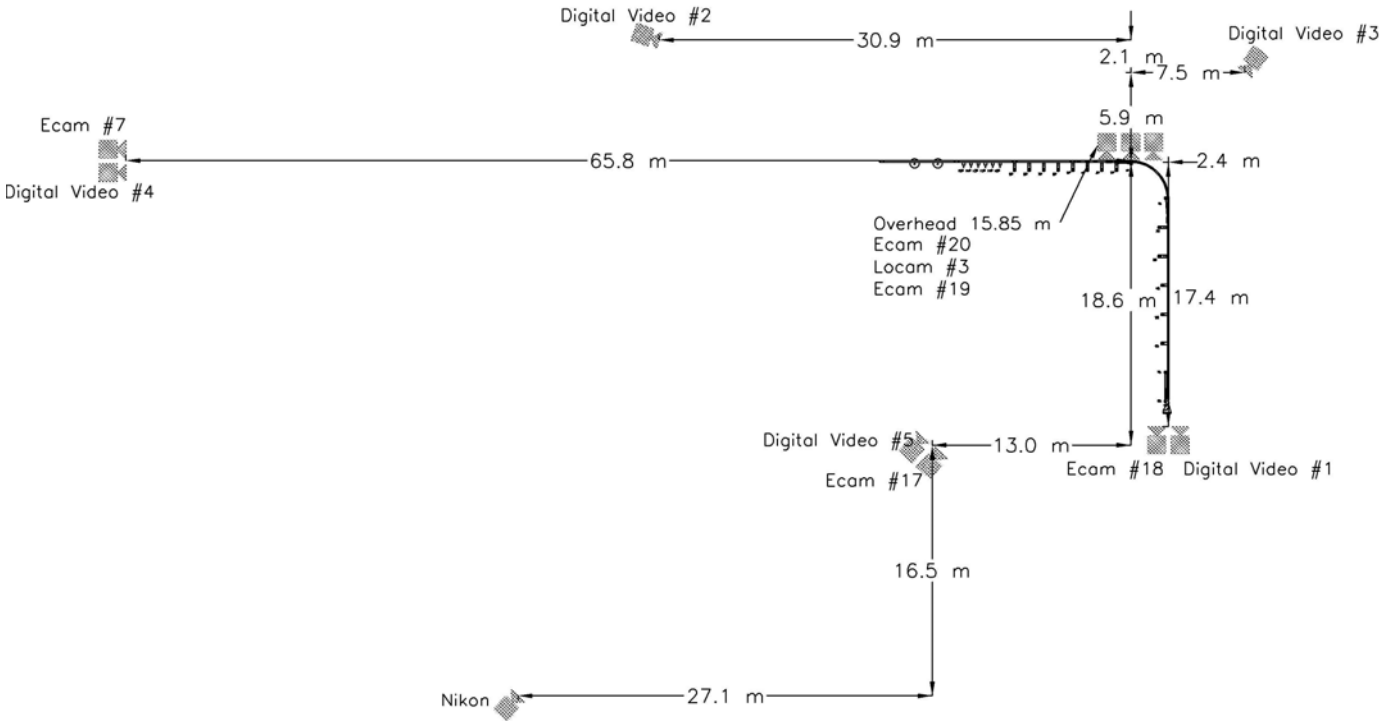

Figure 26. Location of High-Speed Cameras, Test SR-3

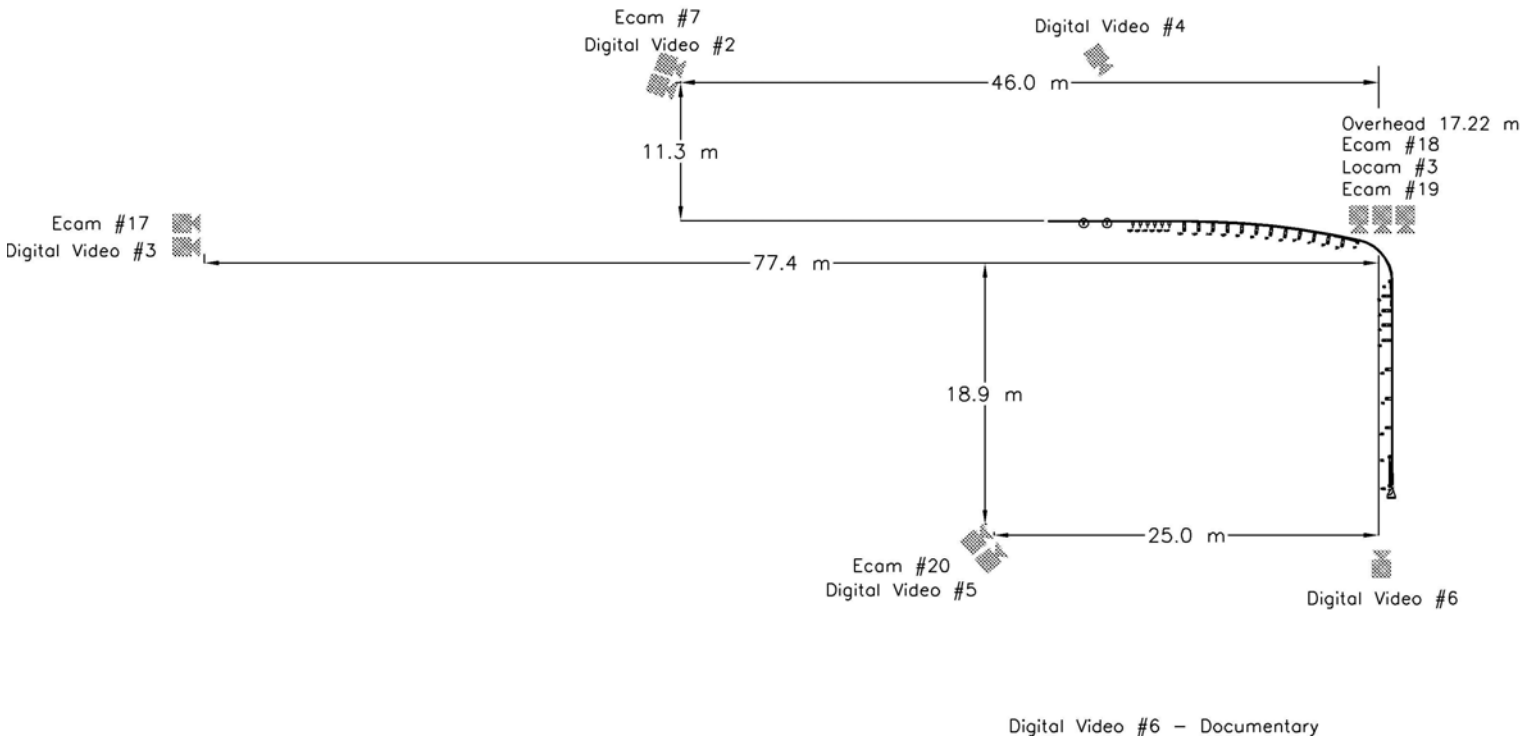

Figure 27. Location of High-Speed Cameras, Test SR-4

4.4.4 Pressure Tape Switches

For test nos. SR-1 though SR-4, two sets of three pressure-activated tape switches, spaced at 2-m intervals, were used to determine the speed of the vehicle before impact with the barrier system. Each tape switch fired a strobe light which sent an electronic timing signal to the data acquisition system as the vehicle's front tire passed over it. For test nos. SR-1 though SR-4, the right-front tire passed over the tape switches. Test vehicle speed was determined from electronic timing mark data recorded using the "Test Point" software. Strobe lights and high-speed film analysis are used only as a backup in the event that vehicle speed cannot be determined from the electronic data.

5 CRASH TEST SR-1

5.1 Test SR-1

Test SR-1 was conducted according to NCHRP Report No. 350 Test Designation 3-33. The 2,029-kg pickup truck impacted the short-radius guardrail at a speed of 98.9 km/hr and at an angle of 19.0 degrees. The impact orientation for this test was the centerline of the pickup truck impacting the center of the curved nose section. A summary of the test results and the sequential photographs are shown in Figure 28. Additional sequential photographs are shown in Figure 30. Documentary photographs of the crash tests are shown in Figures 31 through 34.

5.2 Test Description

The test vehicle impacted the curved section of the short-radius guardrail system, as shown in Figure 35. Upon impact, the front of the pickup truck began to deform the curved section of guardrail inward with the vehicle's front bumper impacting the top of the middle hump of the thrie beam guardrail. As the vehicle deformed the nose of the system inward, the top hump of guardrail became positioned across the bumper, the middle hump was pushed below the bumper, and the bottom hump was pushed beneath the bumper and was rolled over by the left-front tire. At 0.034 sec after impact, post no. 1S was fractured as it was loaded by the deformed guardrail. As the vehicle moved forward, the thrie beam rail wrapped around the right-front corner of the pickup truck, causing the rail to bend around post no. 1P and fracture it at 0.080 sec. By 0.140 sec, the vehicle continued forward into the system with the thrie beam remained locked around its right front corner and post no. 2P was fractured. At approximately 0.160 sec, post no. 2S fractured and the tension holding the thrie beam across the front of the pickup truck was reduced. This allowed the thrie beam to fall off the bumper on the left side of the vehicle while remaining locked around the bumper on the right side.

The uneven loading across the front of the vehicle caused the pickup truck to yaw clockwise and pulled down on the right-front corner of the pickup truck. As the pickup truck continued into the system, the front tires of the vehicle lost contact with the ground due to the moat located behind the guardrail. The loss of contact between the front tires and the slope combined with the downward pitch of the right-front corner of the vehicle, caused the vehicle to roll to the right at approximately 0.300 sec. The thrie beam remained locked around the right-front corner of the vehicle, which loaded the primary side of the system and caused post nos. 2P through 8P to fracture. By approximately 0.760 sec, the pickup truck had rolled completely onto its right side. At this point, the pickup truck became disengaged from the guardrail and continued to roll as it hit the bottom of the moat. The forward momentum and roll of the pickup truck contributed to flipping the vehicle upright just outside the far end of the moat. The final position of the pickup truck was 10.0 m to the left of the primary side of the system and 15.3 m to the right of the secondary side of the system. The trajectory and final position of the pickup truck are shown in Figure 29.

5.3 System and Component Damage

Damage to the short-radius system was extensive, as shown in Figures 36 through 39. Post nos. 1S and 3S on the secondary side were fractured and broken due to the guardrail on the secondary side being pulled towards the middle of the system. Post no. 4S displayed significant deflection but was not fractured. Rail section no. 2 on the secondary side of the system was bent around the post and blockout at post no. 4S. The curved radius, rail section no. 1, displayed completely torn slot tabs along the bottom set of slots in the rail, while only one slot tab was torn in the top set. In addition, the middle hump of the thrie beam was completely torn. The nose cables of the system remained attached to the guardrail by the anchor plates. On the primary side of the system, post nos. 1P through

8P were fractured, while post no. 9P was deflected in the soil. Rail section no. 2 on the primary side was bent around post no. 9P and was twisted as it was pushed into the moat.

5.4 Vehicle Damage

Vehicle damage was extensive, as shown in Figures 40 and 41. Damage due to the impact with the system was difficult to separate from damage due to rollover. The frontal area of the vehicle, including the bumper, radiator, and headlights, was crushed inward due to the impact with the system. The front grill was detached, and the front of the hood was bent slightly. The front fenders of the pickup truck displayed some deformation and crushing. Little or no damage was observed to the undercarriage of the vehicle. The right-rear tire of the pickup truck was knocked of the rim and was deflated. The right side of the box was crushed inward due to rollover, and the right side and rear window glass were broken as well. The bed of the pickup truck was severely deformed. Large dents and deformation were seen near the front of the bed on the right side and in between the wheel well and the end of the box on the left side.

The damage observed to the interior occupant compartment was minor. Complete occupant compartment deformation measurements were not taken after test SR-1 due to the rollover of the test vehicle.

5.5 Occupant Risk Values

The longitudinal occupant impact velocity (OIV) was determined to be 6.27 m/s. The maximum 0.010-sec average occupant ridedown deceleration (ORD) in the longitudinal direction was 9.28 g's. The lateral occupant impact velocity (OIV) was determined to be 1.59 m/s. The maximum 0.010-sec average occupant ridedown deceleration (ORD) in the lateral direction was 7.89 g's. It is noted that the occupant impact velocities and the occupant ridedown decelerations were within the

suggested limits provided in NCHRP Report No. 350. The results of the occupant risk data are summarized in Figure 28. It should be noted that the determination of the occupant risk values was terminated at 0.700 sec because the vehicle had rolled on its side and the data was no longer valid. Results are shown graphically in Appendix A.

5.6 Discussion

Following test SR-1, a safety performance evaluation was conducted, and the short-radius guardrail was determined to be unacceptable according to the NCHRP Report No. 350 criteria. The test article did not safely contain, redirect, or bring the vehicle to a controlled stop. Detached elements and debris from the test article did not penetrate nor show potential for penetrating the occupant compartment or present undue hazard to the other traffic, pedestrians, or personnel in the work zone. Deformations of, or intrusion into, the occupant compartment did not occur. The vehicle did not remain upright during and after the collision. The vehicle's trajectory did not intrude into adjacent traffic lanes. The occupant impact velocities and ridedown accelerations were within the suggested limits imposed by NCHRP Report No. 350.

The failure of test SR-1 to meet the safety performance criteria was directly attributed to the rollover of the pickup truck. The rollover of the truck was believed to be caused by a combination of factors. First, capture of the front of the pickup was not as effective as hoped. The thrie beam guardrail never tore through the top set of slot tabs, and the top hump of the thrie beam rail never completely locked above the front bumper. Instead, the guardrail was only securely locked about the right front corner of the pickup truck. Second, lack of tension from the secondary side of the guardrail allowed the rail to slip below the bumper on the left side of the vehicle. This created an uneven loading across the front of the pickup truck. Third, the presence of the moat added to the instability

of the vehicle by significantly reducing its resistance to roll and pitch motions. This added instability when coupled with the uneven capture and loading of the vehicle pulled the right-front corner of the pickup truck down and rolled the vehicle onto its side as it proceeded into the system.

As a result of this failed test, design changes were deemed necessary in order to improve vehicle containment as well as to provide for a controlled deceleration of the pickup truck.

0.000 sec 0.045 sec 0.128 sec 0.238 sec 0.421 sec

- Test Number SR-1
- Date 10/24/01
- Test Article
  - Type . . . . . Short-Radius Guardrail
  - Key Elements . . . . . One 3,810-mm long curved and slotted thrie beam guardrail section
    Three 3,810-mm long straight thrie beam guardrail sections
    12 breakaway posts
    SKT End Terminal
    Iowa steel post transition
    One W-beam to thrie beam transition
  - Orientation . . . . . Centerline truck with centerline of curved rail
- Soil Type . . . . . Grading B - AASHTO M 147-65 (1990)
- Vehicle Model . . . . . 1995 Ford F250 pickup truck
  - Curb . . . . . 2,000 kg
  - Test Inertial . . . . . 2,029 kg
  - Gross Static . . . . . 2,029 kg
- Vehicle Speed
  - Impact . . . . . 98.9 km/hr
  - Exit . . . . . NA
- Vehicle Angle
  - Impact . . . . . 19.0 deg
  - Exit . . . . . NA
- Vehicle Stability . . . . . Unacceptable (rolled)
- Occupant Ridedown Deceleration (10 msec avg.)
  - Longitudinal . . . . . 9.28 g's < 20g's
  - Lateral (not required) . . . . . 7.89 g's < 20g's
- Occupant Impact Velocity (Normalized)
  - Longitudinal . . . . . 6.27 m/s < 12 m/s
  - Lateral (not required) . . . . . 1.59 m/s < 12 m/s
- Vehicle Damage
  - TAD[20] 12-FD-4
    3-R&T-3
  - SAE[21] 12FDEW2
    03RZAW2
- Vehicle Stopping Distance . . . . . 10.0 m left of primary side
  15.3 m right of secondary side
- Test Article Damage . . . . . Extensive
- Maximum Deflections
  - Permanent Set . . . . . NA
  - Dynamic . . . . . NA

Figure 28. Summary of Test Results and Sequential Photographs, Test SR-1

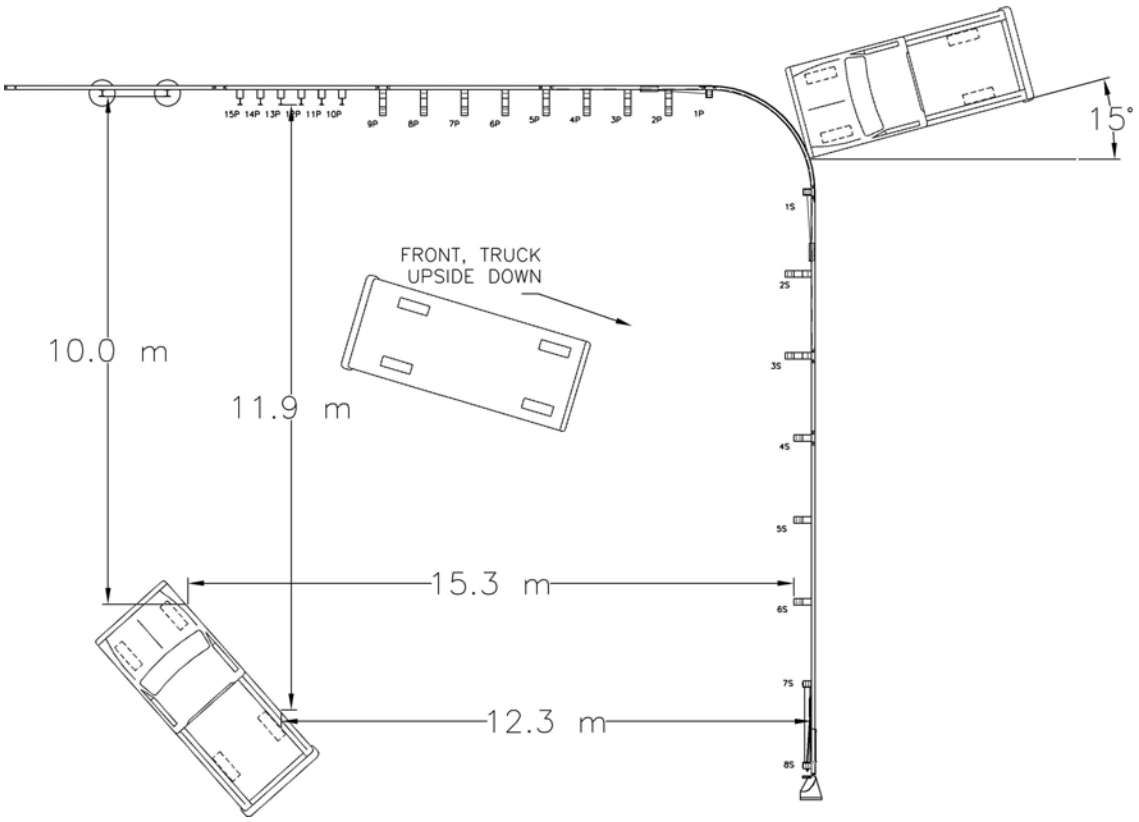

Figure 29. Vehicle Trajectory, Test SR-1

0.000 sec

0.000 sec

0.066 sec

0.050 sec

0.150 sec

0.100 sec

0.246 sec

0.220 sec

0.376 sec

0.350 sec

Figure 30. Additional Sequential Photographs, Test SR-1

Figure 31. Documentary Photographs, Test SR-1

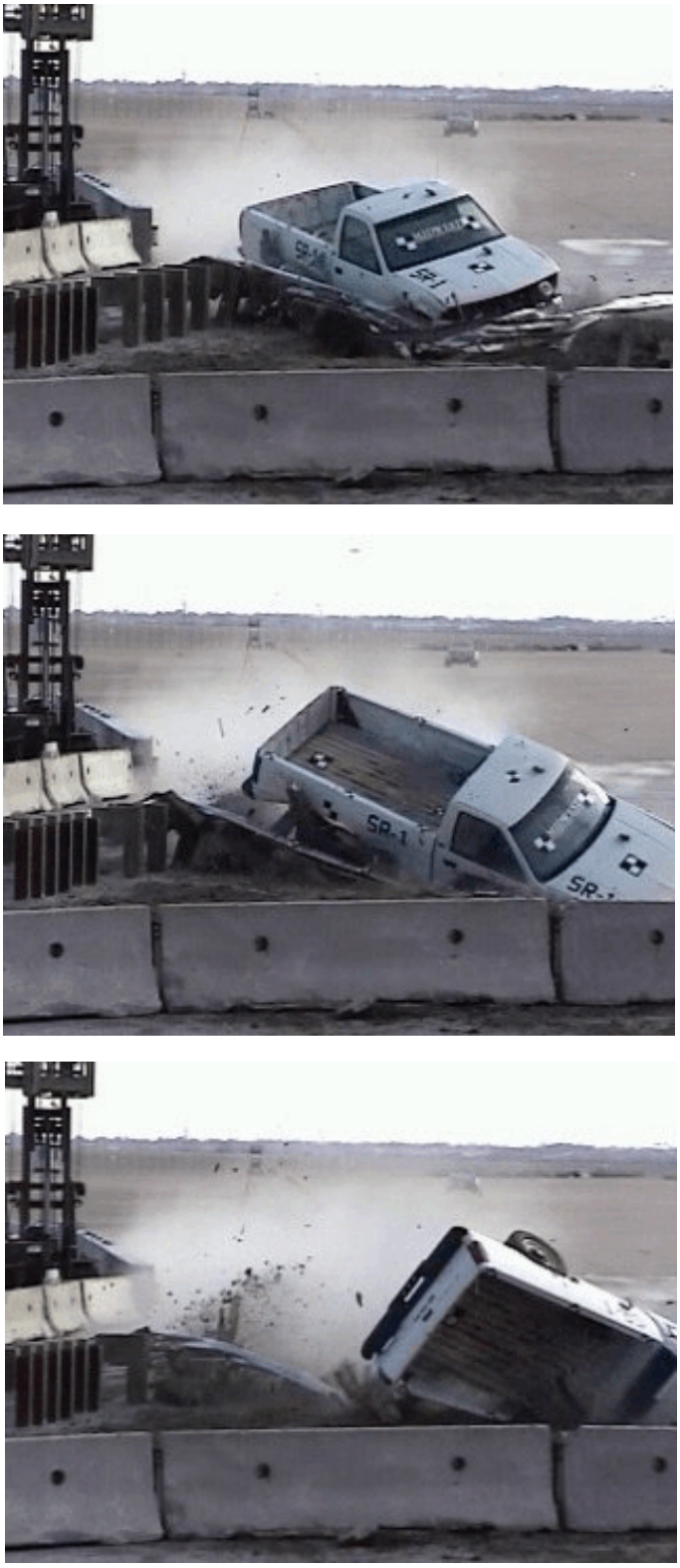

Figure 32. Documentary Photographs, Test SR-1

Figure 33. Documentary Photographs, Test SR-1

Figure 34. Documentary Photographs, Test SR-1

Figure 35. Impact Location, Test SR-1

Figure 36. System Damage, Test SR-1

Figure 37. System Damage, Test SR-1

Figure 38. System Damage, Test SR-1

Figure 39. System Damage, Test SR-1

Figure 40. Vehicle Damage, Test SR-1

Figure 41. Vehicle Damage, Test SR-1

6 DESIGN CHANGES, TEST SR-2

Following a review of the vehicle behavior observed in test SR-1, four design modifications were discussed that would improve the safety performance of the system. The first proposed design modification incorporated a redesign of slot tabs in the nose section. A review of the downstream film of test SR-1 showed that the top slot tabs on the thrie beam did not tear during the impact. This prevented the top hump of guardrail and the top cable from separating from the bottom two humps. Consequently, the top hump of guardrail (and cable) did not effectively capture the pickup truck above the bumper. Redesigning the slot tabs to break more easily could improve the separation of the top hump of the thrie beam and improve capture of the pickup truck. This modification could be accomplished through sizing down the tabs to tear more easily or removing some of the tabs altogether. However, the slot tab redesign option was rejected by the researchers because changing the configuration would result in different patterns for the bullnose and short-radius guardrail systems, and it was desired to keep system components as similar as possible to reduce inventory.

A second option was the addition of single chamfered blockouts on post no. 1 on each side of the system. The addition of chamfered blockouts at post no. 1 could improve vehicle capture by allowing the bottom hump of the thrie beam to separate and slide under the bumper more easily as well as by holding the guardrail up longer during the impact event. This modification was also ruled out in order to make the system simpler by reducing the number of different blockout set ups used in the design.

A third option consisted of increasing the number of posts on the secondary side of the system. The original concept for the short radius developed during Phase I of this research employed an equal number of CRT posts in rail section no. 2 on each side of the system. This concept was

changed to the configuration used in test SR-1 based on the argument that making the secondary side of the system weaker would help counteract the anticipated yaw motion of the pickup truck. The results of test SR-1 showed that this did not happen. Instead, the right-front corner of the pickup truck was locked up by the guardrail. Subsequently, the stiff primary side of the system pushed on the front corner of the truck, thus increasing the yaw and roll of the pickup towards the primary side. The weaker secondary side did not counteract the yaw in this case, rather it allowed it to occur more easily. Increasing the number of posts on the secondary side of the system would stiffen the secondary side and help reduce the roll and yaw of the pickup truck. Additionally, analysis of the film from test SR-1 showed that the rail on the secondary side of the system began to lay back after the fracture of post no. 1S. In addition, the guardrail rode lower on the front of the truck near the secondary side of the system, resulting in uneven capture of the front of the pickup. Increasing the number of posts on the secondary side would allow the guardrail to more effectively contain and capture of the pickup truck. Lastly, the added posts on the secondary side of the system would serve to absorb additional energy. Based on these factors, two CRT posts were added to the secondary side of the system in rail section no 2. This change basically reduced the post spacing in rail section no. 2S to 953 mm.

The final design modification implemented in the system prior to test SR-2 was removal of the moat that was placed behind the system. The moat was removed since it added unnecessary complexity to the design problem and significantly increased the instability of the pickup truck during the impact. The modified short-radius guardrail system for test SR-2 is shown in Figure 42.

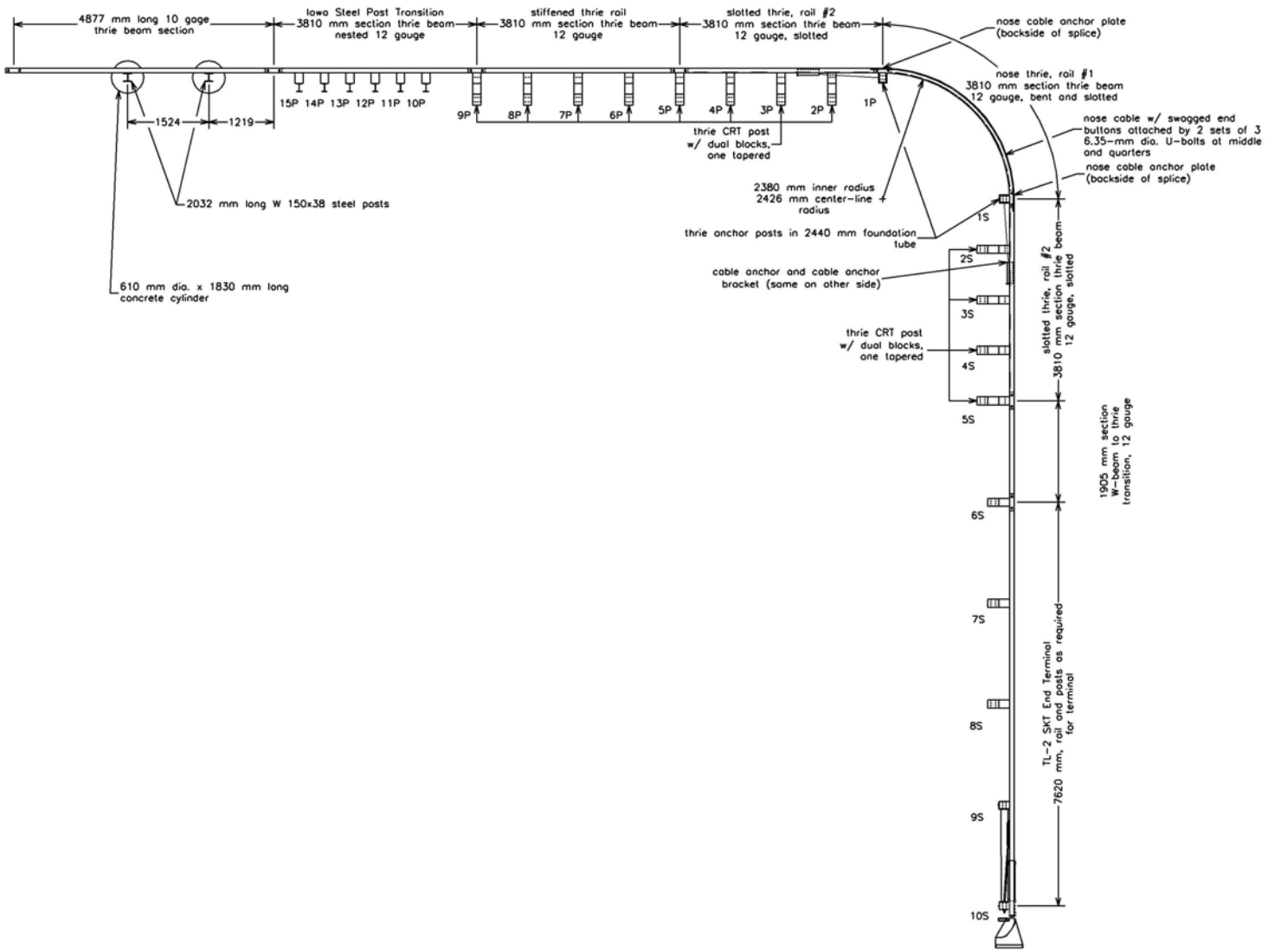

Figure 42. System Details, Test SR-2

7 CRASH TEST SR-2

7.1 Test SR-2

Test SR-2 was conducted according to NCHRP Report No. 350 Test Designation 3-33. The 2,014-kg pickup truck impacted the short-radius guardrail at a speed of 104.2 km/hr and at an angle of 16.1 degrees. The impact orientation for this test was the centerline of the pickup truck impacting the center of the curved nose section of the system. A summary of the test results and the sequential photographs are shown in Figure 43. Additional sequential photographs are shown in Figure 45. Documentary photographs of the crash tests are shown in Figures 46 through 49.

7.2 Test Description

The test vehicle impacted the curved section of the short-radius guardrail system, as shown in Figure 50. Upon impact, the front of the pickup truck began to deform the curved section of guardrail inward with the vehicle's front bumper impacting the middle hump of the thrie beam guardrail. As the vehicle deformed the nose of the system inward, the top and middle humps of guardrail were pushed above the bumper, and the bottom hump was pushed beneath the bumper and was rolled over by the left-front tire. At 0.080 sec after impact, post no. 1S was fractured as it was loaded by the deformed guardrail. As the vehicle moved forward, the thrie beam rail wrapped around the right-front corner of the pickup truck, causing the rail to bend around post no. 1P and fracture it at 0.080 sec. In addition, complete fracture of the middle hump of the thrie beam nose section was observed near the left-front corner of the pickup truck, but the nose cables remained positioned above the front bumper. At approximately 0.130 sec, post no. 2S fractured. As the pickup truck continued into the system, the guardrail on the primary side of the system bent around and was pulled downstream, and the guardrail on the secondary side of the system was pulled back at an

angle. The resulting loading, combined with the impact orientation of the pickup truck, caused the vehicle to begin to yaw to the right at approximately 0.150 sec. By 0.192 sec, post nos. 2P and 3S were fractured due to tension in guardrail as it was pulled downstream. The vehicle continued to yaw as it moved downstream becoming perpendicular to the primary side of the system at approximately 0.640 sec. At this point, the deflecting guardrail promoted the fracture of post nos. 3P through 8P and post no. 4S. After becoming perpendicular to the primary side of the system, the left side of the pickup truck lifted of the ground, and the right side of the pickup truck rolled over the thrie beam. Because the velocity of the vehicle at the time was minimal, the vehicle came to rest on its right side after rolling over the rail. The final position of the pickup truck was 6.8 m to the left of the primary side of the system and 8.6 m to the right of the secondary side of the system . The trajectory and final position of the pickup truck are shown in Figure 44.

7.3 System and Component Damage

Damage to the short-radius system was extensive, as shown in Figures 51 through 55. Post nos. 1S and 4S on the secondary side were fractured due to the guardrail on the secondary side being pulled towards the middle of the system. Post no. 5S pulled out of the ground but was not fractured. Rail section no. 2 on the secondary side of the system was bent around the post and blockout at post no. 6S. The nose section of guardrail, rail section no. 1, displayed completely torn slot tabs along the bottom set of slots in the rail. In addition, the top and middle humps of the thrie beam were completely torn near the start of the secondary side of the system. The nose cables of the system remained attached to the guardrail by the anchor plates. On the primary side of the system, post nos. 1P through 8P were fractured, while post no. 9P was deflected in the soil. Rail section no. 2 on the primary side was bent around post no. 9P and twisted due to the vehicle rolling over it.

7.4 Vehicle Damage

Vehicle damage was extensive, as shown in Figure 56. Damage due to the impact with the system was difficult to separate from damage due to rollover. The frontal area of the vehicle, including the bumper, radiator, and headlights, was crushed inward due to the impact with the system. The front grill was detached, and the front of the hood was bent. The front fenders of the pickup truck displayed some deformation and crushing. Little or no damage was observed to the undercarriage of the vehicle. A slight bend in the frame rail was observed behind the right-front wheel. The right side of the box of the pickup truck was crushed inward due to rollover. The right-front tire of the pickup truck was cut and deflated.

The damage observed to the interior occupant compartment was minor. Complete occupant compartment deformation measurements were not taken after test SR-2 due to the rollover of the test vehicle.

7.5 Occupant Risk Values

The longitudinal occupant impact velocity (OIV) was determined to be 7.18 m/s. The maximum 0.010-sec average occupant ridedown deceleration (ORD) in the longitudinal direction was 7.05 g's. The lateral occupant impact velocity (OIV) was determined to be 2.94 m/s. The maximum 0.010-sec average occupant ridedown deceleration (ORD) in the lateral direction was 8.51 g's. It is noted that the occupant impact velocities and the occupant ridedown decelerations were within the suggested limits provided in NCHRP Report No. 350. The results of the occupant risk data are summarized in Figure 43. Results are shown graphically in Appendix B. The results from the rate transducer also shown graphically in Appendi

7.6 Discussion

Following test SR-2, a safety performance evaluation was conducted, and the short-radius guardrail was determined to be unacceptable according to the NCHRP Report No. 350 criteria. The test article did not safely contain, redirect, or bring the vehicle to a controlled stop. Detached elements and debris from the test article did not penetrate nor show potential for penetrating the occupant compartment or present undue hazard to the other traffic, pedestrians, or personnel in the work zone. Deformations of, or intrusion into, the occupant compartment did not occur. The vehicle did not remain upright during and after the collision. The vehicle's trajectory did not intrude into adjacent traffic lanes. The occupant impact velocities and ridedown accelerations were within the suggested limits imposed by NCHRP Report No. 350.

The failure of test SR-2 to meet the safety performance criteria was directly attributed to the rollover of the pickup truck. Analysis of the data from the test and the high-speed film suggested that the rollover was due to a combination of factors. First, the vehicle displayed sufficient yaw during the impact to place it perpendicular to the primary roadway side of the system prior to rollover. Second, debris from the fractured posts and guardrail gathered in front of the right side of the vehicle as the impact progressed. It was believed that the combination of the yaw of the vehicle and the debris collected along the right side caused the vehicle to trip and rollover the thrie beam guardrail.

Based on the results of this test, the researchers decided to run a modified version of NCHRP Report No. 350 test designation no. 3-31 on the same short-radius guardrail system in order to examine the behavior of the system under different impact conditions. No changes were to be made to the system until the results from the new impact condition were known.

0.000 sec | 0.079 sec | 0.172 sec | 0.313 sec | 0.404 sec

- Test Number SR-2
- Date 5/1/01
- Test Article
  - Type . . . . . Short-Radius Guardrail
  - Key Elements . . . . . One 3,810-mm long curved and slotted thrie beam guardrail section
    Two 3,810-mm long straight thrie beam guardrail sections
    16 breakaway posts
    SKT End Terminal
    Iowa steel post transition
  - Orientation . . . . . Centerline truck with center of curved nose
- Soil Type . . . . . Grading B - AASHTO M 147-65 (1990)
- Vehicle Model . . . . . 1994 Chevy C2500 pickup truck
  - Curb . . . . . 2,009 kg
  - Test Inertial . . . . . 2,014 kg
  - Gross Static . . . . . 2,014 kg
- Vehicle Speed
  - Impact . . . . . 104.2 km/hr
  - Exit . . . . . NA
- Vehicle Angle
  - Impact . . . . . 16.1 deg
  - Exit . . . . . NA
- Vehicle Stability . . . . . Satisfactory
- Occupant Ridedown Deceleration (10 msec avg.)
  - Longitudinal . . . . . 7.05 g's < 20g's
  - Lateral (not required) . . . . . 8.51 g's < 20g's
- Occupant Impact Velocity (Normalized)
  - Longitudinal . . . . . 7.18 m/s < 12 m/s
  - Lateral (not required) . . . . . 2.94 m/s < 12m/s
- Vehicle Damage
  - TAD[20] 12-FD-3
    . . . . . 3-R&T-2
  - SAE[21] 12FDEW2
    . . . . . 03RDEW2
- Vehicle Stopping Distance . . . . . 6.8 m left of primary side
  8.6 m right of secondary side
- Test Article Damage . . . . . Extensive
- Maximum Deflections
  - Permanent Set . . . . . NA
  - Dynamic . . . . . NA

Figure 43. Summary of Test Results and Sequential Photographs, Test SR-2

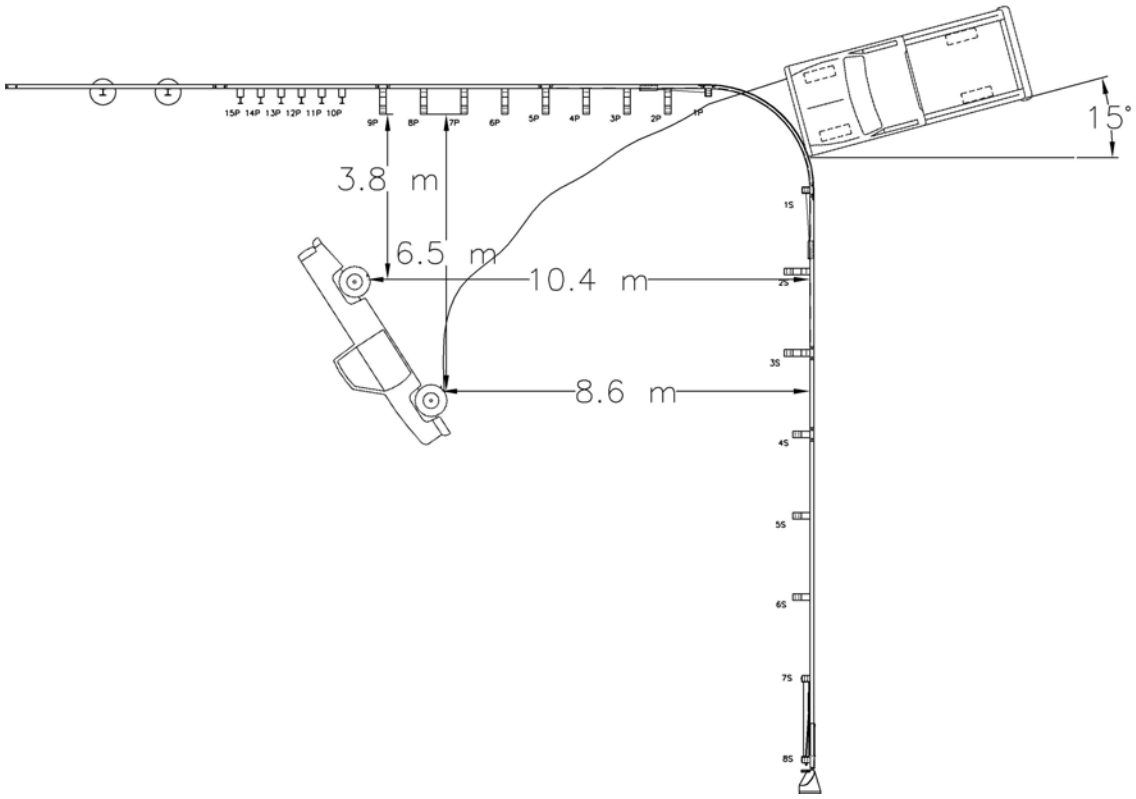

Figure 44. Vehicle Trajectory, Test SR-2

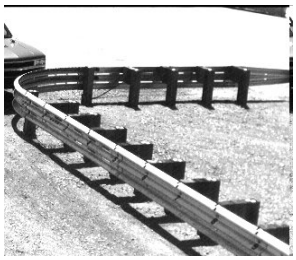

0.000 sec

0.000 sec

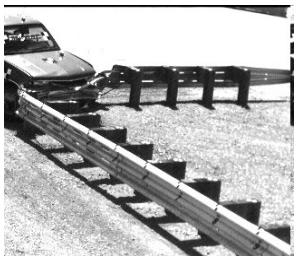

0.060 sec

0.110 sec

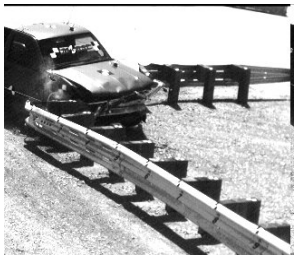

0.122 sec

0.176 sec

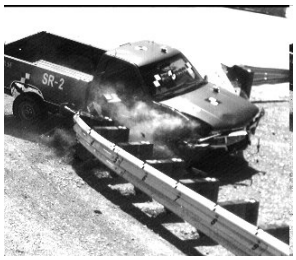

0.230 sec

0.368 sec

0.378 sec

0.906 sec

Figure 45. Additional Sequential Photographs, Test SR-2

Figure 46. Documentary Photographs, Test SR-2

Figure 47. Documentary Photographs, Test SR-2

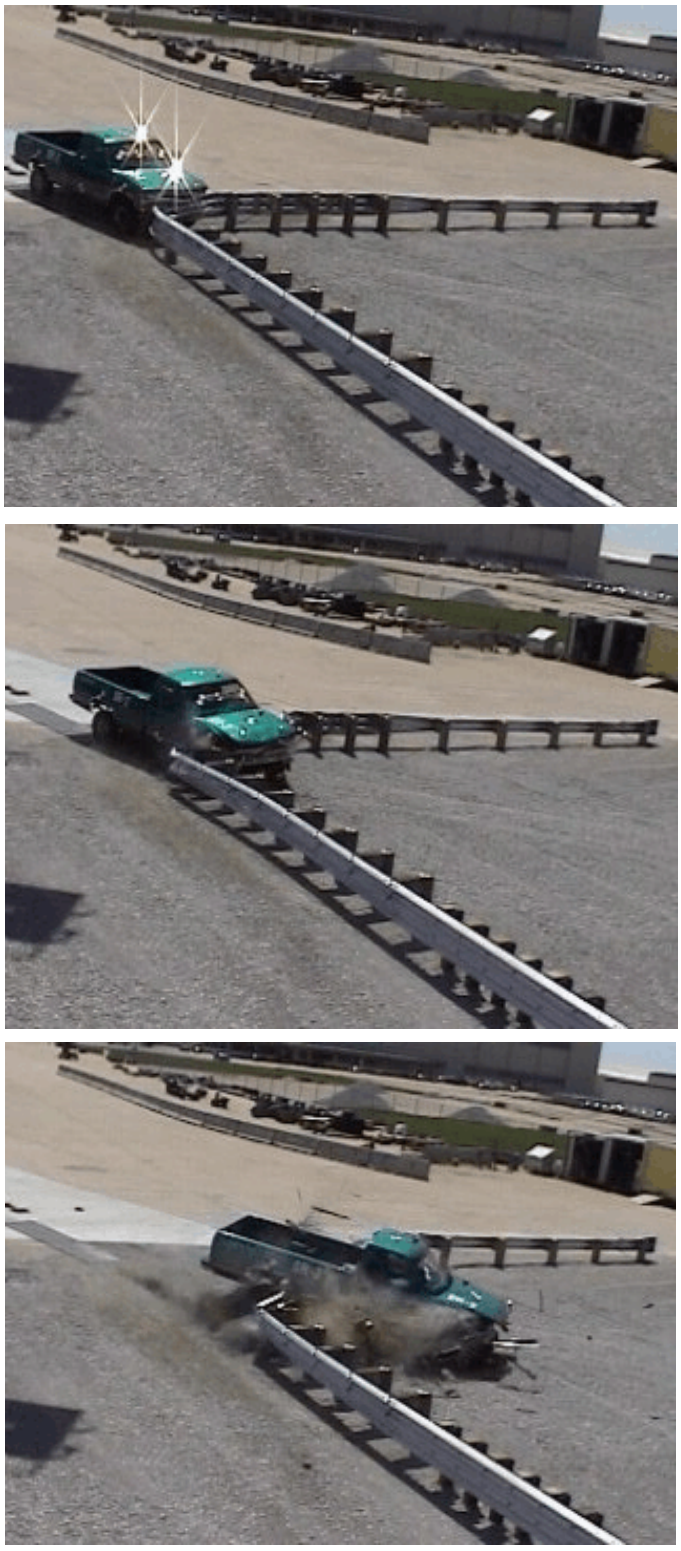

Figure 48. Documentary Photographs, Test SR-2

Figure 49. Documentary Photographs, Test SR-2

Figure 50. Impact Location, Test SR-2

Figure 51. System Damage, Test SR-2

Figure 52. System Damage, Test SR-2

Figure 53. System Damage, Test SR-2

Figure 54. System Damage, Test SR-2

Figure 55. System Damage, Test SR-2

Figure 56. Vehicle Damage, Test SR-2

8 CRASH TEST SR-3

8.1 Test SR-3

Test SR-3 was conducted as a modified version of NCHRP Report No. 350 Test Designation 3-31. In test 3-31, a 2,000-kg pickup truck would impact the centerline of the nose of the barrier at 100 km/hr and at an angle of 0 degrees. In reviewing this impact condition and the geometry of the system, the researchers decided that a more critical impact location would exist with the centerline of the pickup truck directly aligned with the primary side of the system. Therefore, the impact conditions in this test were modified to force the vehicle to impact with the centerline of the pickup truck on the centerline of post no. 1P on the primary side. The 2,036-kg pickup truck impacted the short-radius guardrail at a speed of 102.9 km/hr and at an angle of 0.9 degrees. A summary of the test results and the sequential photographs are shown in Figure 57. Additional sequential photographs are shown in Figure 59. Documentary photographs of the crash tests are shown in Figures 60 through 62.

8.2 Test Description

The test vehicle impacted the curved section of the short-radius guardrail, as shown in Figure 63. Upon impact, the front of the pickup truck began to deform the curved section of guardrail inward with the vehicle's front bumper pushing in between the top two humps of the thrie beam guardrail. As the bumper slid through the slots in the guardrail, several of the slot tabs between the top and middle humps were torn. The top hump of guardrail then moved above the bumper, while the middle and bottom humps were pushed beneath the bumper and were rolled over by the left-front tire. At 0.078 sec after impact, the pickup truck impacted and fractured post no. 1P. As the vehicle moved forward past post no. 1P, the thrie beam guardrail was buckled inward towards the middle

of the system and ahead of the pickup truck. By 0.098 sec, guardrail section no. 2 on the primary side stopped buckling ahead of the vehicle, and instead began to flex outward. Without the guardrail buckling, the loading of the guardrail on the front of the truck increased significantly. Consequently, the deformation to the front of the vehicle was significantly increased. The vehicle continued to move down the center of the primary side of the system and impacted and fractured post no. 2P at 0.114 sec. By 0.124 sec, guardrail section no. 1, now on the left side of the vehicle, was pulled tight across the front of the pickup truck, and the top hump of the thrie beam guardrail was ruptured. However, the cable remained intact after the rupture of the guardrail and locked above the front bumper of the vehicle. In addition, guardrail section no. 2 on the primary side was moving toward the ground, and the top of the rail was rotating away from the posts. This caused the front of the pickup truck to pitch down toward the ground as well. At 0.148 sec, the pickup truck impacted and fractured post no. 3P. Definite flex between the box and the cab of the truck was visible and likely due to the pitch and deceleration of the vehicle. At 0.174 sec, the top nose cable pulled through the cable plate which anchored it at post no. 1S. By 0.224 sec, the pickup truck impacted and fractured post no. 4. Shortly afterward, the guardrail in front of post no. 5P was pushed down toward the ground ahead of the vehicle. The pickup truck then began to roll to the right and yaw counterclockwise. By 0.345 sec, only the right-front corner pickup truck remained in contact with the ground as the truck continued to yaw and roll. At 0.594 sec, the vehicle was completely off of the ground and on its side in the air. The right-front corner of the truck bed landed on the primary side guardrail near post no. 9P at 1.024 sec, causing the truck bed to deform. The pickup truck then began to roll onto its top. By 1.290 sec, both sides of the pickup truck bed were on top of the guardrail and the top of the truck was on the ground. The vehicle continued to roll until it landed

back on its wheels with the rear of the truck still propped up on the primary side guardrail. The final position of the pickup truck was 10.6-m downstream and 0.8 m to the left of post no. 1P. The trajectory and final position of the pickup truck are shown in Figure 58.

8.3 System and Component Damage

Damage to the short-radius guardrail system was extensive, as shown in Figures 64 through 66. Post nos. 1S and 2S on the secondary side were fractured due to the guardrail on the secondary side being pulled towards the middle of the system. Post nos. 3S and 4S displayed significant deflection but were not fractured. Rail section no. 2 on the secondary side of the system was bent around the post and blockout at post no. 3S. Damage was more severe to both the nose section and the primary side of the system. The curved radius, rail section no. 1, displayed torn slot tabs along both the top and bottom set of slots in the rail. The top hump of the section was completely ruptured 864-mm downstream of post no. 1S. Other minor tearing of rail section no. 1 was observed near the guardrail splice at post no. 1P. The top nose cable of the system detached on the secondary side by pulling the button ferrule through the cable anchor plate. On the primary side of the system, post nos. 1P through 5P were fractured, while post no. 6P was partially fractured. Rail section no. 2 on the primary side was severely buckled and crushed. The crushing of rail section no. 2 was evident from the beginning of the section to approximately post no. 6P. Post no. 9P displayed damage to the top of the post and minor deflection due to the pickup truck landing on it as it rolled.

8.4 Vehicle Damage

Vehicle damage was extensive, as shown in Figures 67 and 68. Damage due to the impact with the system was difficult to separate from damage due to rollover. The frontal area of the vehicle, including the bumper, radiator, and headlights, was crushed inward due to the impact with

the system. The majority of this frontal crush damage was due to the impact with the posts along the centerline of the vehicle and crushing of the guardrail along the primary side of the system. The front grill was detached, and the front of the hood was bent slightly. The front fenders of the pickup truck were deformed and dented. The front suspension on the right side of the vehicle was damaged due to the disengagement of the tie rod. The left-front tire of the pickup truck was knocked of the rim, and both of the front tires were deflated. The left-front corner of the cab of the pickup truck was crushed inward due to the rollover, and the windshield glass was broken in that area as well. The bed of the pickup truck was severely deformed. Large dents and deformation were seen near the front of the bed on the right side and in between the wheel well and the end of the truck box on the left side.

Damage to the interior occupant compartment of the vehicle was minimal. Deformations of both the floor pan and the dash were also observed. Maximum vertical deflections of 44 mm were measured at two locations on the driver-side floor pan. A maximum lateral deflection of 38 mm was measured near the front of the passenger-side floor plan. A maximum longitudinal deflection of 25 mm was measured on the hump in the middle of the floor plan. Maximum deflection of the dashboard was measured to be 13 mm in the longitudinal direction. These occupant compartment deformations were not sufficient to cause concern with regards to occupant safety. Complete occupant compartment deformation details are given in Appendix C.

8.5 Occupant Risk Values

The longitudinal occupant impact velocity (OIV) was determined to be 8.83 m/s. The maximum 0.010-sec average occupant ridedown deceleration (ORD) in the longitudinal direction was 12.21 g's. The lateral occupant impact velocity (OIV) was determined to be 1.30 m/s. The

maximum 0.010-sec average occupant ridedown deceleration (ORD) in the lateral direction was 8.01 g's. It is noted that the occupant impact velocities and the occupant ridedown decelerations were within the suggested limits provided in NCHRP Report No. 350. The results of the occupant risk data are summarized in Figure 57. Results are shown graphically in Appendix C. The results from the rate transducer are also shown graphically in Appendix C.

8.6 Discussion

Following test SR-3, a safety performance evaluation was conducted, and the short-radius guardrail was determined to be unacceptable according to the NCHRP Report No. 350 criteria. The test article did not safely contain, redirect, or bring the vehicle to a controlled stop. Detached elements and debris from the test article did not penetrate nor show potential for penetrating the occupant compartment or present undue hazard to the other traffic, pedestrians, or personnel in the work zone. Deformations of, or intrusion into, the occupant compartment did not occur. The vehicle did not remain upright during and after the collision. The vehicle's trajectory did not intrude into adjacent traffic lanes. The occupant impact velocities and ridedown accelerations were within the suggested limits imposed by NCHRP Report No. 350.

The failure of test SR-3 to meet the safety performance criteria was directly attributed to the rollover of the pickup truck. The rollover of the truck was believed to be caused by a combination of factors. First, the impact of the vehicle into the guardrail and closely spaced breakaway posts along the primary side of the system caused very rapid deceleration of the pickup truck. Second, the orientation of the impact caused the short-radius system to capture only the left side of the impacting vehicle, and therefore, an uneven loading was created on the front of the pickup truck. Third, guardrail section no. 2 on the primary side did not buckle in front of the vehicle, but it was crushed

and bunched up directly in front of the right-front corner of the pickup truck. Finally, the left-front side of the pickup truck did not interlock effectively with the guardrail during impact. Only the top hump of the thrie beam guardrail and the top nose cable captured the vehicle above the bumper, and this capture was lost when the top nose cable pulled through the cable plate. In addition, with only the top hump and nose cable above the bumper, the middle hump and lower nose cable were unable to disengage and allow the guardrail to feed past the lap splice at post no. 1P. Thus, the vehicle was forced to push through the splice rather than having the guardrail feed smoothly. These factors combined to cause the vehicle to pitch forward and roll to the right about its right-front corner. This led to the vehicle cartwheeling into the air and rolling over.

As a result of this failed test, design changes were deemed necessary in order to allow for the successful containment or redirection of the pickup truck.

0.000 sec

0.092 sec

0.230 sec

0.452 sec

1.042 sec

- Test Number SR-3
- Date 10/24/01
- Test Article
  - Type . . . . . Short-Radius Guardrail
  - Key Elements . . . . . One 3,810-mm long curved and slotted thrie beam guardrail section
    Two 3,810-mm long straight thrie beam guardrail sections
    14 breakaway posts
    SKT End Terminal
    Iowa steel post transition
  - Orientation . . . . . Centerline truck with centerline post no. 1P
- Soil Type . . . . . Grading B - AASHTO M 147-65 (1990)
- Vehicle Model . . . . . 1995 Ford F250 pickup truck
  - Curb . . . . . 2,000 kg
  - Test Inertial . . . . . 2,036 kg
  - Gross Static . . . . . 2,036 kg
- Vehicle Speed
  - Impact . . . . . 102.9 km/hr
  - Exit . . . . . NA
- Vehicle Angle
  - Impact . . . . . 0.9 deg
  - Exit . . . . . NA
- Vehicle Stability . . . . . Satisfactory
- Occupant Ridedown Deceleration (10 msec avg.)
  - Longitudinal . . . . . 12.21 g's < 20 g's
  - Lateral (not required) . . . . . 8.01 g's < 20 g's
- Occupant Impact Velocity (Normalized)
  - Longitudinal . . . . . 8.83 m/s < 12 m/s
  - Lateral (not required) . . . . . 1.30 m/s < 12 m/s
- Vehicle Damage
  - TAD[20] 12-FC-6
    . . . . . L&T/R&T-4
  - SAE[21] 12FCEN3
    . . . . . 00TDDO3
- Vehicle Stopping Distance . . . . . 10.6 m downstream
  0.80 m right
- Test Article Damage . . . . . Extensive
- Maximum Deflections
  - Permanent Set . . . . . NA
  - Dynamic . . . . . NA

Figure 57. Summary of Test Results and Sequential Photographs, Test SR-3

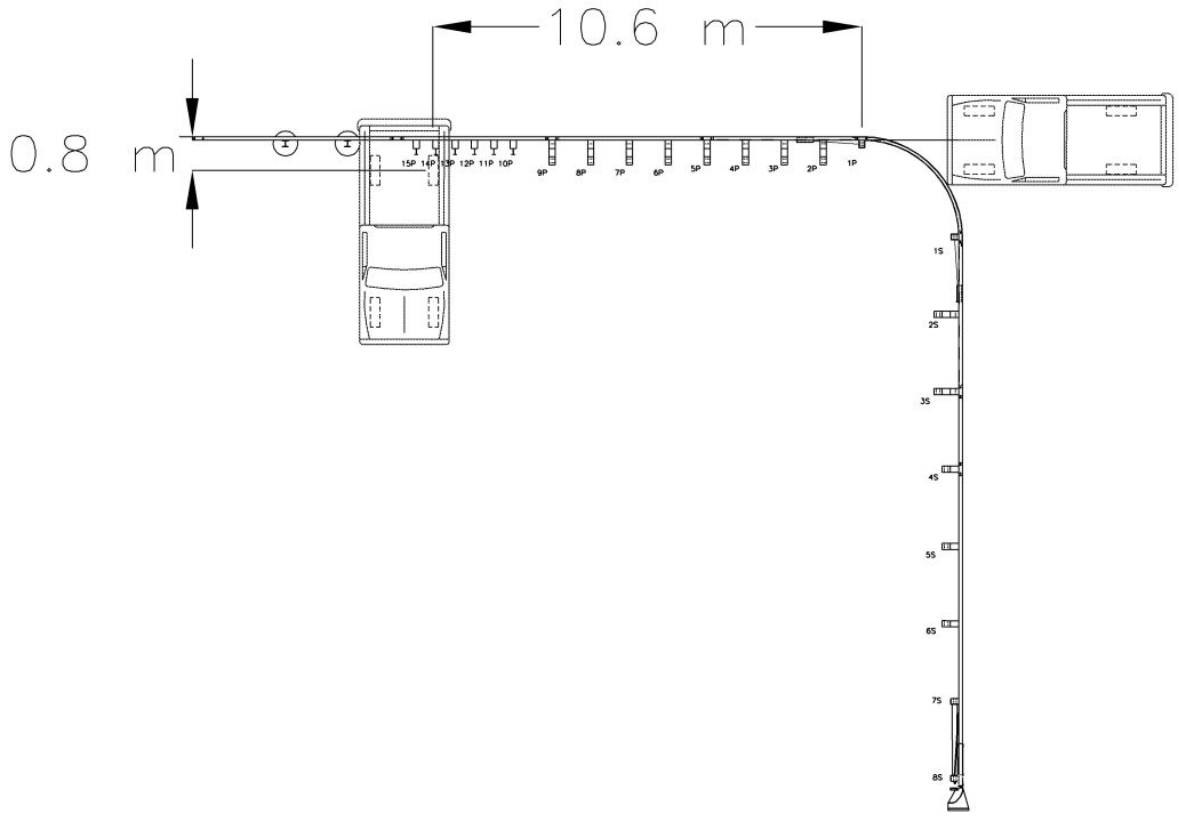

Figure 58. Vehicle Trajectory, Test SR-3

0.034 sec

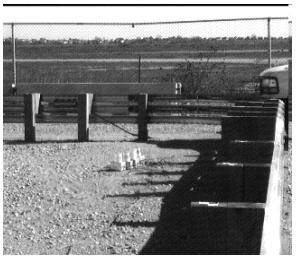

0.000 sec

0.114 sec

0.072 sec

0.228 sec

0.122 sec

0.296 sec

0.178 sec

0.506sec

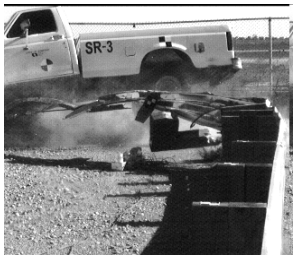

0.288 sec

Figure 59. Additional Sequential Photographs, Test SR-3

Figure 60. Documentary Photographs, Test SR-3

Figure 61. Documentary Photographs, Test SR-3

Figure 62. Documentary Photographs, Test SR-3

Figure 63. Impact Location, Test SR-3

Figure 64. System Damage, Test SR-3

Figure 65. System Damage, Test SR-3

Figure 66. System Damage, Test SR-3

Figure 67. Vehicle Damage, Test SR-3

Figure 68. Vehicle Damage, Test SR-3

9 DESIGN MODIFICATIONS, TEST SR-4

The failure of the short-radius guardrail system to safely contain or redirect the vehicle during test nos. SR-2 and SR-3 demonstrated the need for additional design modifications in order to improve its safety performance. A review of the prior test results led to three design modifications for test SR-4.

The first modification consisted of a redesign of the primary roadway side in order to improve the ability of the system to capture and gradually decelerate the vehicle for impacts on the nose of the system but without compromising the safe redirection of the vehicle along the primary side. Redesign of the primary side consisted of the addition of a parabolic flare and the addition of one more section of 3,810-mm long, 12 gauge thrie beam, as shown in Figures 69 and 70. The additional section of thrie beam was supported by four new CRT posts with double, chamfered blockouts similar to those used throughout the system. Following this modification, a total of thirteen breakaway posts were located on the primary side of the system. Rail section nos. 3P and 4P were given slots in the valleys of the thrie beam similar to those used in rail section no. 2.

There were several advantages to the redesign of the primary side of the short-radius guardrail system. First, it was believed that the use of the additional guardrail section would give the system more stroke to absorb energy and safely decelerate those vehicles impacting on the nose of the short-radius system but parallel to the primary side. It was also believed that the parabolic flare and the additional slotted rail sections would allow for easier buckling of the guardrail ahead of the vehicle during impacts similar to test SR-3, thus preventing the high loads and the vehicle vaulting observed in that test.

The second design modification to the short-radius system was to raise the entire system 51

mm. This modification positioned the top of the thrie beam at 854 mm and the top of the W-beam at 756 mm. In order to accommodate the new guardrail height, BCT post nos. 1S and 1P were made 51 mm longer in order to keep the holes at the proper height. The remaining posts in the system were left unchanged and simply installed with 51 mm less embedment. The system height was increased in order to improve vehicle capture by forcing the top two humps of thrie beam and the corresponding nose cables to engage the vehicle above the bumper. In addition, forcing the top humps and both cables above the bumper would allow the bottom section of the rail to tear away and prevent the vehicle from having to push through the guardrail splice, as was observed in test SR-3. Although the researchers recognized that the increased system height would result in compatibility problems with regards to attachment to existing guardrail and bridge rail designs, theses issues were not addressed at this time.

The final design modification consisted of increasing the capacity of the cable plate used to secure the nose cables at post nos. 1S and 1P. During test SR-3, the button ferrule on the top nose cable pulled through the space between the cable plate and the guardrail due to the combination of the high tensile loads on the cable and the deformation of the cable plate and adjacent guardrail. The thickness of the cable plate was increased from 4.76 mm to 6.35 mm. The change in plate thickness provided increased bending capacity as well as resulted in a reduced clearance between the cable plate and the guardrail, thus making it more difficult for the button ferrule to pull through the connection.

Details and photographs of the modified short-radius system for use in test SR-4 are shown in Figures 69 through 84.

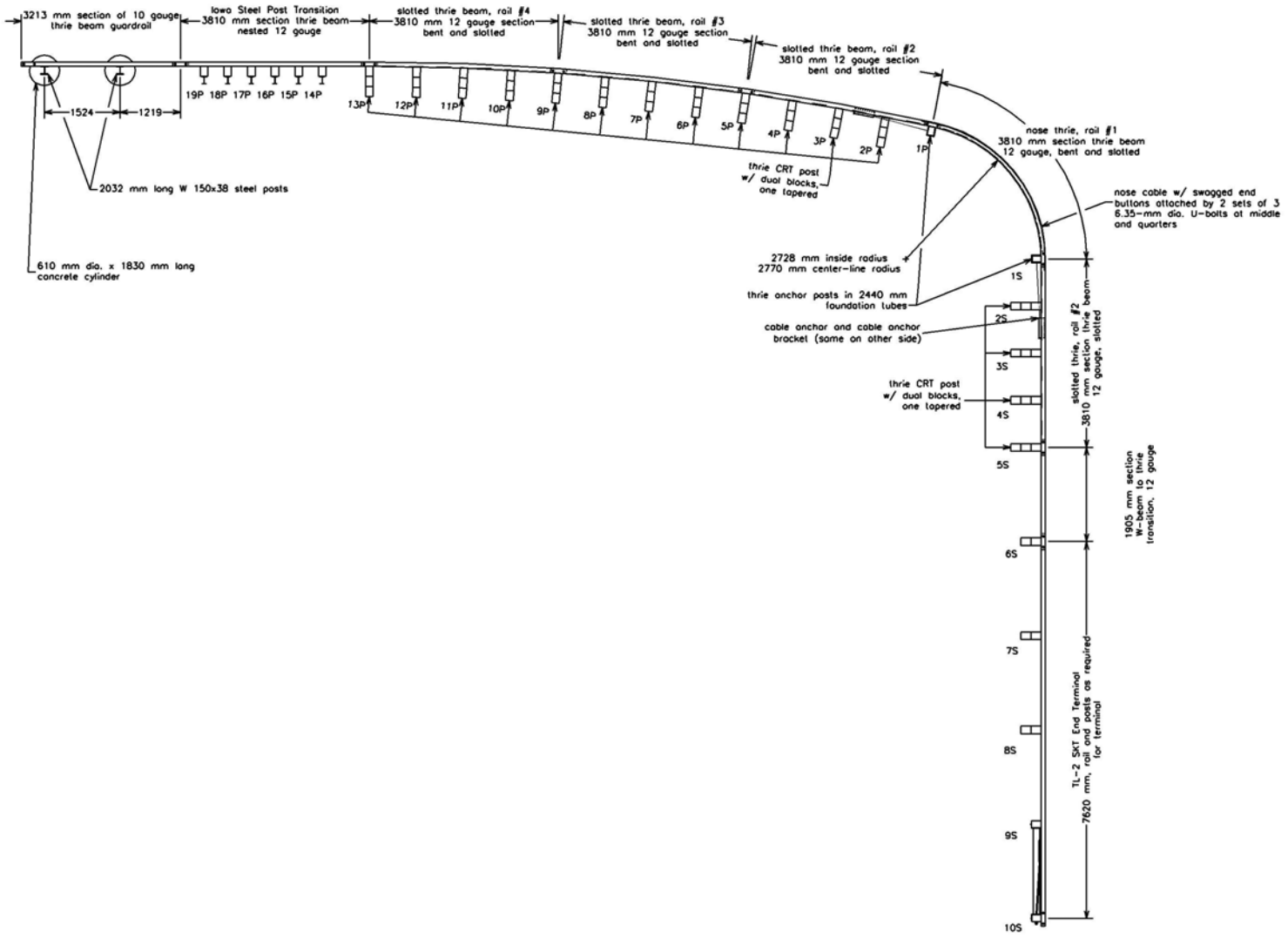

Figure 69. Overall System Layout, Test SR-4

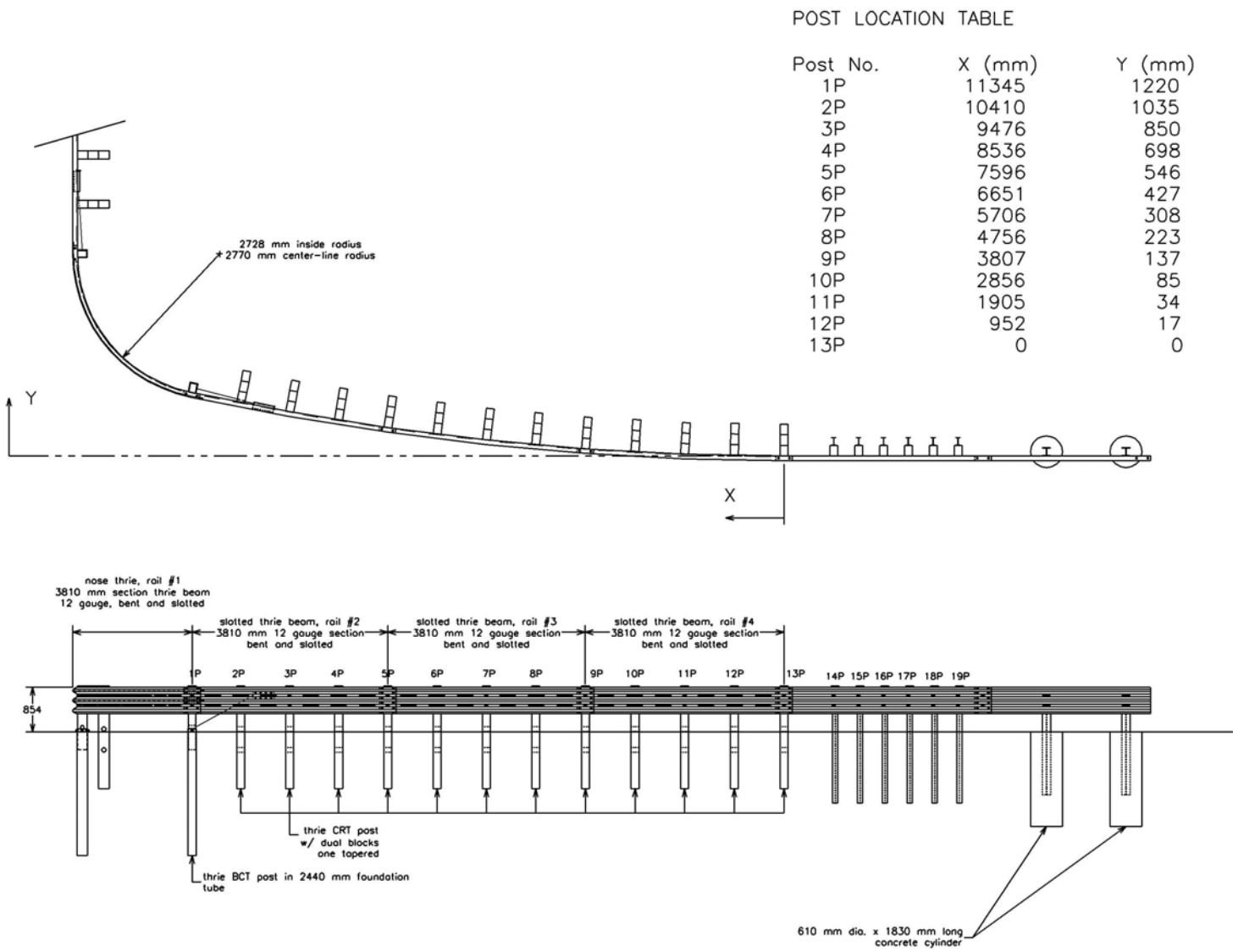

Figure 70. Primary Side System Layout, Test SR-4

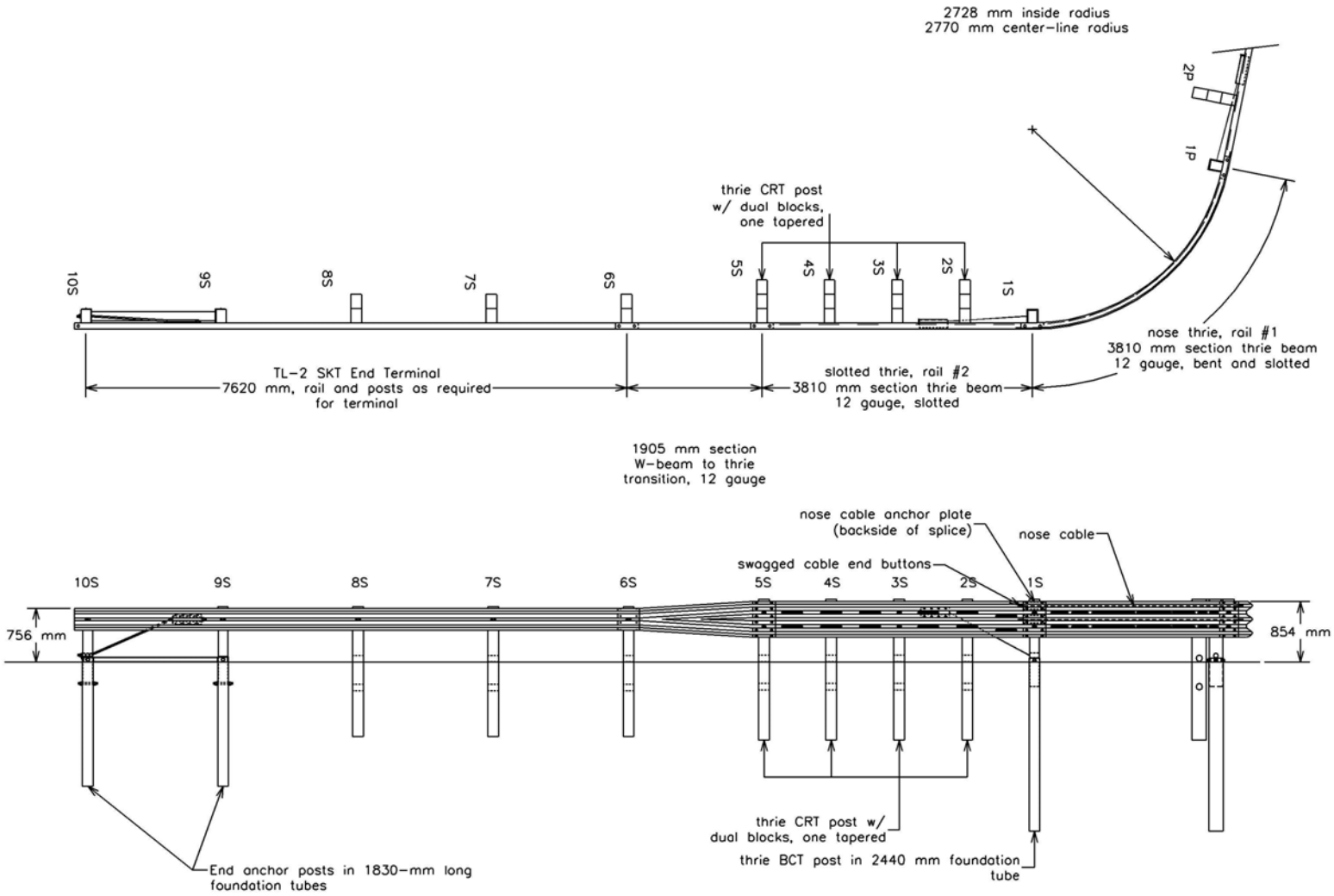

Figure 71. Secondary Side System Layout, Test SR-4

Rail Section 1 ("Nose" Section)

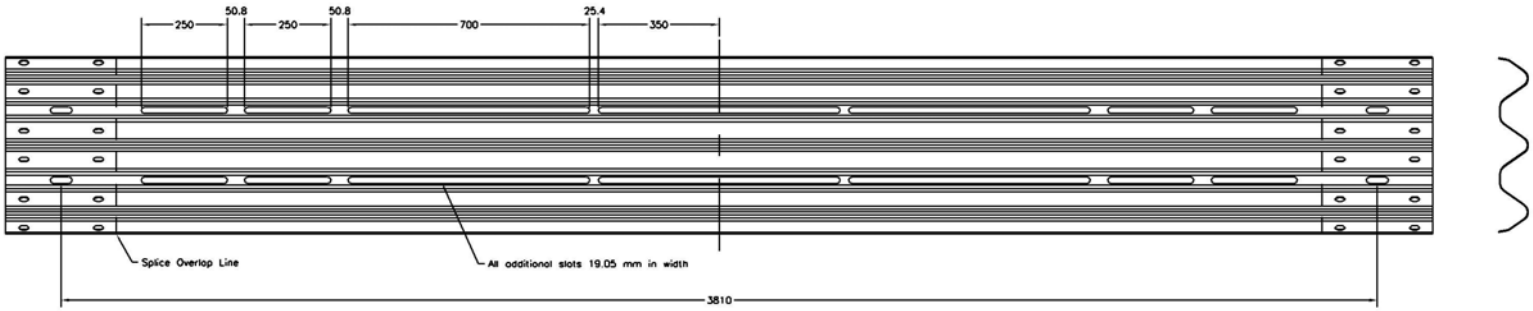

Rail Section 1 ("Nose" Section)

Note: All units are in mm unless specifed otherwise

Figure 72. System Details, Test SR-4

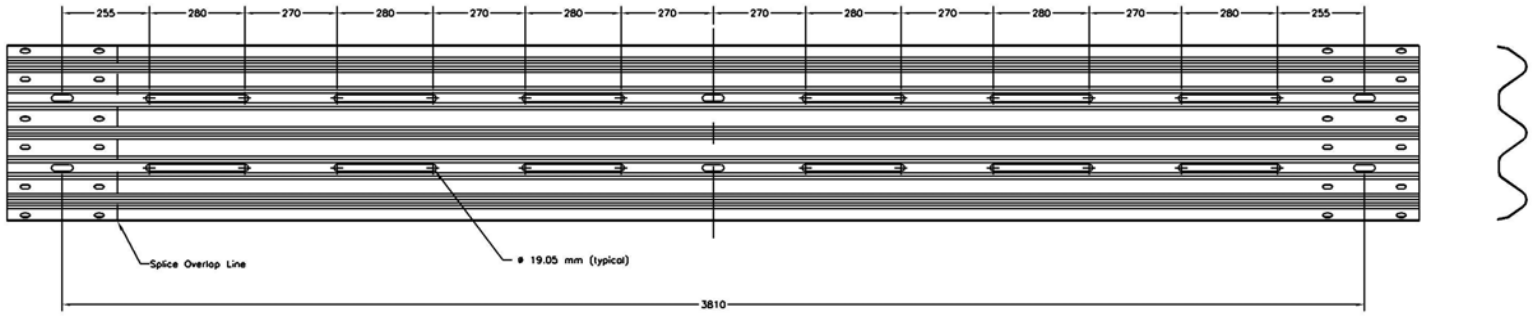

Rail Section 2

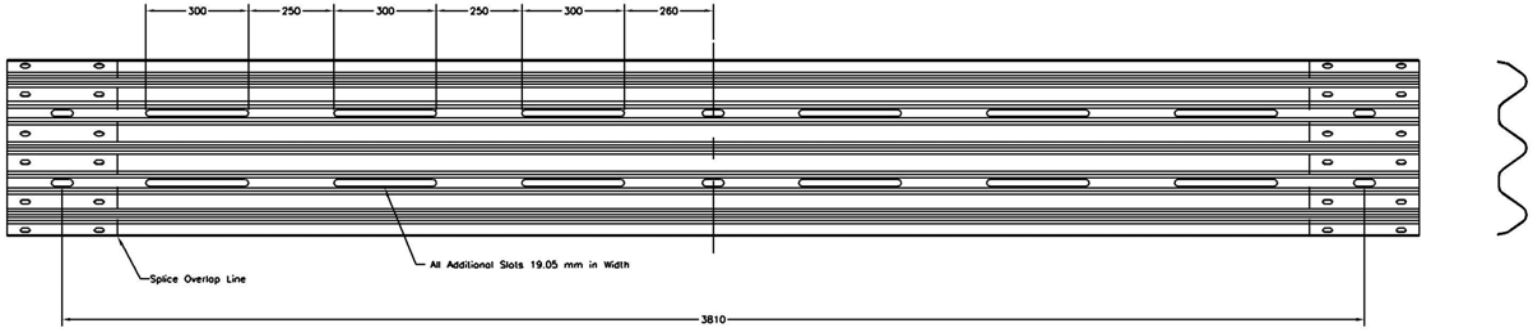

Rail Section 2

Note: All units are in mm unless specified otherwise

Figure 73. System Details, Test SR-4

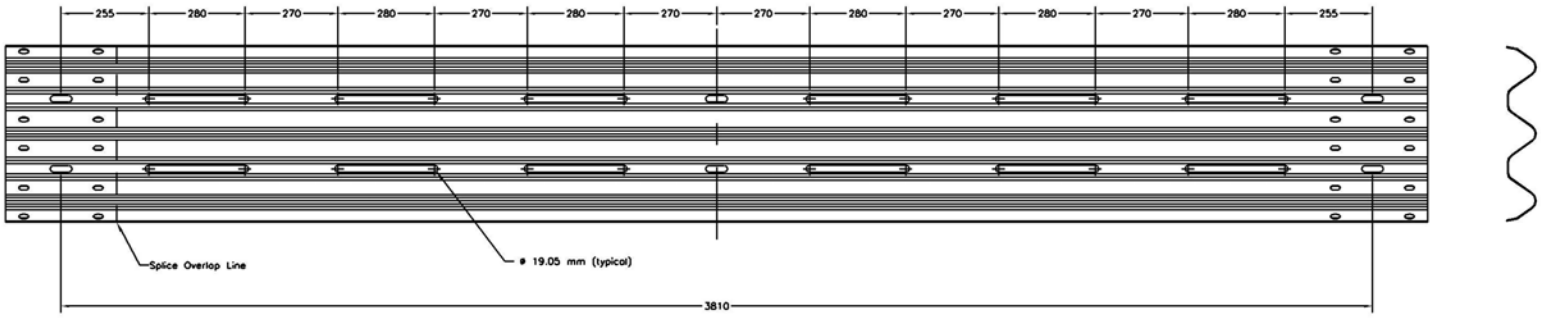

Rail Section 3 on Primary Side

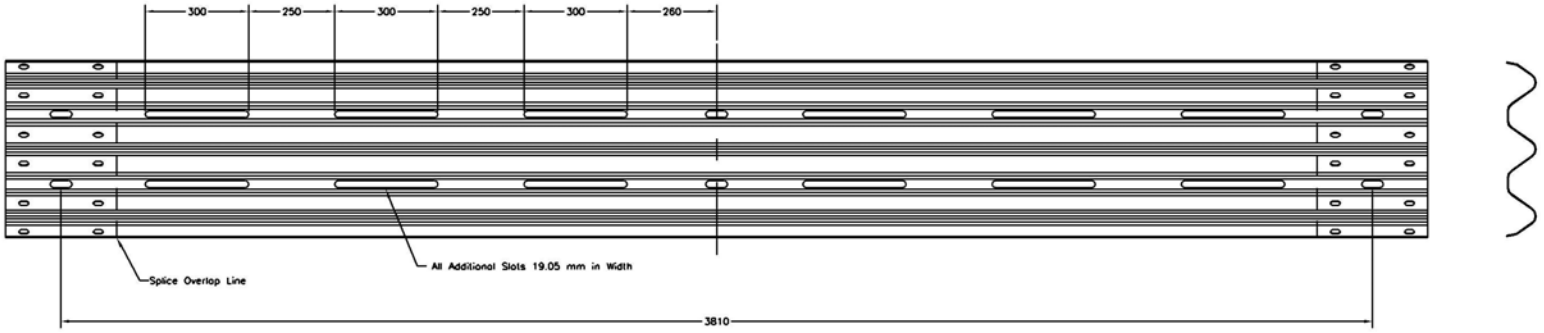

Rail Section 3 on Primary Side

Note: All units are in mm unless specified otherwise

Figure 74. System Details, Test SR-4

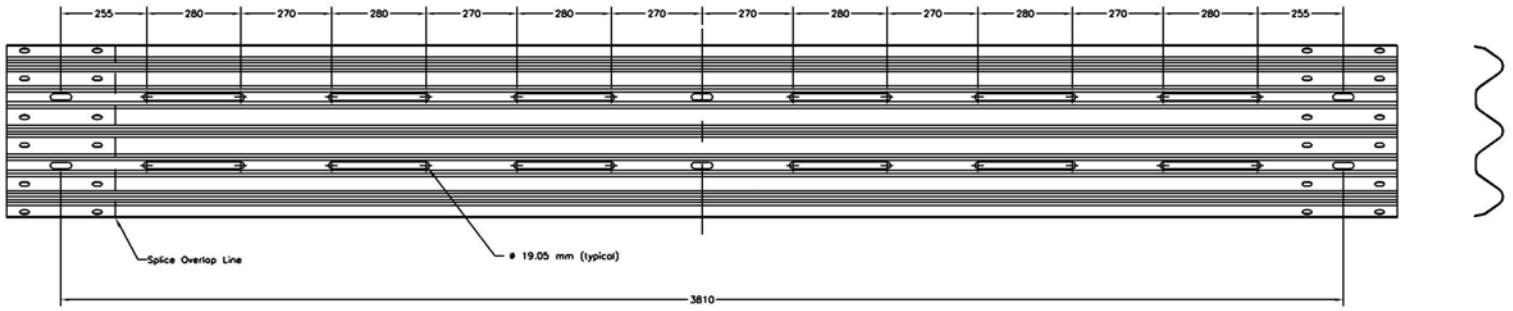

Rail Section 4 – Primary Side

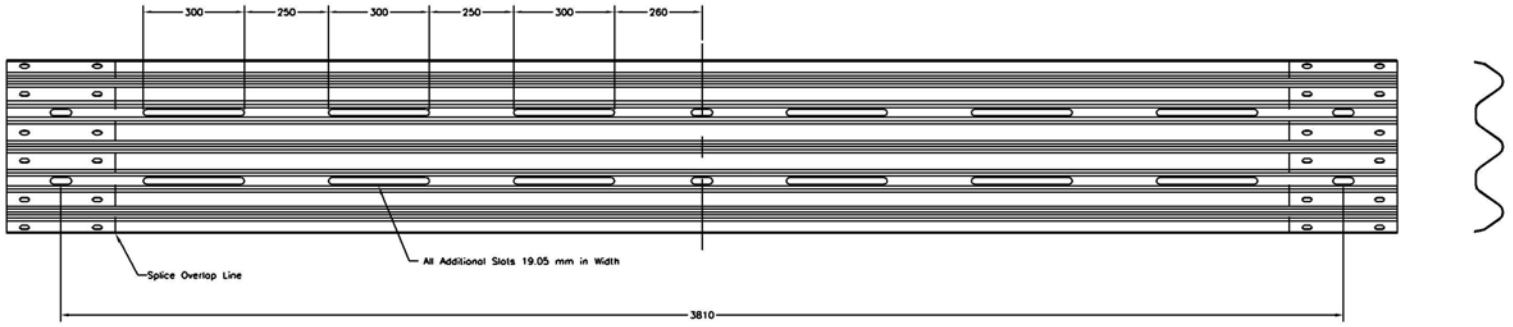

Rail Section 4 – Primary Side

Note: All units are in mm unless specified otherwise

Figure 75. System Details, Test SR-4

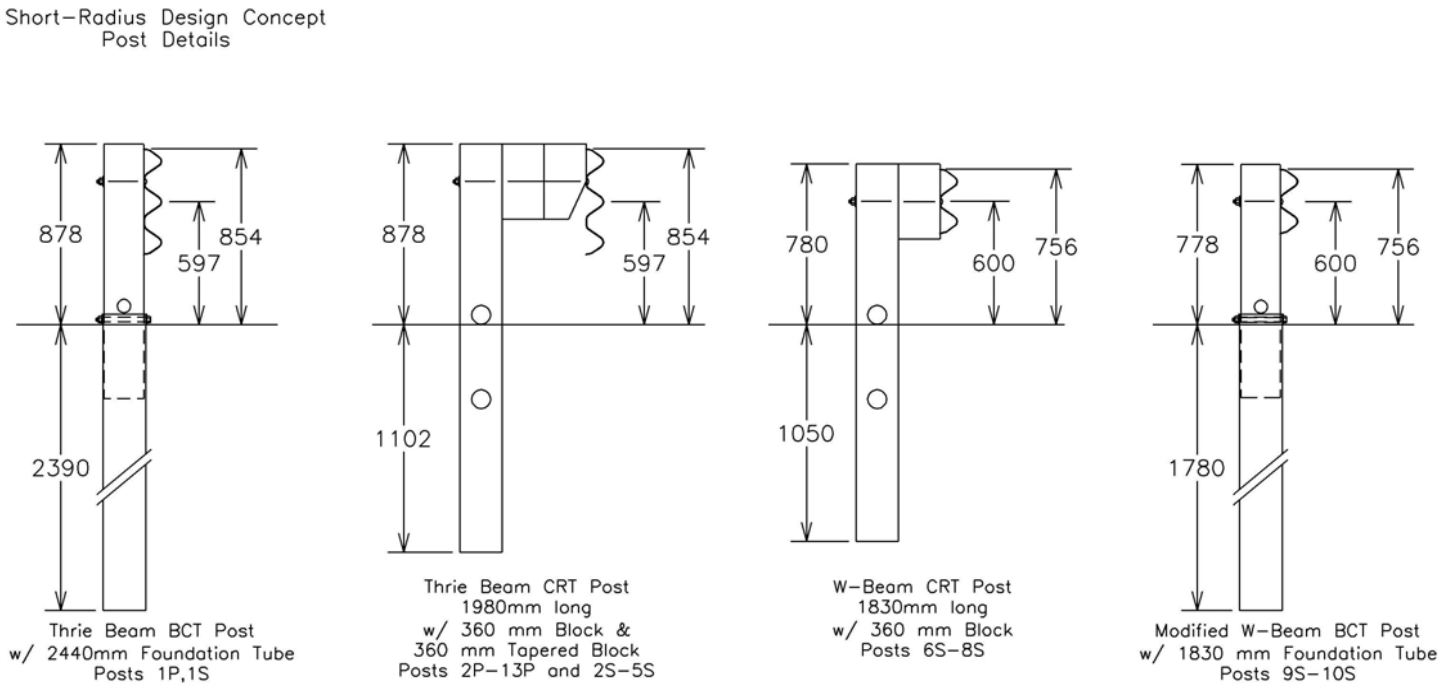

Figure 76. System Details, Test SR-4

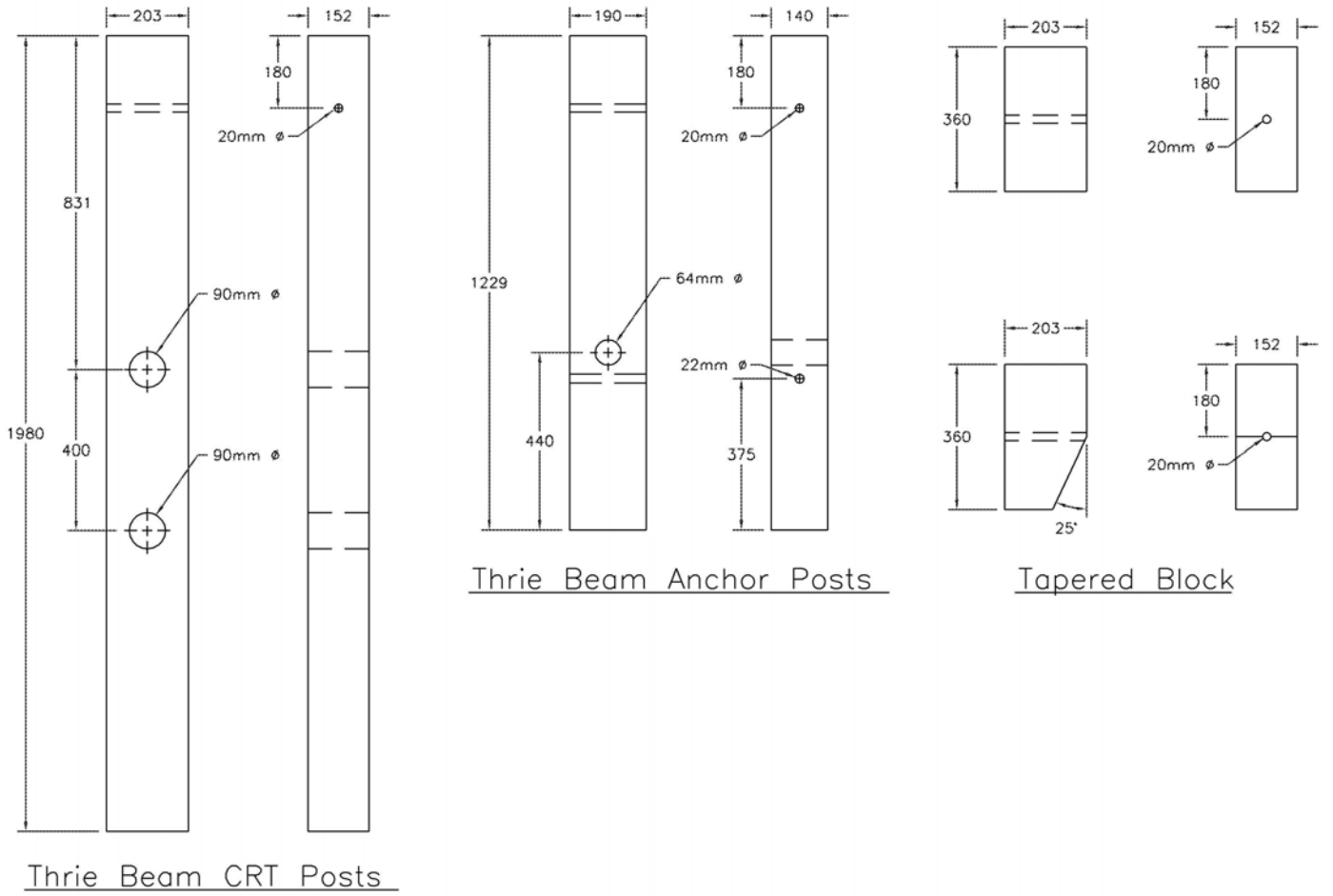

Figure 77. System Details, Test SR-4

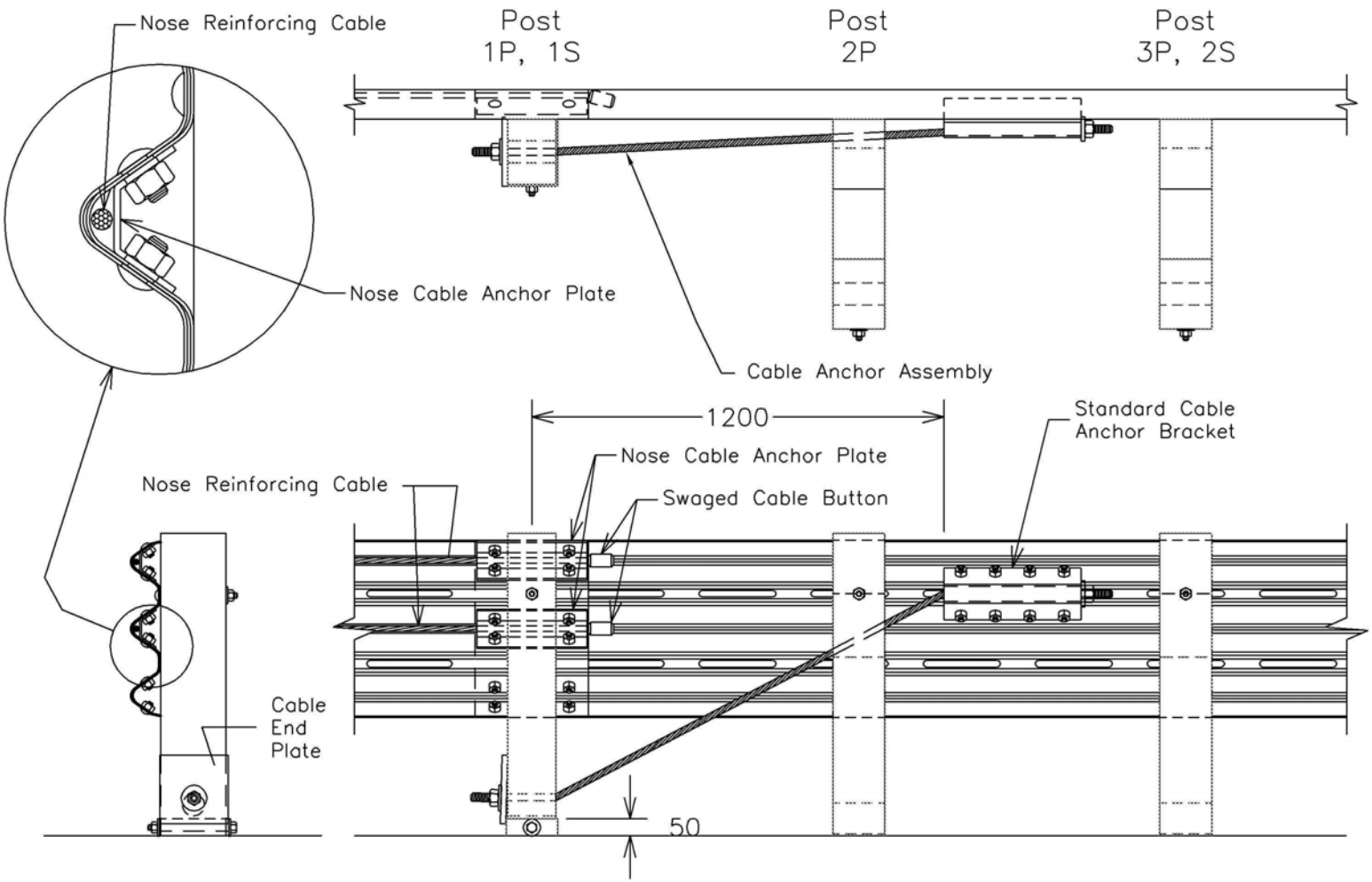

Figure 78. System Details, Test SR-4

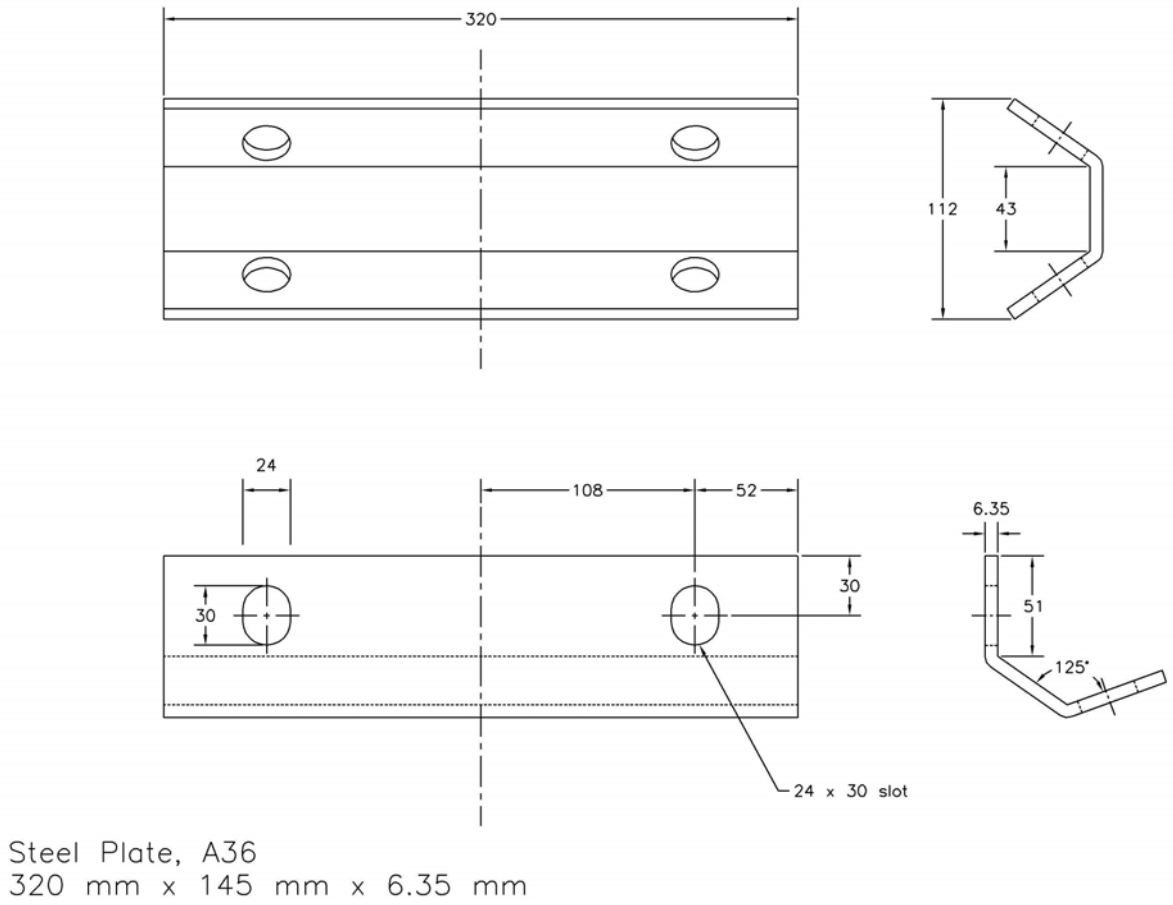

Figure 79. System Details, Test SR-4

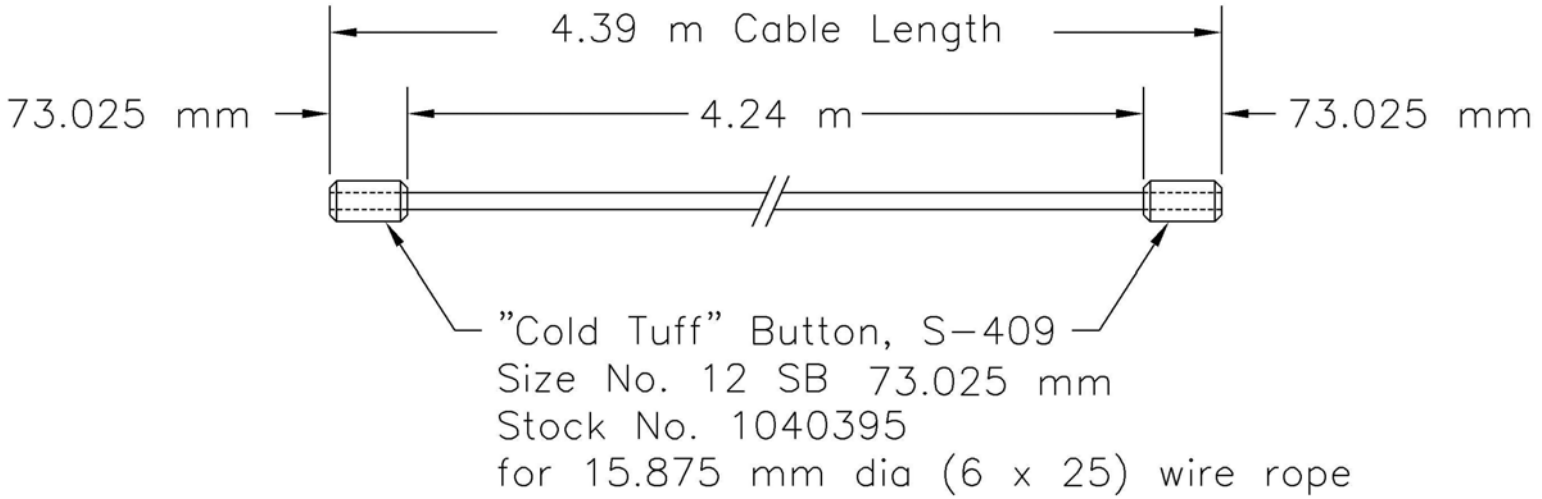

Figure 80. System Details, Test SR-4

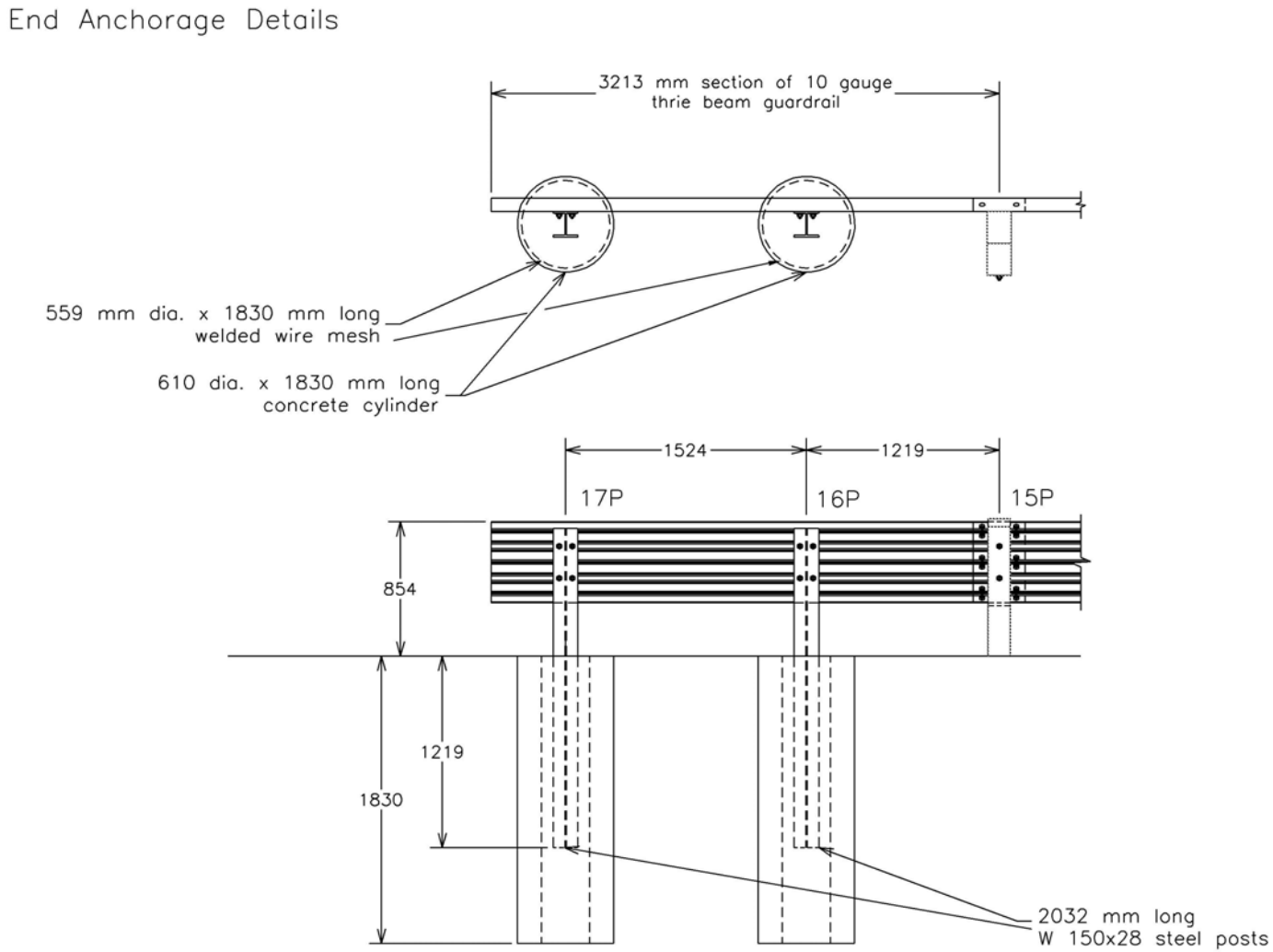

Figure 81. Primary Side End Anchorage Details, Test SR-4

Figure 82. System Photographs, Test SR-4

Figure 83. System Photographs, Test SR-4

Figure 84. System Photographs, Test SR-4

10 CRASH TEST SR-4

10.1 Test SR-4

Test SR-4 was a repeat of test SR-3 and was conducted as a modified version of NCHRP Report No. 350 Test Designation 3-31. The 2,036-kg pickup truck impacted the short-radius guardrail at a speed of 106.3 km/hr and at an angle of 1.8 degrees. Due to the added parabolic flare, the impact location for this test aligned the centerline of the pickup truck with the back face of post no.13P. A summary of the test results and the sequential photographs are shown in Figure 85. Additional sequential photographs are shown in Figure 87. Documentary photographs of the crash tests are shown in Figures 88 through 89.

10.2 Test Description

The left-front corner of the test vehicle impacted the curved nose section of the short-radius guardrail just upstream of post no. 1P, as shown in Figure 90. At 0.036 sec, the left-front corner of the pickup truck impacted and fractured post no. 1P. The pickup truck continued downstream fracturing post no. 2P at 0.69 sec and pushing the thrie beam to the left of the vehicle. By 0.100 sec, the pickup truck had reached post no. 3P and began to redirect. The pickup truck proceeded downstream while pushing the deflected thrie beam off of the left-front corner of the vehicle and towards the inside of the system, fracturing post nos. 3P through 8P by 0.284 sec. At 0.306 sec, the leading edge of the thrie beam guardrail formed a bent knee and slid off of the left-front corner of the pickup truck and into the wheel well. The bent knee of guardrail impacted and snagged the rear of the wheel well and the firewall. This caused the pickup truck to decelerate rapidly and yaw counterclockwise before coming to rest 1.85 m to the right of post no. 10P. The trajectory and final position of the pickup truck are shown in Figure 86.

10.3 System and Component Damage

Damage to the short-radius system was extensive, as shown in Figures 91 through 93. Post no. 1S on the secondary side was fractured due to the guardrail on the secondary side being pulled towards the middle of the system. Post nos. 2S and 3S displayed minor deflections but were not fractured. Rail section no. 2S on the secondary side of the system was bent around the post and blockout at post no. 2S. Damage was more severe on the primary side of the system. On the primary side of the system, post nos. 1P through 9P were completely fractured, while post nos. 10P through 13P were deflected in the soil. Rail section no. 2 on the primary side was severely buckled and crushed. Rail section nos. 2P and 3P were deformed from the impact and redirection of the vehicle. Rail section no. 3P was severely crushed and buckled due to snagging in the wheel well, beginning approximately 254-mm upstream of post no. 9P.

10.4 Vehicle Damage

Vehicle damage was extensive, as shown in Figures 94 through 96. The left-front area of the vehicle, including the bumper, radiator, and headlights, was crushed inward due to the impact with the system. The front grill was detached, and the left-front corner of the hood was bent slightly. The left-front fender of the pickup truck was deformed and crushed. The front suspension on the left side of the vehicle was damaged as well. This damage consisted of bent upper and lower control arms, a bent stabilizer bar, and failed connections on the tie rod and upper control arm. The left-front wheel was still attached at the lower control arm connection. Some deformation of the left-front rim was observed. The driver-side door was jarred shut and displayed some deformation.

Damage to the interior occupant compartment of the vehicle is shown in Figure 96. The damage included a 254-mm long rupture on the front of the floor pan near the left side.

Deformations of both the floor pan and the dash were also observed. Maximum vertical deflections of 146 mm and 159 mm were measured near the right-front corner of the driver's-side floor pan. A maximum lateral deflection of 57 mm was measured near the left-front corner of the driver's-side floor plan. A maximum longitudinal deflection of 260 mm was measured near the rear of the driver's-side floor plan. Maximum deflection of the dashboard was measured to be 38 mm in the vertical direction. The large rupture in the floor pan and the significant longitudinal floor pan deformation were unacceptable according to the criteria in NCHRP Report No. 350. Complete occupant compartment deformation details are given in Appendix E.

10.5 Occupant Risk Values

The longitudinal occupant impact velocity (OIV) was determined to be 4.32 m/s. The maximum 0.010-sec average occupant ridedown deceleration (ORD) in the longitudinal direction was 23.61 g's. The lateral occupant impact velocity (OIV) was determined to be 3.02 m/s. The maximum 0.010-sec average occupant ridedown deceleration (ORD) in the lateral direction was 11.68 g's. It is noted that the occupant ridedown deceleration in the longitudinal direction exceeded the NCHRP Report No. 350 suggested limit of 20 g's. The remaining occupant risk values were within the suggested limits provided in NCHRP Report No. 350. The results of the occupant risk data are summarized in Figure 85. Results are shown graphically in Appendix F.

10.6 Discussion

Following test SR-4, a safety performance evaluation was conducted, and the short-radius guardrail was determined to be unacceptable according to the NCHRP Report No. 350 criteria. The test article did not safely contain, redirect, or bring the vehicle to a controlled stop. Detached elements and debris from the test article did not penetrate nor show potential for penetrating the

occupant compartment or present undue hazard to the other traffic, pedestrians, or personnel in the work zone. Deformations of, or intrusion into, the occupant compartment did occur. The vehicle did remain upright during and after the collision. The vehicle's trajectory did not intrude into adjacent traffic lanes. The occupant impact velocities and ridedown accelerations were not within the suggested limits imposed by NCHRP Report No. 350.

The failure of test SR-4 to meet the safety performance criteria was directly attributed to the intrusion and snagging of the thrie beam guardrail into the wheel well region of the pickup truck. Through the initial portion of the impact, the thrie beam guardrail was impacted by the left-front corner of the vehicle and deflected towards the inside of the short-radius guardrail system. After approximately 0.300 sec, the leading edge of impacting guardrail slid past the left-front corner and into the wheel well. The intruding guardrail punched a large hole in the floor pan of the occupant compartment and causing a rapid deceleration and yaw of the vehicle. The intrusion of the thrie beam was caused by the combination of the orientation of the impact vehicle, the geometry of the system, and the lack of upstream tension in the guardrail. Because the cable anchorage at post no. 1P was disengaged almost immediately, there was little or no upstream tension in the flared guardrail section. Therefore, the vehicle moved downstream along the system with very little redirection. This in turn led to the intrusion of the thrie beam into the wheel well region.

0.000 sec 0.134 sec 0.328 sec 0.387 sec 0.454 sec

- Test Number SR-4
- Date 10/24/01
- Test Article
  - Type . . . . . Short-Radius Guardrail
  - Key Elements . . . . . Four 3,810-mm long curved and slotted thrie beam guardrail sections
    One 3,810-mm long straight thrie beam guardrail section
    18 breakaway posts
    SKT End Terminal
    Iowa steel post transition
  - Orientation . . . . . Centerline truck with centerline post no. 1P
- Soil Type . . . . . Grading B - AASHTO M 147-65 (1990)
- Vehicle Model . . . . . 1999 Chevy C2500 pickup truck
  - Curb . . . . . 1,986 kg
  - Test Inertial 2,005kg
  - Gross Static . . . . . 2,005 kg
- Vehicle Speed
  - Impact . . . . . 106.3 km/hr
  - Exit . . . . . NA
- Vehicle Angle
  - Impact . . . . . 1.8 deg
  - Exit . . . . . NA
- Vehicle Stability . . . . . Satisfactory
- Occupant Ridedown Deceleration (10 msec avg.)
  - Longitudinal . . . . . 23.61 g's > 20 g's
  - Lateral (not required) . . . . . 11.69g's < 20 g's
- Occupant Impact Velocity (Normalized)
  - Longitudinal . . . . . 4.32 m/s < 12 m/s
  - Lateral (not required) . . . . . 3.02 m/s < 12 m/s
- Vehicle Damage
  - TAD[20] 11-FL-5
  - SAE[21] 11FLEA3
- Vehicle Stopping Distance . . . . . 8.49 m downstream post no. 1P
  1.85 m right
- Test Article Damage . . . . . Extensive
- Maximum Deflections
  - Permanent Set . . . . . NA
  - Dynamic . . . . . NA

Figure 85. Summary of Test Results and Sequential Photographs, Test SR-4

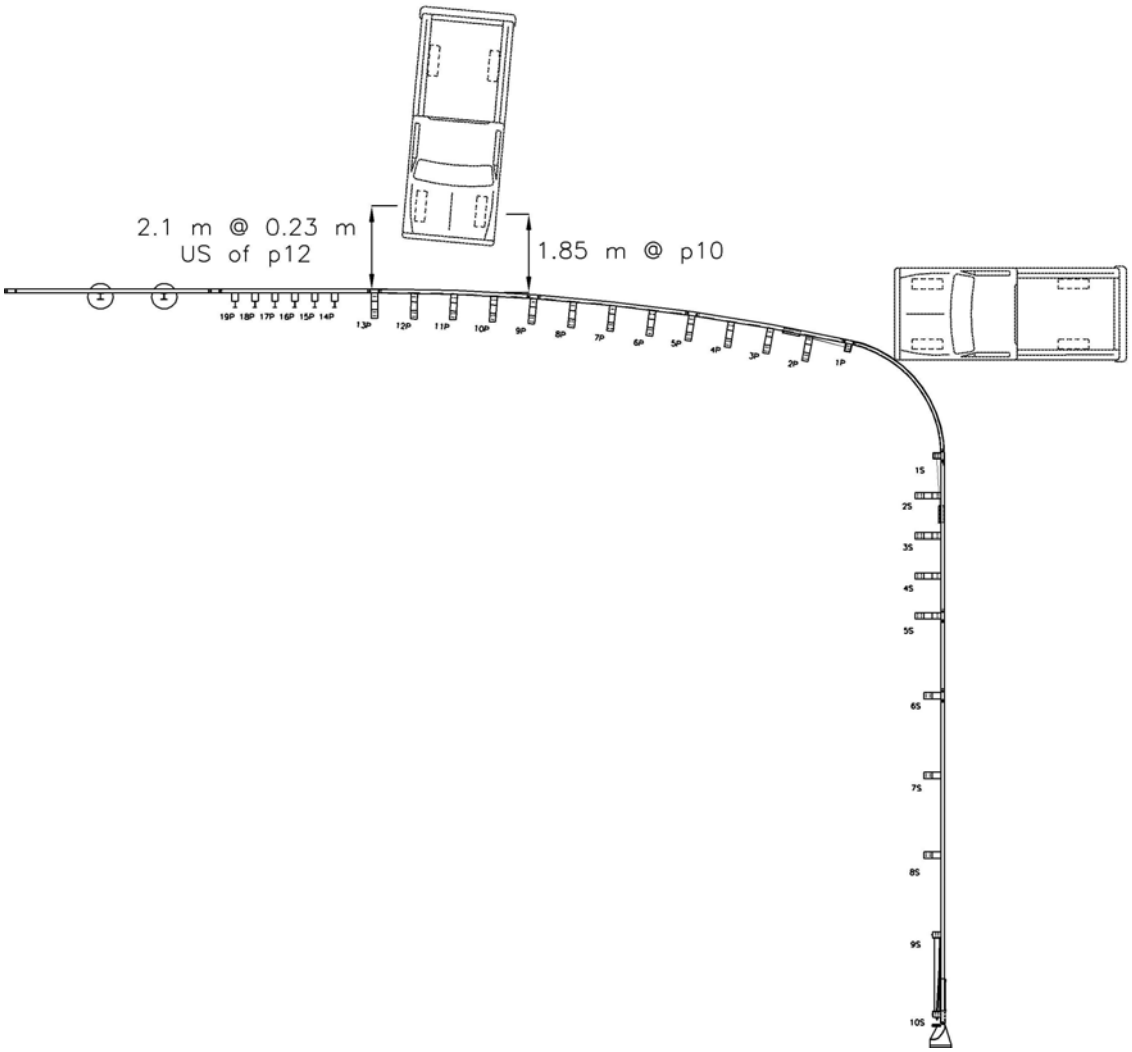

Figure 86. Vehicle Trajectory, Test SR-4

0.000 sec

0.000 sec

0.088 sec

0.134 sec

0.222 sec

0.212 sec

0.368 sec

0.372 sec

0.576 sec

0.434 sec

Figure 87. Additional Sequential Photographs, Test SR-4

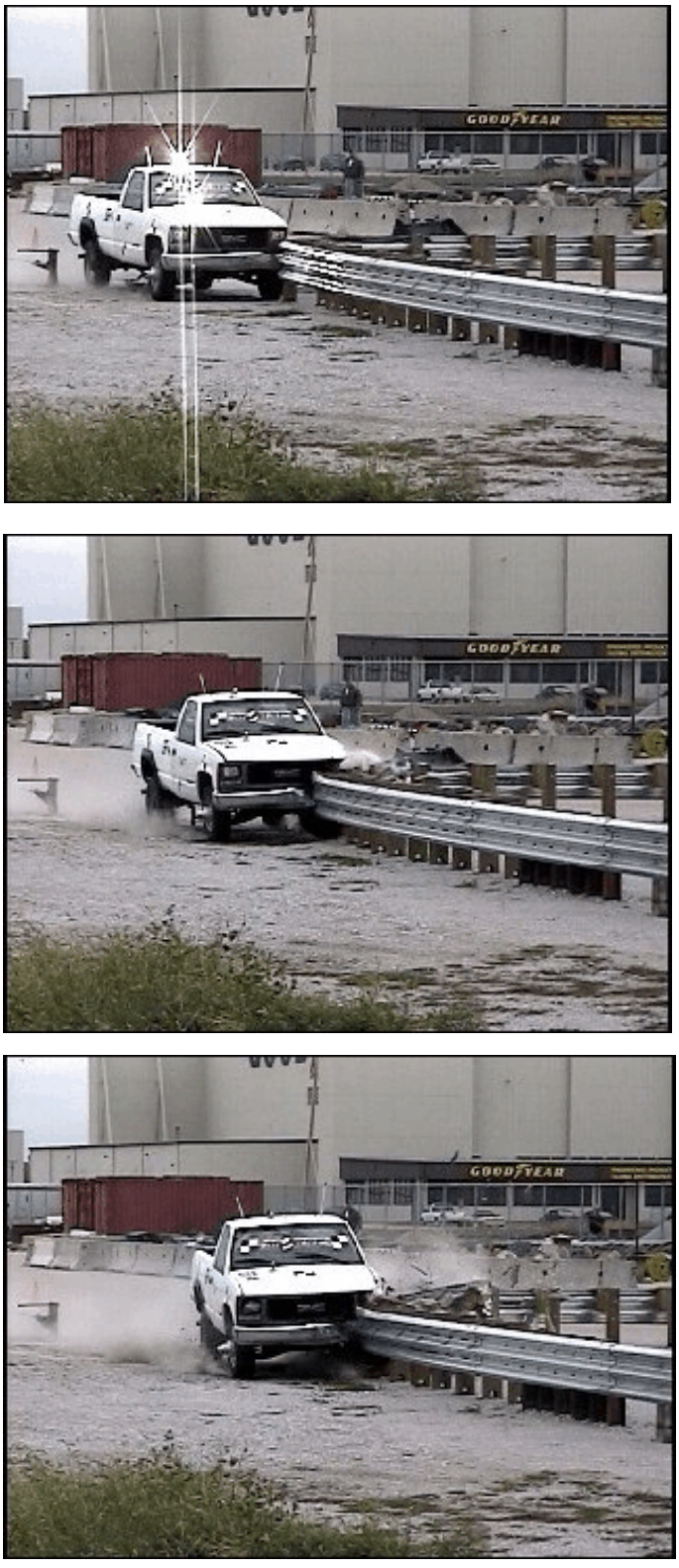

Figure 88. Documentary Photographs, Test SR-4

Figure 89. Documentary Photographs, Test SR-4

Figure 90. Impact Location, Test SR-4

Figure 91. System Damage, Test SR-4

Figure 92. System Damage, Test SR-4

Figure 93. System Damage, Test SR-4

Figure 94. Vehicle Damage, Test SR-4

Figure 95. Vehicle Damage, Test SR-4

Figure 96. Vehicle Damage, Test SR-4

10 LS-DYNA COMPUTER SIMULATION MODELING

During the concept development phase of the short-radius guardrail system, finite-element computer simulation using LS-DYNA (22) was used to demonstrate the potential for the system to meet the NCHRP Report No. 350 safety requirements for test 3-33. Simulations of the original short-radius design concept using the test 3-33 impact conditions showed that the system effectively captured and contained the pickup truck.

Further simulation modeling of the short-radius system was performed in unison with the full-scale crash testing and development of the short-radius system described herein. The focus of the simulation effort was to develop models of the short-radius system that would help investigate the failed tests in the development of the system as to well as provide a tool for examining potential design changes. To this end, LS-DYNA models of both the test 3-33 and test 3-31 impact conditions into the short-radius system were developed, as shown in Figure 97.

The modeling of the short-radius system displayed good correlation with full-scale test results for approximately the first 150 msec to 200 msec of the impact. The models were capable of accurately replicating the initial portion of the impact event, including the deformation of the system and the capture and/or redirection of the impacting vehicle. Basic comparisons of LS-DYNA simulations and full-scale test nos. SR-2, SR-3, and SR-4 are shown in Figures 98, 99, and 100, respectively.

Beyond the 150 msec to 200 msec event length, contact instabilities and numerical errors in the simulation prevented accurate representation of the crash event. This is a typical short-coming seen in roadside safety simulations using LS-DYNA. LS-DYNA is most effective when simulating impact events with a duration of 200 msec or less. However, typical impact events involving

roadside safety devices can vary in duration from 150 msec to well over 1000 msec. In the case of the short-radius system, the events leading to the failure of the full-scale crash tests all occurred well after 250 msec. As such, the simulation models were capable of effectively examining these failures or investigating potential design changes. However, it should be noted that the LS-DYNA computer simulation effort will continuing to be used during the development of the short-radius guardrail where applicable.

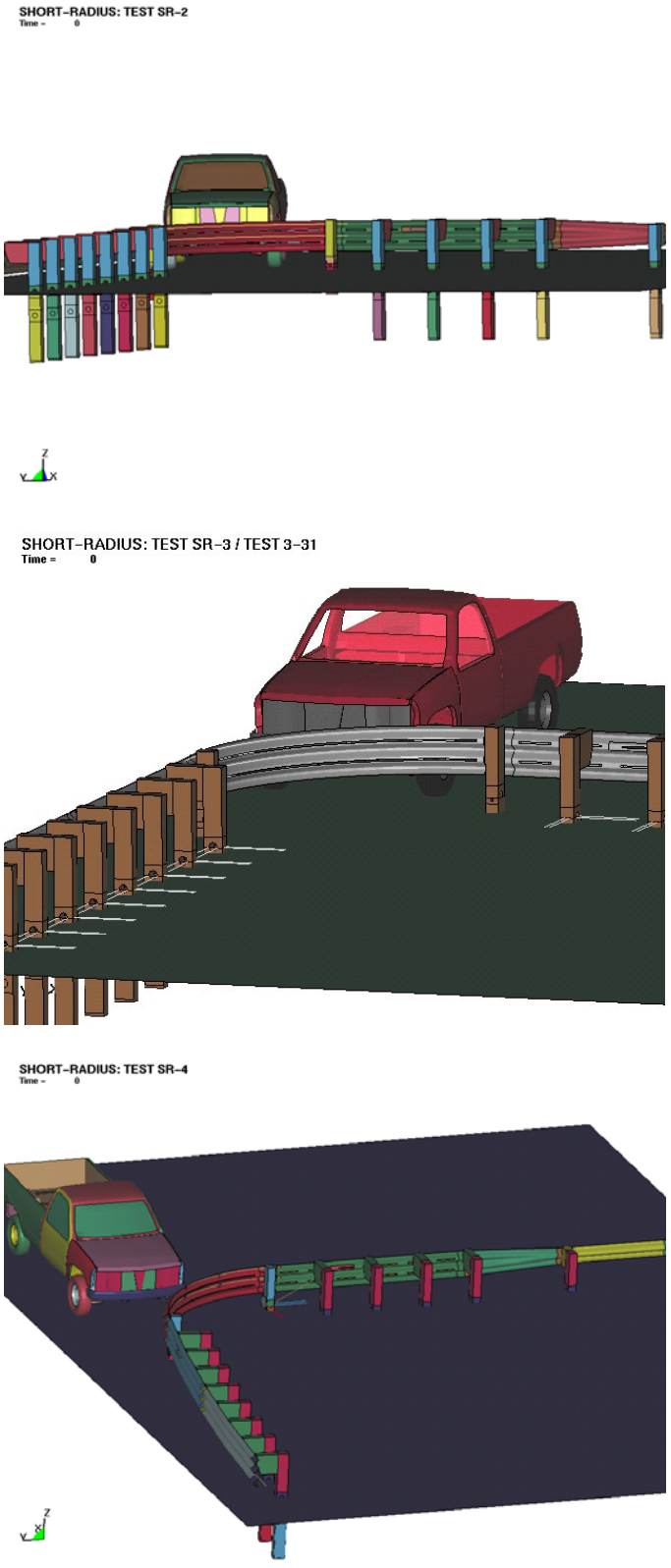

Figure 97. LS-DYNA Simulation Models, Test Nos. SR-2, SR-3, and SR-4

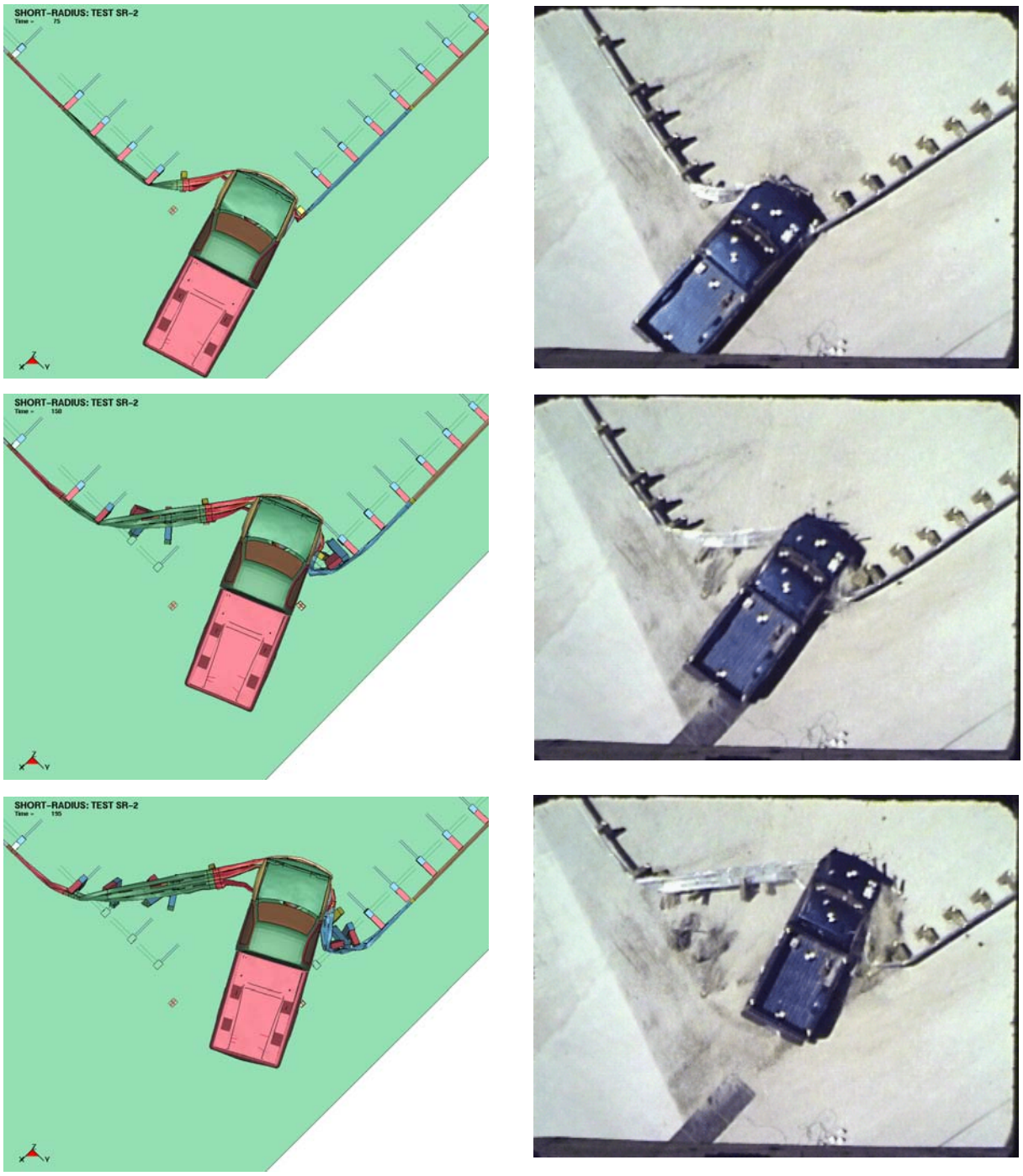

Figure 98. Comparison of Full-Scale Test and LS-DYNA Simulation Model, Test No. SR-2

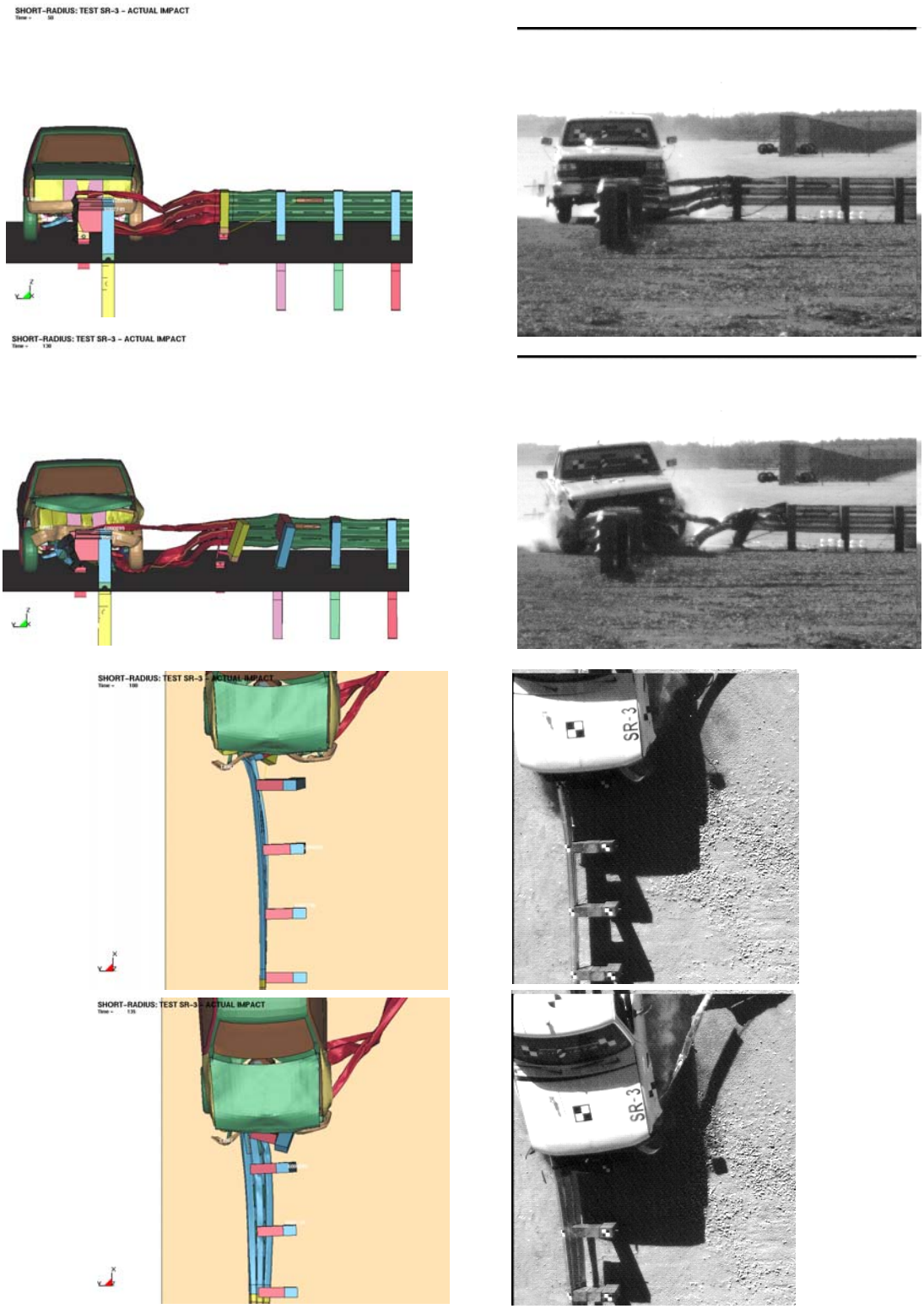

Figure 99. Comparison of Full-Scale Test and LS-DYNA Simulation Model, Test No. SR-3

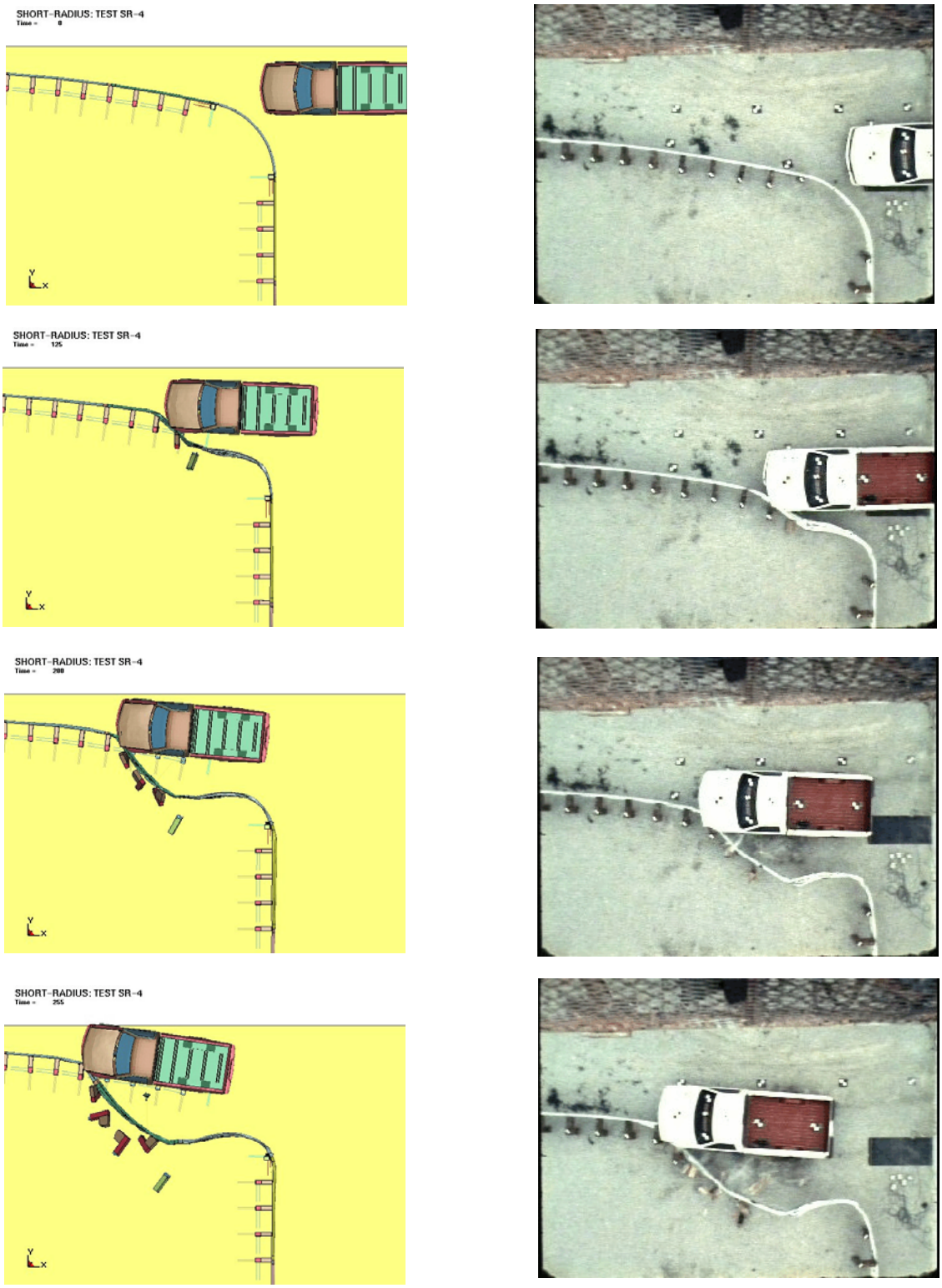

Figure 100. Comparison of Full-Scale Test and LS-DYNA Simulation Model, Test No. SR-4

11 SUMMARY

The Phase II development of a TL-3 short-radius guardrail system for intersecting roadways began with the construction of a barrier system consisting of a curved and slotted thrie beam nose section, two adjacent slotted thrie beam sections, and breakaway CRT posts. One side of the system attached to a TL-3 steel post approach guardrail transition while the other side attached to a TL-2 guardrail end terminal.

The first full-scale crash test, test SR-1, was conducted according to NCHRP Report No. 350 Test Designation 3-33. The test consisted of a 2,029-kg pickup truck impacting the nose of center of the short-radius at a speed of 98.9 km/hr and at an angle of 19.0 degrees. The results of test SR-1 were deemed unacceptable according to NCHRP Report No. 350 criteria due to rollover of the test vehicle. Vehicle rollover was attributed to ineffective capture, uneven loading of the front of the vehicle, and instability caused by the presence of a moat behind the test article. Design modifications were made to improve the performance of the system prior to the next test. These changes included the addition of two posts to the secondary side of the system and the removal of the moat.

Test SR-2 was conducted as a repeat of test SR-1. In this test, a 2,014-kg pickup truck impacted the center of the nose of the short-radius system at speed of 104.2 km/hr and at an angle of 16.1 degrees. Test SR-2 was again judged unacceptable according to NCHRP Report No. 350 criteria due to rollover of the test vehicle. It was believed that a combination of the yaw induced into the test vehicle and the accumulation of debris in front of the vehicle caused the vehicle to trip and roll over the thrie beam near the end of the impact event. After test SR-2, it was decided to leave the system unchanged and investigate another impact condition before proposing additional design changes to the system.

Test SR-3 was conducted as a modified version of NCHRP Report No. 350 Test Designation 3-31. In test 3-31, a 2,000-kg pickup truck should impact along the centerline of the nose of the barrier at 100 km/hr and at an angle of 0 degrees. In reviewing this impact condition as well as the geometry of the system, the researchers decided that a more critical impact location would exist with the pickup truck directly aligned with the primary side of the system. Therefore, the impact conditions in this test were modified in order to allow the centerline of the pickup truck to impact along the centerline of post no.1P and parallel to the primary side of the system. The 2,036-kg pickup truck impacted the short-radius guardrail at a speed of 102.9 km/hr and at an angle of 0.9 degrees. Test SR-3 was judged unacceptable according to NCHRP Report No. 350 criteria due to rollover of the test vehicle. As a result of this failed test, design changes were deemed necessary in order to allow for the successful containment or redirection of the pickup truck. Prior to test SR-4, a series of design modifications were implemented in order to improve the performance of the short-radius system, including the addition of a parabolic flare to the primary side (and the additional slotted rail sections that accompanied it), raising the system 51 mm, and increasing the capacity of the nose cable plates.

Test SR-4 was conducted as a repeat of test SR-3. Due to the added parabolic flare, the impact location for this test aligned the centerline of the pickup truck with the back face of post no.13P. The 2,005-kg pickup truck impacted the short-radius guardrail at a speed of 106.3 km/hr and at an angle of 1.8 degrees. During this test, the thrie beam guardrail intruded into the wheel well of the pickup truck, causing rapid deceleration and significant penetration into the interior occupant compartment. Based on these results, test SR-4 was judged unacceptable according to NCHRP Report No. 350 criteria.

A schematic of the impact conditions for test nos. SR-1 through SR-4 is shown in Figure 101 and a summary of the full-scale test performance evaluation results is shown in Table 2.

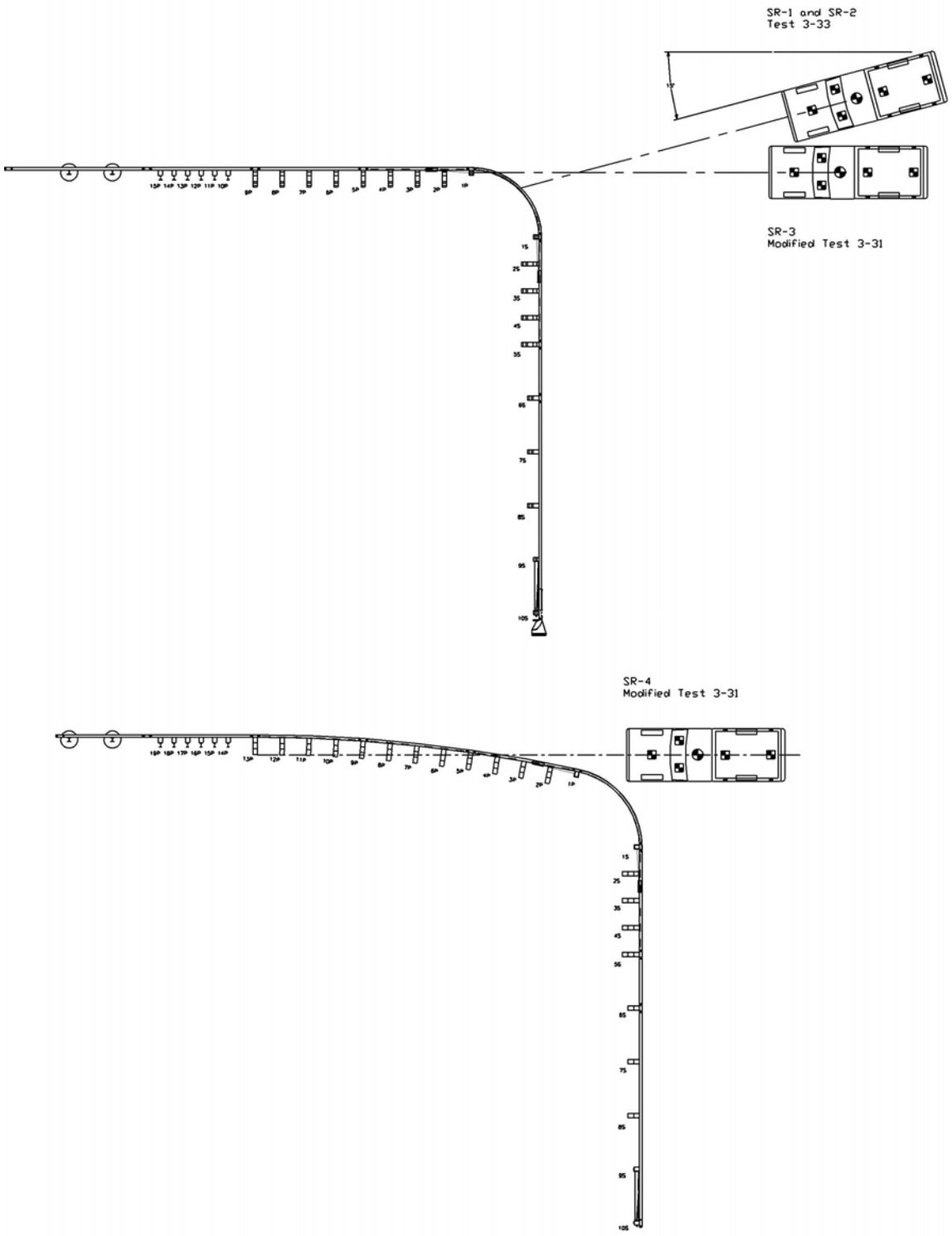

Figure 101. Summary of Short-Radius Guardrail Impacts

Table 2. Summary of Safety Performance Evaluation Results

Evaluation Factors	Evaluation Criteria	Test SR-1	Test SR-2	Test SR-3	Test SR-4
Structural Adequacy	A	NA	NA	NA	NA
	C	U	U	U	U
Occupant Risk	D	U	S	S	U
	F	U	U	U	S
	H	S	S	S	S
	I	S	S	S	U
Vehicle Trajectory	K	S	S	S	S
	L	NA	NA	NA	NA
	M	NA	NA	NA	NA
	N	U	U	S	S
NCHRP Report No. 350 Test Level		TL-3	TL-3	TL-3	TL-3
NCHRP Test No.		3-33	3-33	3-31 (modified)	3-31 (modified)
Pass/Marginal/Fail		FAIL	FAIL	FAIL	FAIL

S - Satisfactory
M - Marginal
U - Unsatisfactory
NA - Not Applicable

12 RECOMMENDATIONS

The development of a TL-3 short-radius guardrail system for intersecting roadways has proven difficult due to the complex system geometry and the demanding impact conditions. To date, no successful tests have been conducted on the system. However, the most recent test of the short-radius design, test SR-4, displayed some promising results.

The addition of the parabolic flare and the corresponding additional slotted guardrail sections should greatly improve vehicle capture while providing additional stroke for gradual deceleration of impacting vehicles. However, the failure of the test due to intrusion of the thrie beam guardrail into the wheel well region demonstrated the need for some design modifications. These modifications should help eliminate shortcomings in the current short-radius guardrail system while improving the system's safety performance. Review of the test results suggested two possible modifications for future short-radius guardrail system development.

The first proposed modification was to reduce the height of the thrie beam in the system to its original 803-mm level. In test SR-4, the rail height was increased in order to improve vehicle capture and allow the pickup truck to push through the guardrail splice. After reviewing the results of test SR-4, the researchers believe that the addition of the flare to the primary side of the system should improve vehicle capture and eliminate the potential for the impacting vehicle to push through the splice. Therefore, it was believed that the height could be reduced to the original level without impairing the safety performance of the system. In addition, the increased rail height created far too many compatibility issues with regards to connection to adjacent guardrails, end terminals, and bridge rails.

The second proposed modification to the short-radius guardrail system was the addition of

an upstream anchor along the primary side. Review of test SR-4 demonstrated that the intrusion of the thrie beam was partially precipitated by the lack of upstream tension in the guardrail. The cable anchorage at post no. 1P was disengaged almost immediately and there was little or no upstream tension in the flared guardrail section to redirect the impacting vehicle. Therefore, the addition of a second anchorage for the primary side would improve redirection and prevent the intrusion of the thrie beam into the wheel well. Placement and design of such an anchor is both complicated and critical to the safety performance of the system. First, the anchor needs to be nearly tangent or parallel to the primary side in order to develop tension effectively. Second, the design of the anchor needs to be such that remains in place for redirection impacts and can be triggered to release when the system captures a vehicle.

13 REFERENCES

1. Ross, H. E. Jr., D. L. Sicking, R. A. Zimmer, and J. D. Michie, *Recommended Procedures for the Evaluation of Highway Features*, NCHRP 350, Transportation Research Board, Washington, D. C., 1993.

2. Michie, Jarvis D., *Recommended Procedures for the Safety Performance Evaluation of Highway Appurtenances*, NCHRP 230, Transportation Research Board, Washington, D.C., March 1981.

3. Bielenberg, R.W., Reid, J.D., Faller, R.K., Rohde, J.R., Sicking, D.L., Keller, E.A., Holloway, J.C., *Concept Development of a Short-Radius Guardrail System for Intersecting Roadways*, Final Report to the Midwest State's Regional Pooled Fund Program, Transportation Research Report No. TRP-03-100-00, Project No. SPR-3(017)-Year 8, Midwest Roadside Safety Facility, University of Nebraska-Lincoln, September 12, 2000.

4. Bronstad, M.E., L.R. Calcote, M. H. Ray, and J.B. Mayer, *Guardrail-Bridge Rail Transition Designs, Volume I*, Report No. FHWA/RD-86/178, Southwest Research Institute, San Antonio, Texas, April 1988.

5. Bronstad, M.E., Ray, M.H., Mayer, J.B., Jr., and McDevitt, C.F., *W-Beam Approach Treatment at Bridge Rail Ends Near Intersecting Roadways*, Transportation Research Record No. 1133, Transportation Research Board, National Research Council, Washington, D.C., 1987.

6. Mayer, J.B., *Full-Scale Crash Testing of Approach Guardrail for Yuma County Public Works Department*, Final Report, Project No. 06-2111, Southwest Research Institute, San Antonio Texas, 1989.

7. *1989 Guide Specifications for Bridge Railings*, American Association of State Highway and Transportation Officials, Washington, D.C., 1989.

8. Ross, H.E. Jr., Bligh, R.P., Parnell, C.B., *Bridge Railing End Treatments at Intersecting Streets and Drives*, Report No. FHWA TX-91/92-1263-1F, Texas Transportation Institute, College Station, Texas, August 1992.

9. Bligh, Roger P., Hayes E. Ross, Jr., and Dean C. Alberson, *Short-Radius Thrie Beam Treatment for Intersecting Streets and Drives*, Report No. FHWA/TX-95/1442-1F, Texas Transportation Institute, College Station, Texas, November 1994.

10. *Curved W-Beam Guardrail Installations at Minor Roadway Intersections*, Federal Highway Administration (FHWA), U.S. Department of Transportation, Technical Advisory T 5040.32, April 13, 1992.

11. Bielenberg, B.W., Faller, R.K., Reid, J.D., Rohde, J.R., Sicking, D.L., and Keller, E.A., *Concept Development of a Bullnose Guardrail System for Median Applications*, Final Report to the Midwest State's Regional Pooled Fund Program, Transportation Research Report No. TRP-03-73-98, Project No. SPR-3(017)-Year 7, Midwest Roadside Safety Facility, University of Nebraska-Lincoln, May 22, 1998.

12. Bielenberg, B.W., Reid, J.D., Faller, R.K., Rohde, J.R., Sicking, D.L., Keller, E.A., and Holloway, J.C., *Phase II Development of a Bullnose Guardrail System for Median Applications*, Final Report to the Midwest State's Regional Pooled Fund Program, Transportation Research Report No. TRP-03-78-98, Project No. SPR-3(017)-Years 7 and 8, Midwest Roadside Safety Facility, University of Nebraska-Lincoln, December 18, 1998.

13. Bielenberg, B.W., Reid, J.D., Faller, R.K., Rohde, J.R., Sicking, D.L., Keller, E.A., Holloway, J.C., and Supencheck, L., *Phase III Development of a Bullnose Guardrail System for Median Applications*, Final Report to the Midwest State's Regional Pooled Fund Program, Transportation Research Report No. TRP-03-95-00, Project No. SPR-3(017)-Years 7 and 8, Midwest Roadside Safety Facility, University of Nebraska-Lincoln, June 1, 2000.

14. Reid, J. R., Bielenberg, B. W., "Using LS-DYNA Simulation to Solve a Design Problem: A Bullnose Guardrail Example", Paper No. 99-0554, Transportation Research Record No. 1690, Transportation Research Board, Washington, D.C., November 1999.

15. Bielenberg, R.W., Reid, J.D., and Faller, R.K., "NCHRP Report No. 350 Compliance Testing of a Bullnose Median Barrier System", Paper No. 01-0204, Transportation Research Record No. 1743, Transportation Research Board, Washington, D.C., January 2001.

16. Faller, R.K., Reid, J.D., and Rohde, J.R., *Approach Guardrail Transition for Concrete Safety Shape Barriers*, Transportation Research Record No. 1647, Transportation Research Board, Washington, D.C., November 1998.

17. Faller, R.K., Reid, J.D., Rohde, J.R., Sicking, D.L., and Keller, E.A., *Two Approach Guardrail Transitions for Concrete Safety Shape Barriers*, Final Report to the Midwest State's Regional Pooled Fund Program, Transportation Research Report No. TRP-03-69-98, Project No. SPR-3(017)-Year 6, Midwest Roadside Safety Facility, University of Nebraska-Lincoln, May 15, 1998.

18. Sicking, DL, JD Reid, and JR Rohde, "Development of a Sequential Kinking Terminal for W-beam Guardrails," Paper No. 98-0614, Transportation Research Record No. 1647, 1998.

19. Hinch, J., Yang, T-L, and Owings, R., *Guidance Systems for Vehicle Testing*, ENSCO, Inc., Springfield, VA 1986.

20. *Vehicle Damage Scale for Traffic Investigators*, Second Edition, Technical Bulletin No. 1, Traffic Accident Data (TAD) Project, National Safety Council, Chicago, Illinois, 1971.

21. *Collision Deformation Classification - Recommended Practice J224 March 1980*, Handbook Volume 4, Society of Automotive Engineers (SAE), Warrendale, Pennsylvania, 1985.

22. Hallquist, J.O., *LS-DYNA Keyword User's Manual*, Livermore Software Technology Corporation, California, 1997.

14 APPENDICES

APPENDIX A

ACCELEROMETER DATA ANALYSIS, TEST SR-1

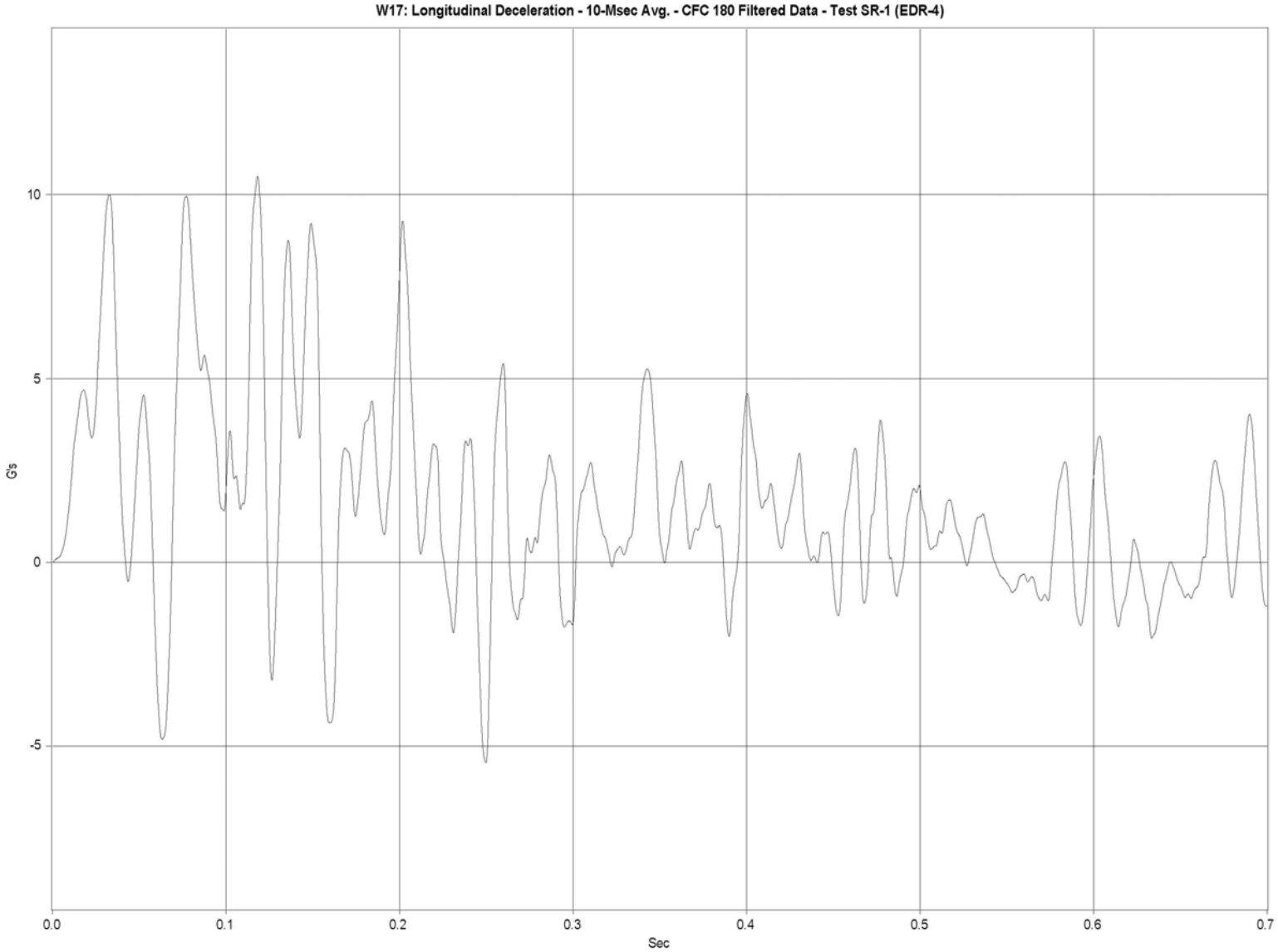

Figure A-1. Graph of Longitudinal Deceleration - Filtered Data, Test SR-1

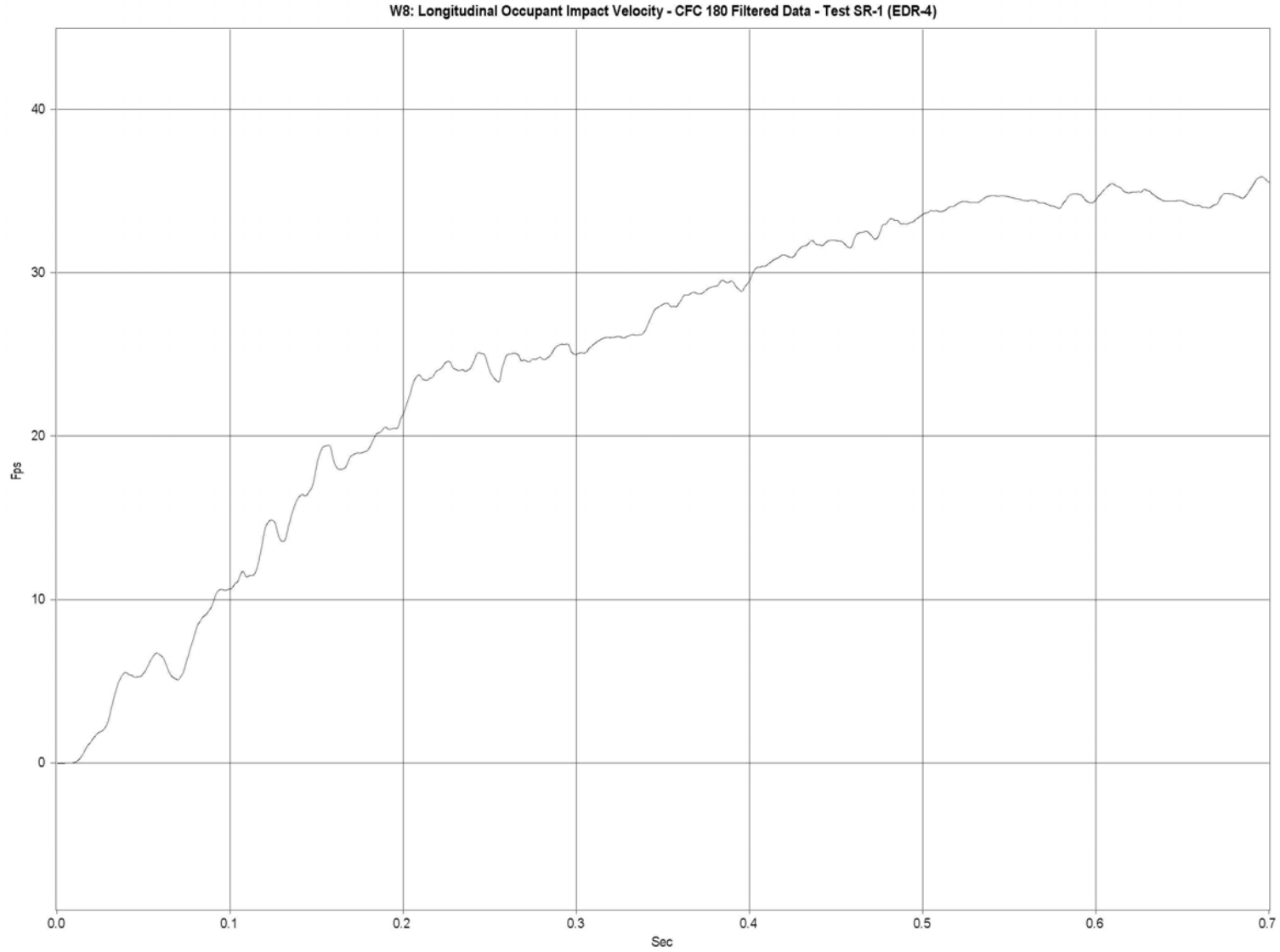

Figure A-2. Graph of Longitudinal Occupant Impact Velocity - Filtered Data, Test SR-1

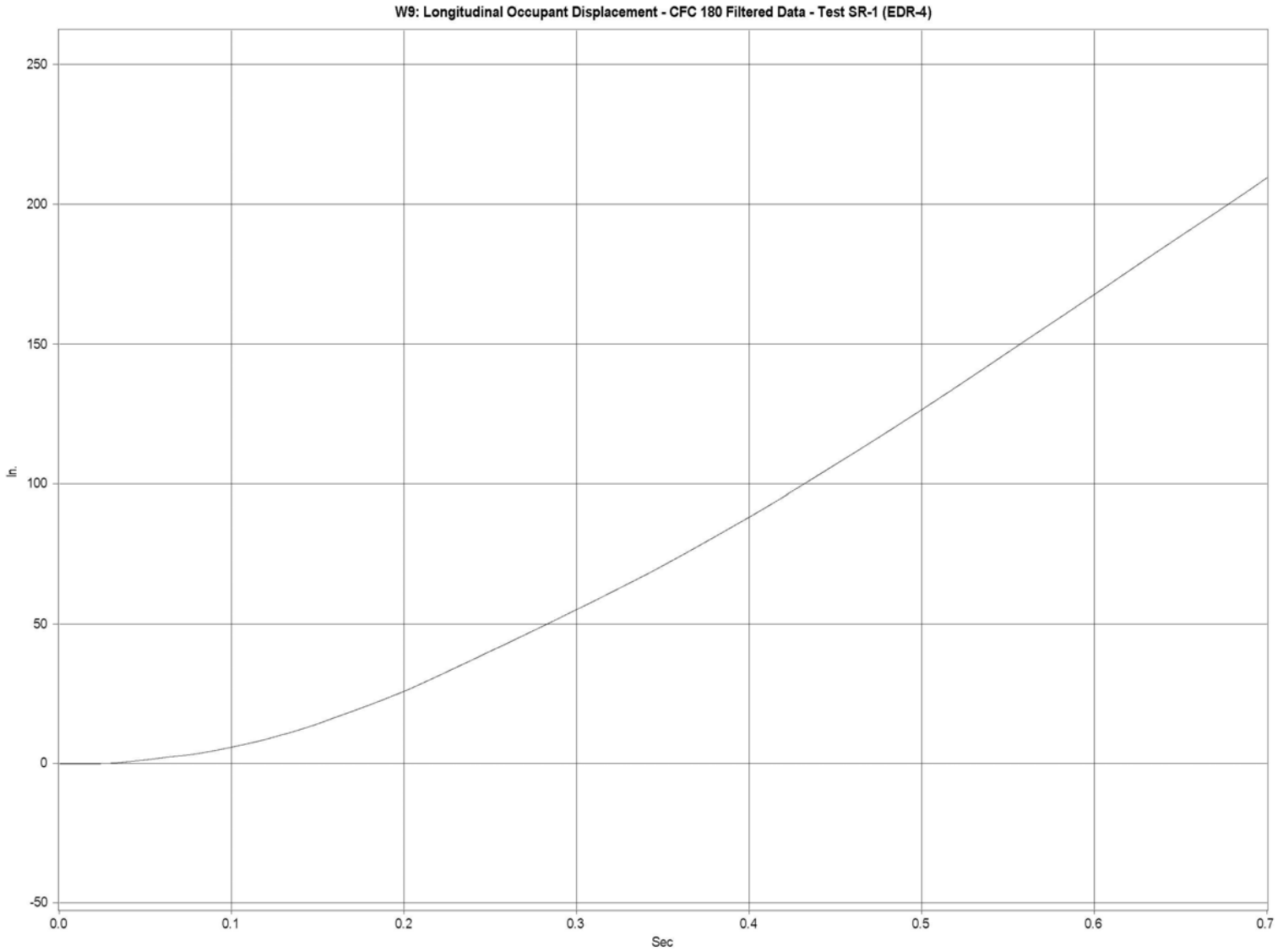

Figure A-3. Graph of Longitudinal Occupant Displacement - Filtered Data, Test SR-1

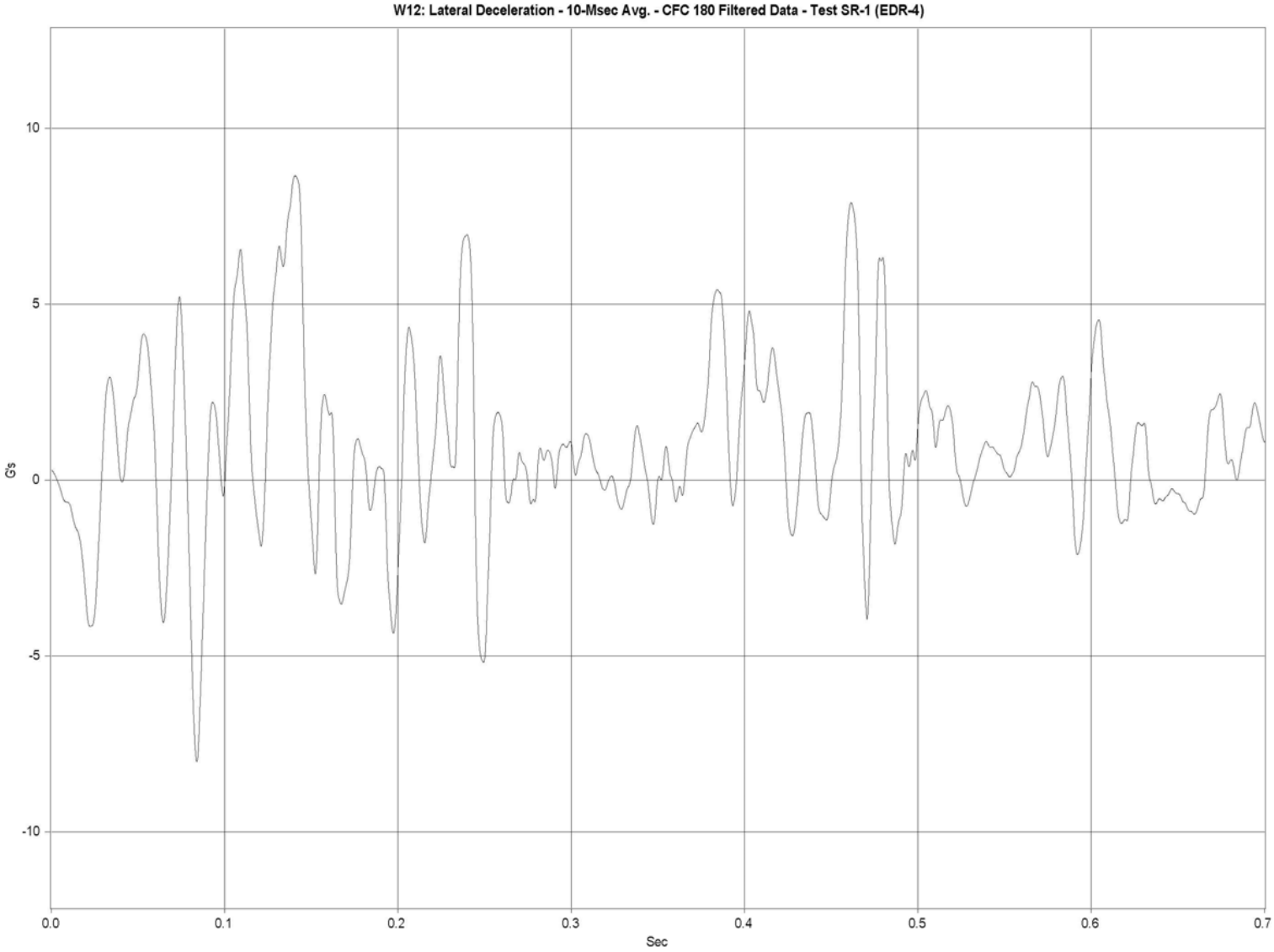

Figure A-4. Graph of Lateral Deceleration - Filtered Data, Test SR-1

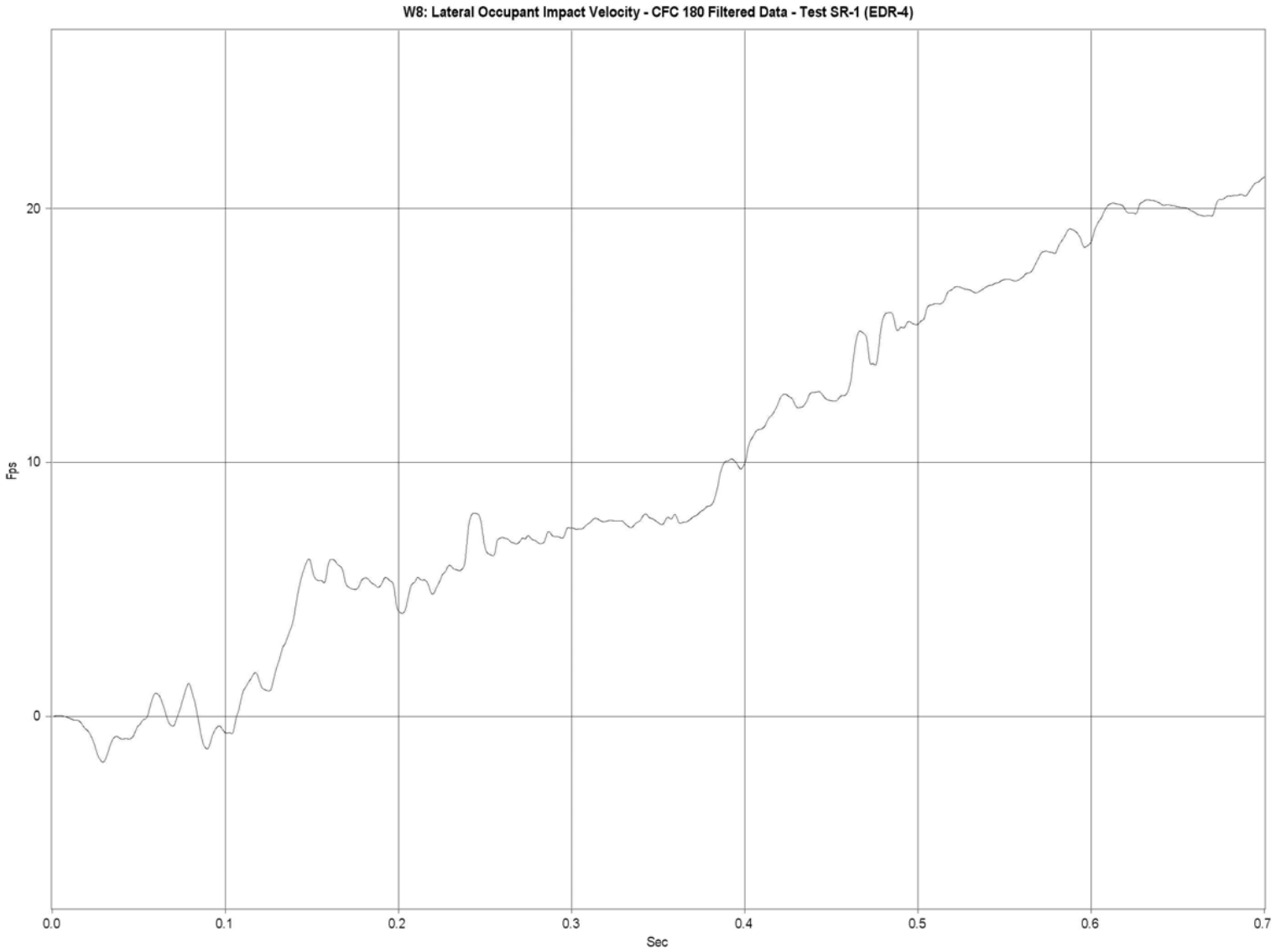

Figure A-5. Graph of Lateral Occupant Impact Velocity - Filtered Data, Test SR-1

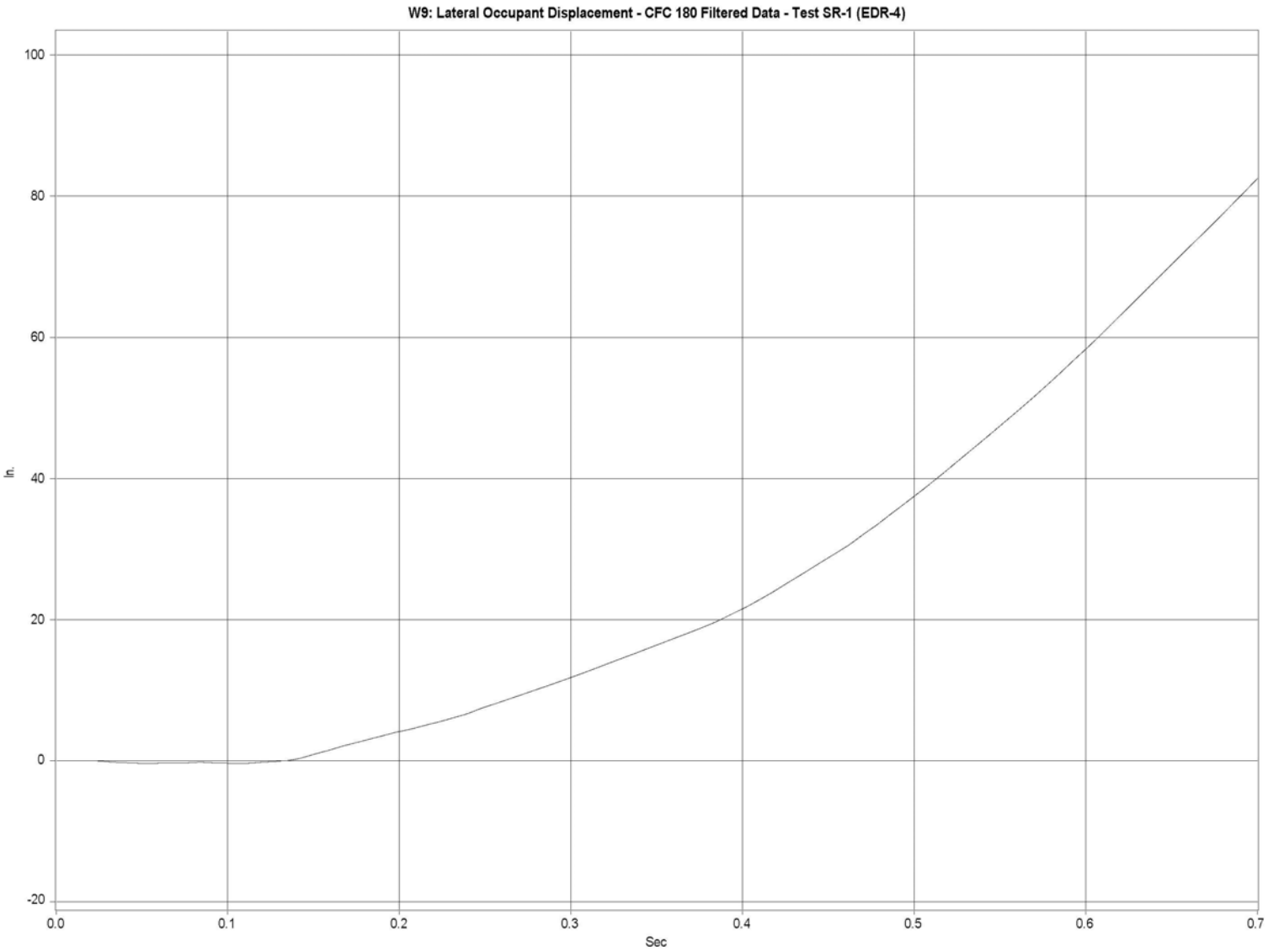

Figure A-6. Graph of Lateral Occupant Displacement - Filtered Data, Test SR-1

APPENDIX B

ACCELEROMETER DATA ANALYSIS, TEST SR-2

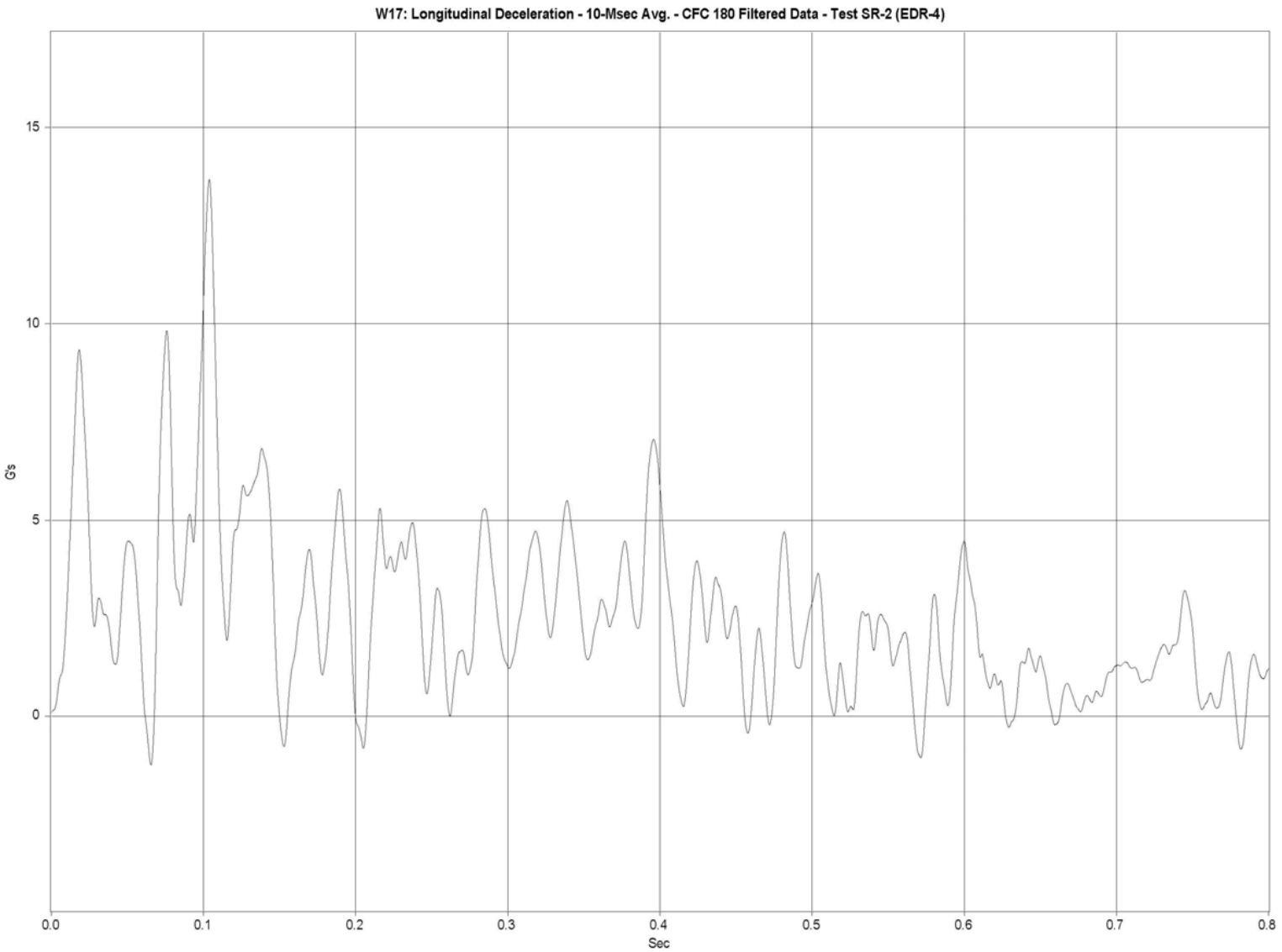

Figure B-1. Graph of Longitudinal Deceleration - Filtered Data, Test SR-2

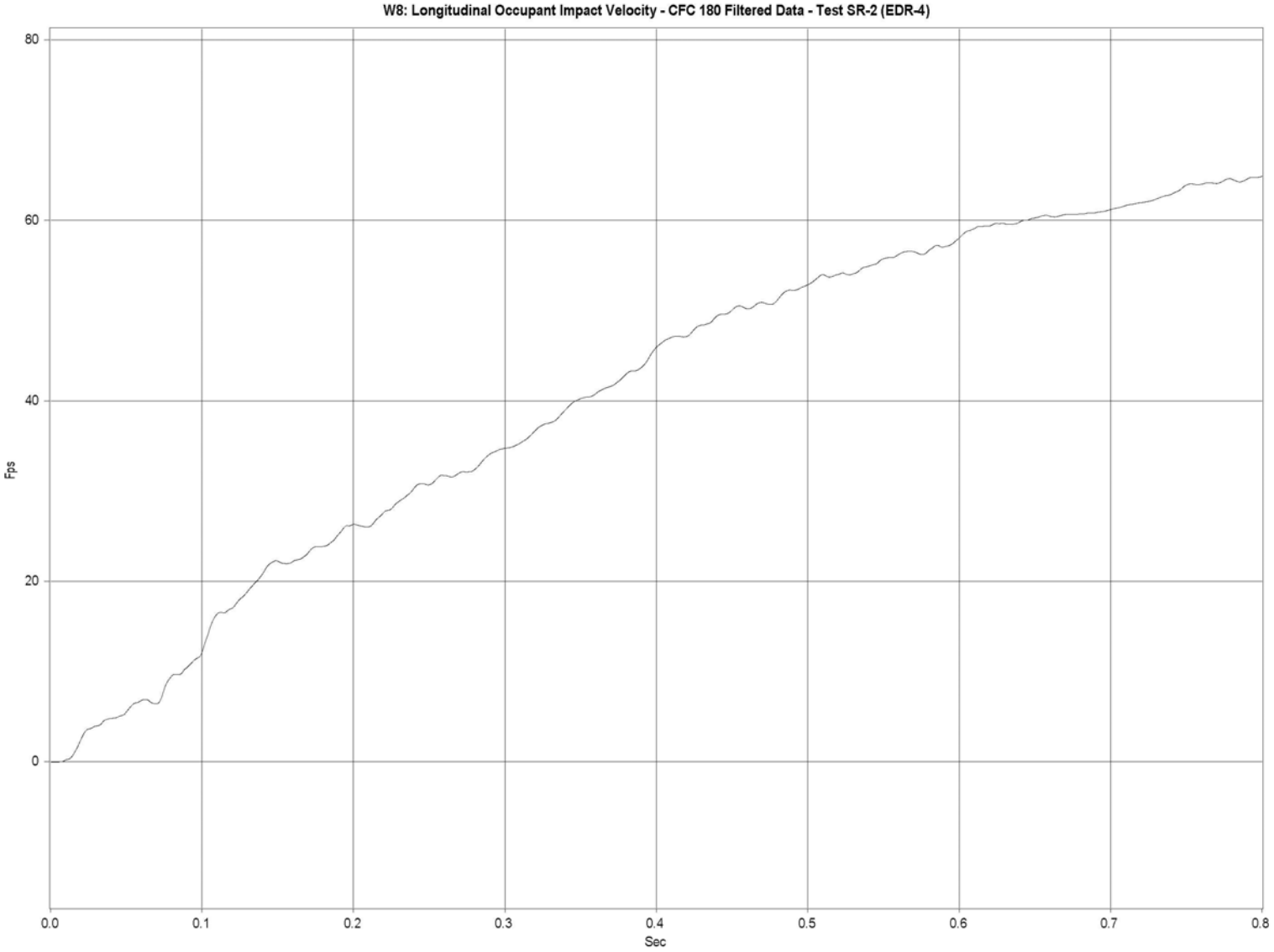

Figure B-2. Graph of Longitudinal Occupant Impact Velocity - Filtered Data, Test SR-2

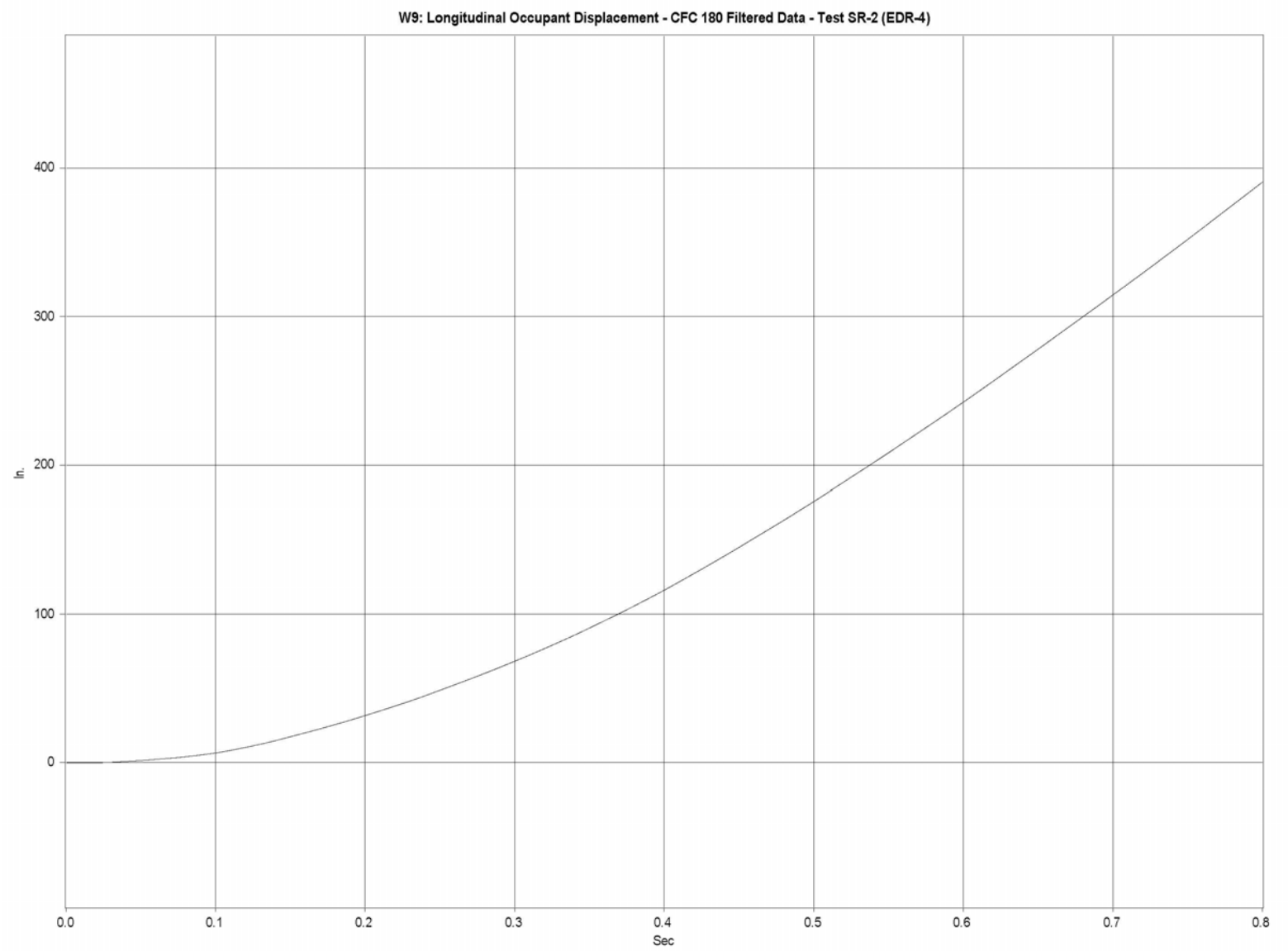

Figure B-3. Graph of Longitudinal Occupant Displacement - Filtered Data, Test SR-2

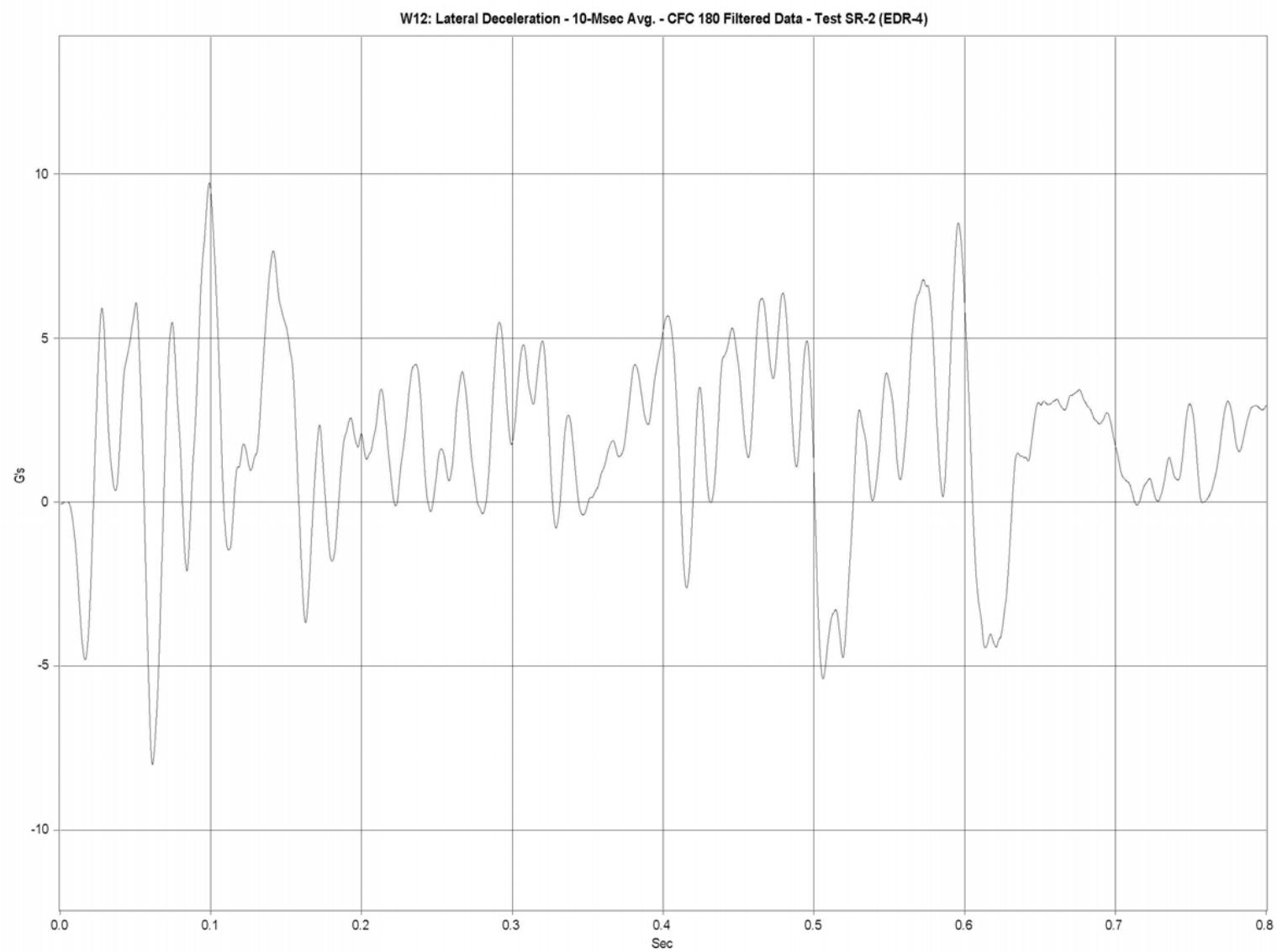

Figure B-4. Graph of Lateral Deceleration - Filtered Data, Test SR-2

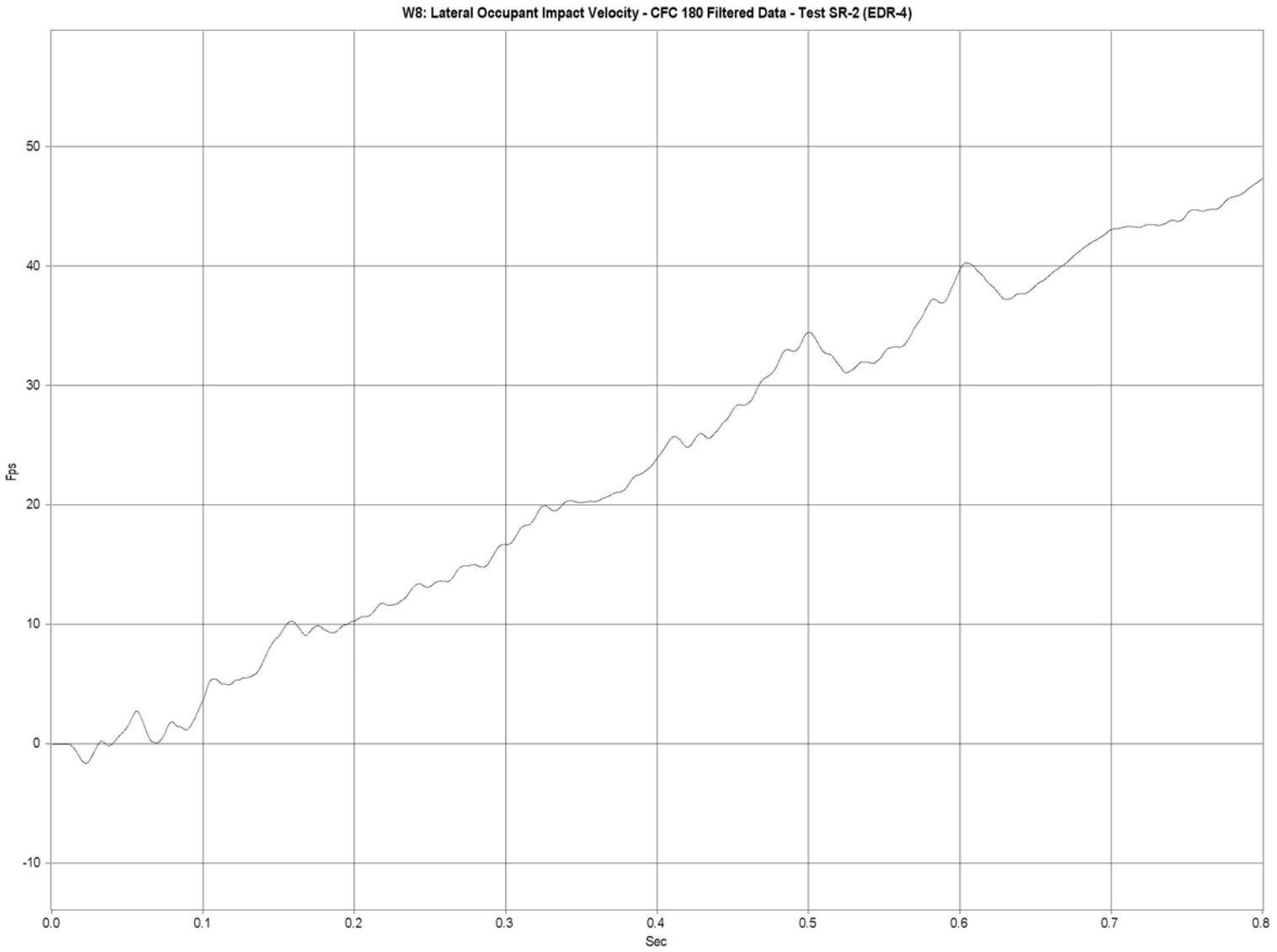

Figure B-5. Graph of Lateral Occupant Impact Velocity - Filtered Data, Test SR-2

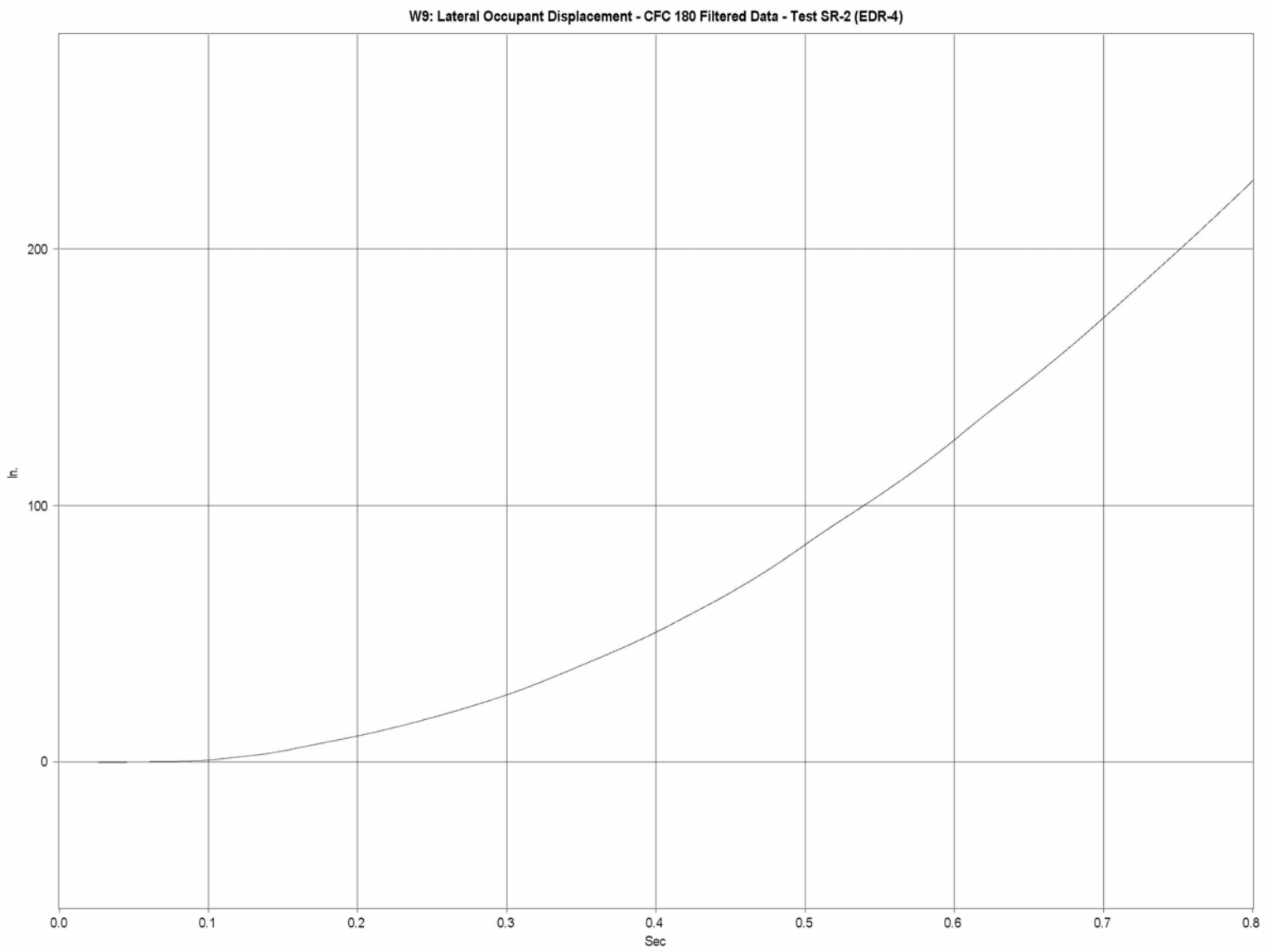

Figure B-6. Graph of Lateral Occupant Displacement - Filtered Data, Test SR-2

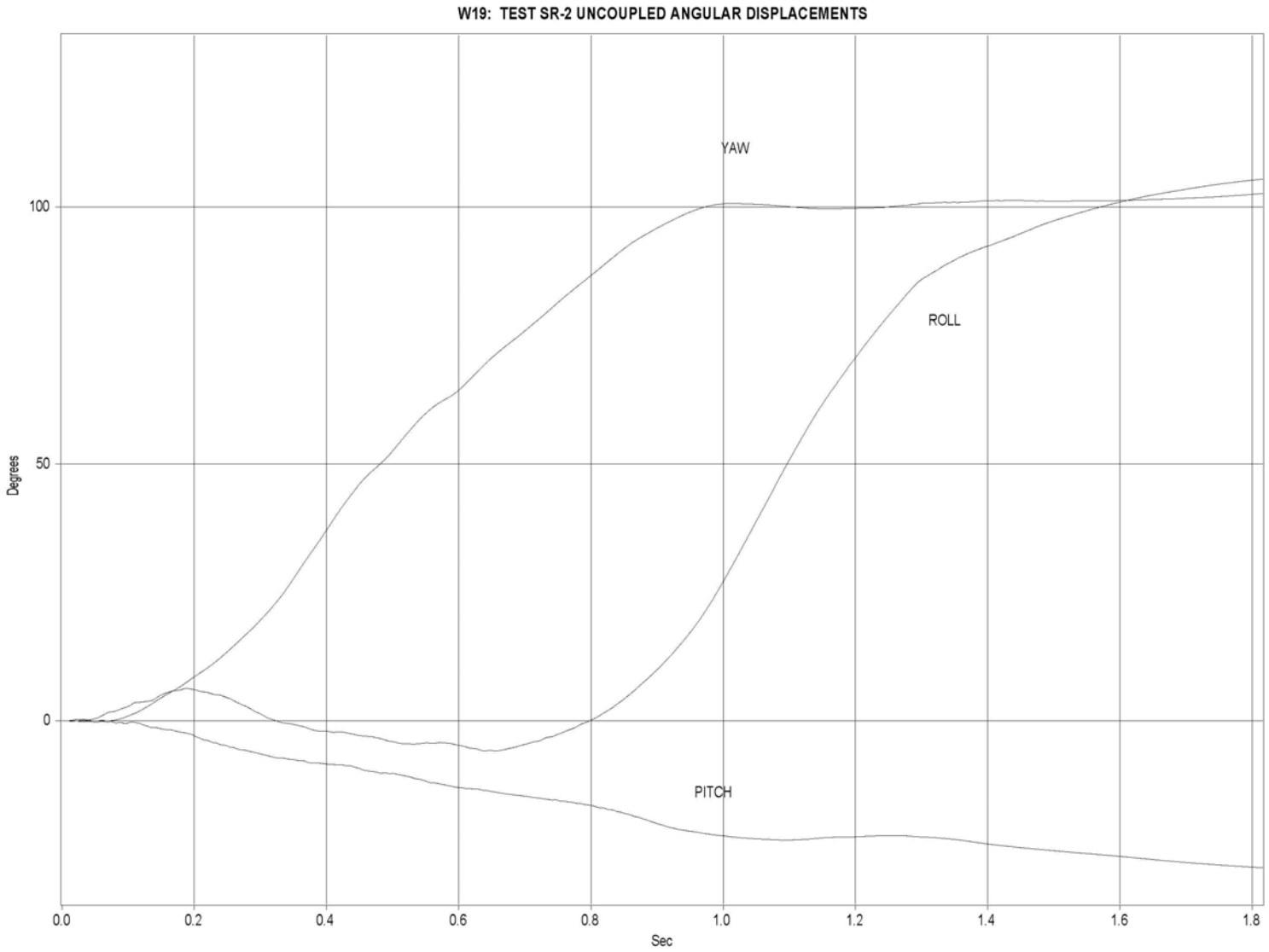

Figure B-7. Rate Transducer Data, Test SR-2

APPENDIX C

OCCUPANT COMPARTMENT DEFORMATION, TEST SR-3

Figure C-1. Occupant Compartment Deformation, Test SR-3

VEHICLE PRE/POST CRUSH INFO

TEST: SR-3
VEHICLE: 1995/FORD/F250/WHITE

POINT	X	Y	Z	X'	Y'	Z'	DEL X	DEL Y	DEL Z
1	-28.25	52.25	-6	-27.5	53	-5.75	0.75	0.75	0.25
2	-18	53.5	-5.5	-17.5	53.75	-4.75	0.5	0.25	0.75
3	-4.25	47.75	0	-4	48.5	1	0.25	0.75	1
4	8.25	49	1.25	8.5	49.5	2.75	0.25	0.5	1.5
5	15.5	53.5	-2.75	14.75	53.5	-2	-0.75	0	0.75
6	27.5	54.25	-2.75	27.5	54	-2.5	0	-0.25	0.25
7	-28.75	48	-8.5	-27.25	48.5	-8	1.5	0.5	0.5
8	-18.75	48.25	-8.25	-17.75	49	-7	1	0.75	1.25
9	-8	47.25	-8.25	-8.75	48	-7.25	-0.75	0.75	1
10	-5.5	43	-3.5	-5.25	43.25	-2.5	0.25	0.25	1
11	7.25	45	-1.75	7.25	45	0	0	0	1.75
12	15.25	49.75	-6	14.5	49.5	-5.25	-0.75	-0.25	0.75
13	26.5	50.25	-6.25	26.25	50	-6	-0.25	-0.25	0.25
14	-28.25	44.5	-9	-27.5	45	-8.25	0.75	0.5	0.75
15	-18.75	43.5	-9	-18.75	44	-7.75	0	0.5	1.25
16	-5.75	38.5	-4.5	-5.25	38.75	-3.75	0.5	0.25	0.75
17	8	36.25	-4.25	7.75	36.25	-2.5	-0.25	0	1.75
18	13.75	36.25	-8	13.25	35.75	-6.5	-0.5	-0.5	1.5
19	27.25	35.5	-9	27	35.75	-8.5	-0.25	0.25	0.5
20	-27.5	35.5	-8.75	-27.25	36.5	-7.75	0.25	1	1
21	-17.5	36.5	-8.5	-17	36.5	-7.5	0.5	0	1
22	-3.25	30.25	-5	-3	30.25	-4	0.25	0	1
23	10.25	29.25	-4.5	10.25	29.25	-3	0	0	1.5
24	22.75	28.75	-7.25	22.25	29	-6.5	-0.5	0.25	0.75
25	1.75	18	-5	1.75	18.25	-4.5	0	0.25	0.5
26	-26.25	40.5	22.25	-26.75	41.25	23	-0.5	0.75	0.75
27	1	41.75	20.75	1	42.25	21	0	0.5	0.25
28	27.25	41.25	19.25	27.25	41.5	19.5	0	0.25	0.25
29									
30									

ORIENTATION AND REFERENCE INFO

Head On Impact

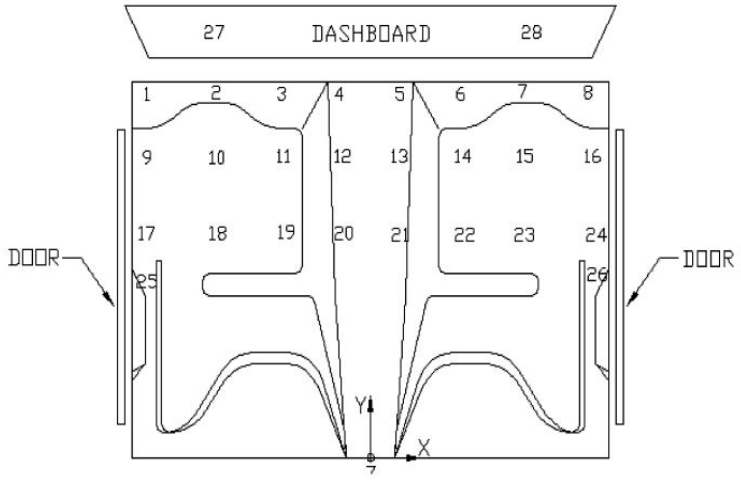

Figure C-1. Occupant Compartment Deformation, Test SR-3

APPENDIX D

ACCELEROMETER DATA ANALYSIS, TEST SR-3

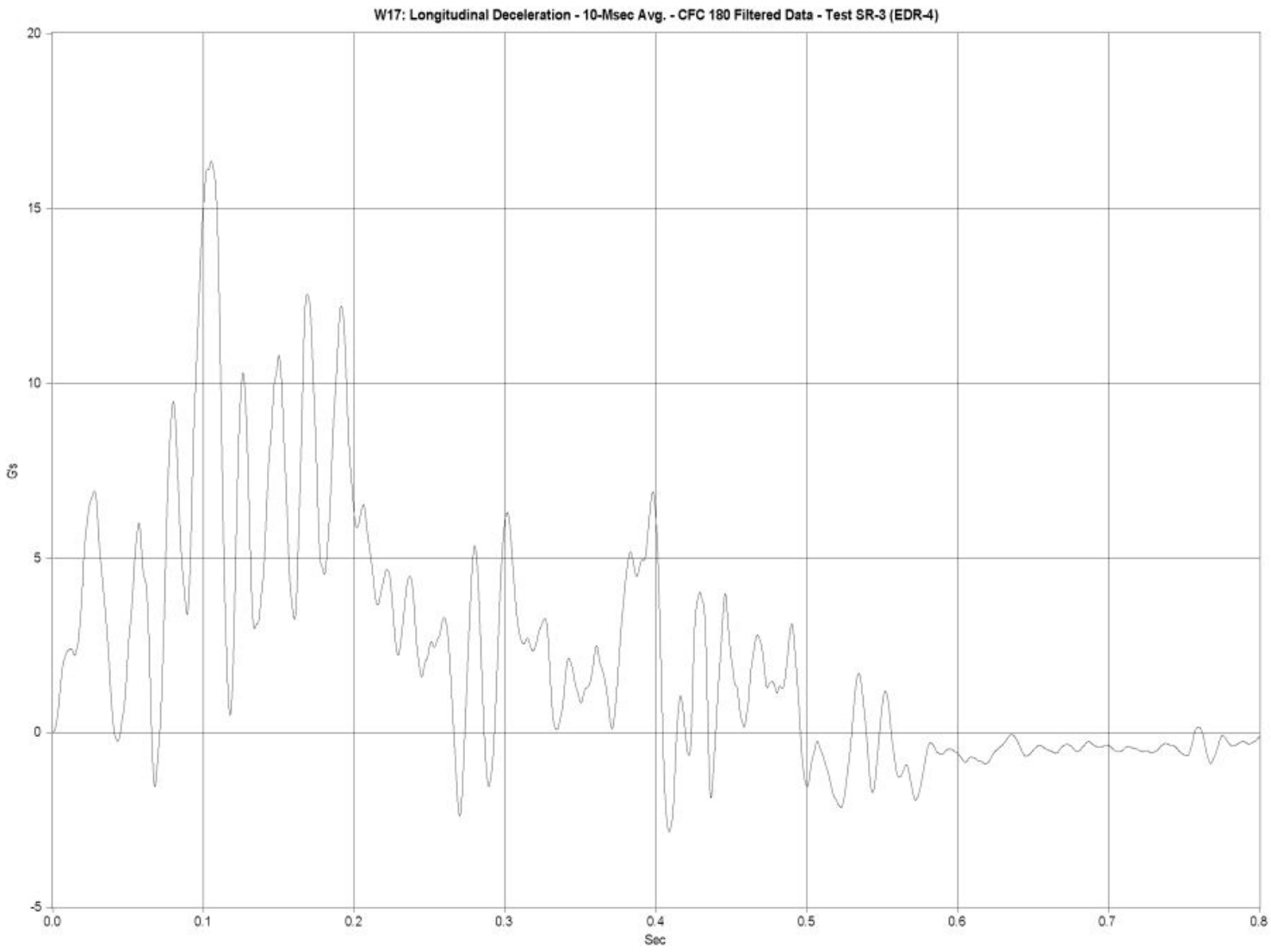

Figure D-1. Graph of Longitudinal Deceleration - Filtered Data, Test SR-3

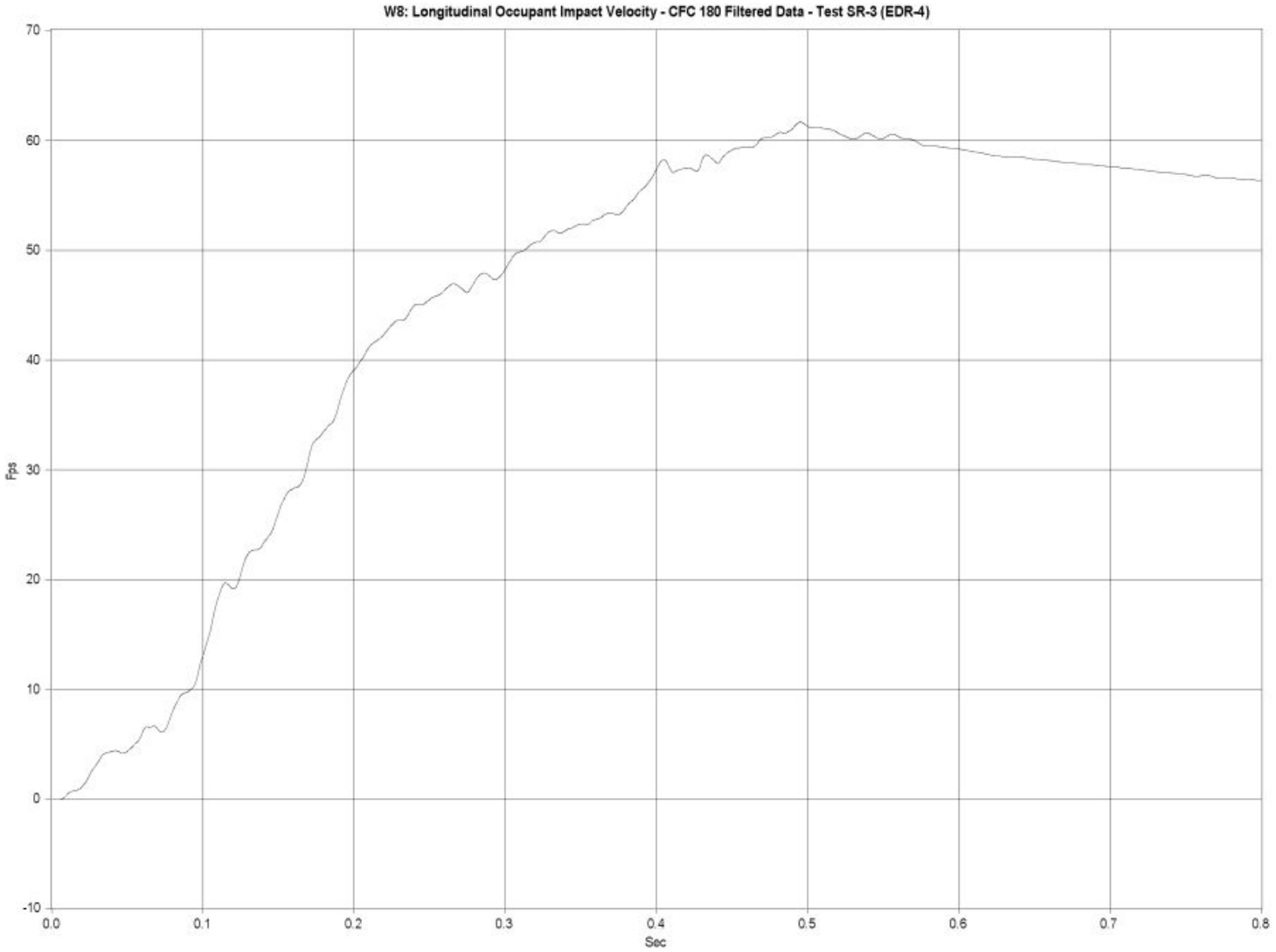

Figure D-2. Graph of Longitudinal Occupant Impact Velocity - Filtered Data, Test SR-3

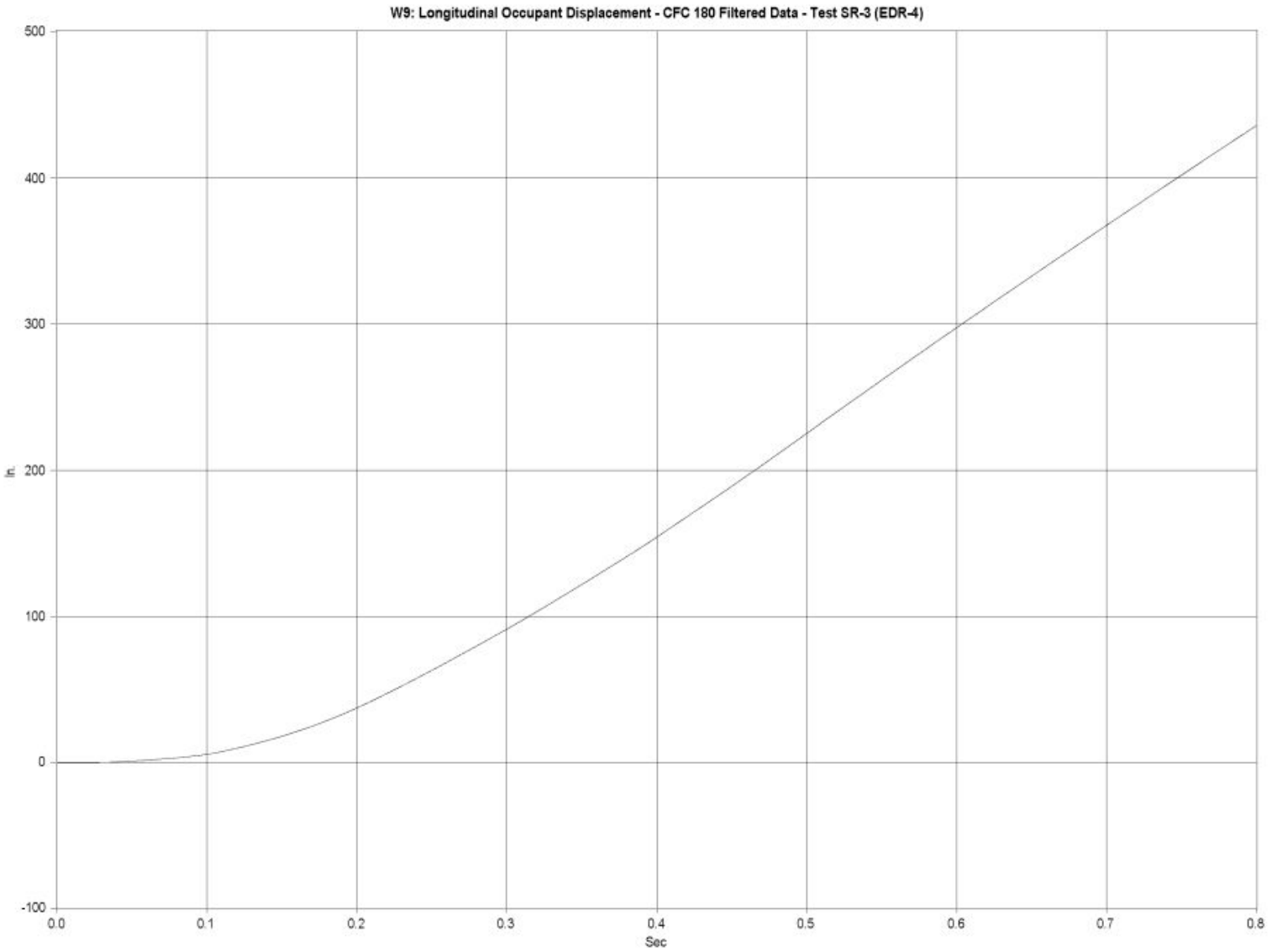

Figure D-3. Graph of Longitudinal Occupant Displacement - Filtered Data, Test SR-3

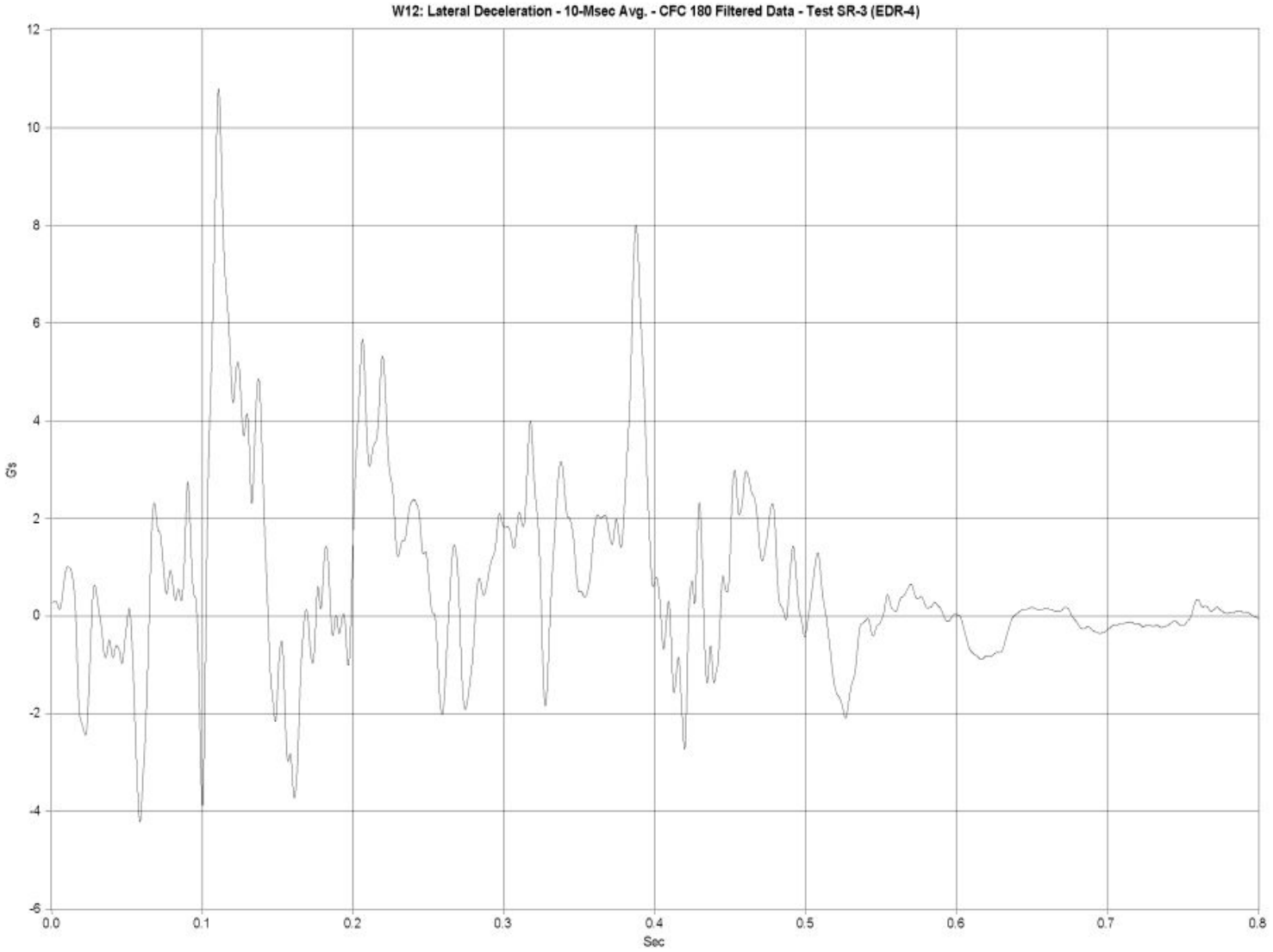

Figure D-4. Graph of Lateral Deceleration - Filtered Data, Test SR-3

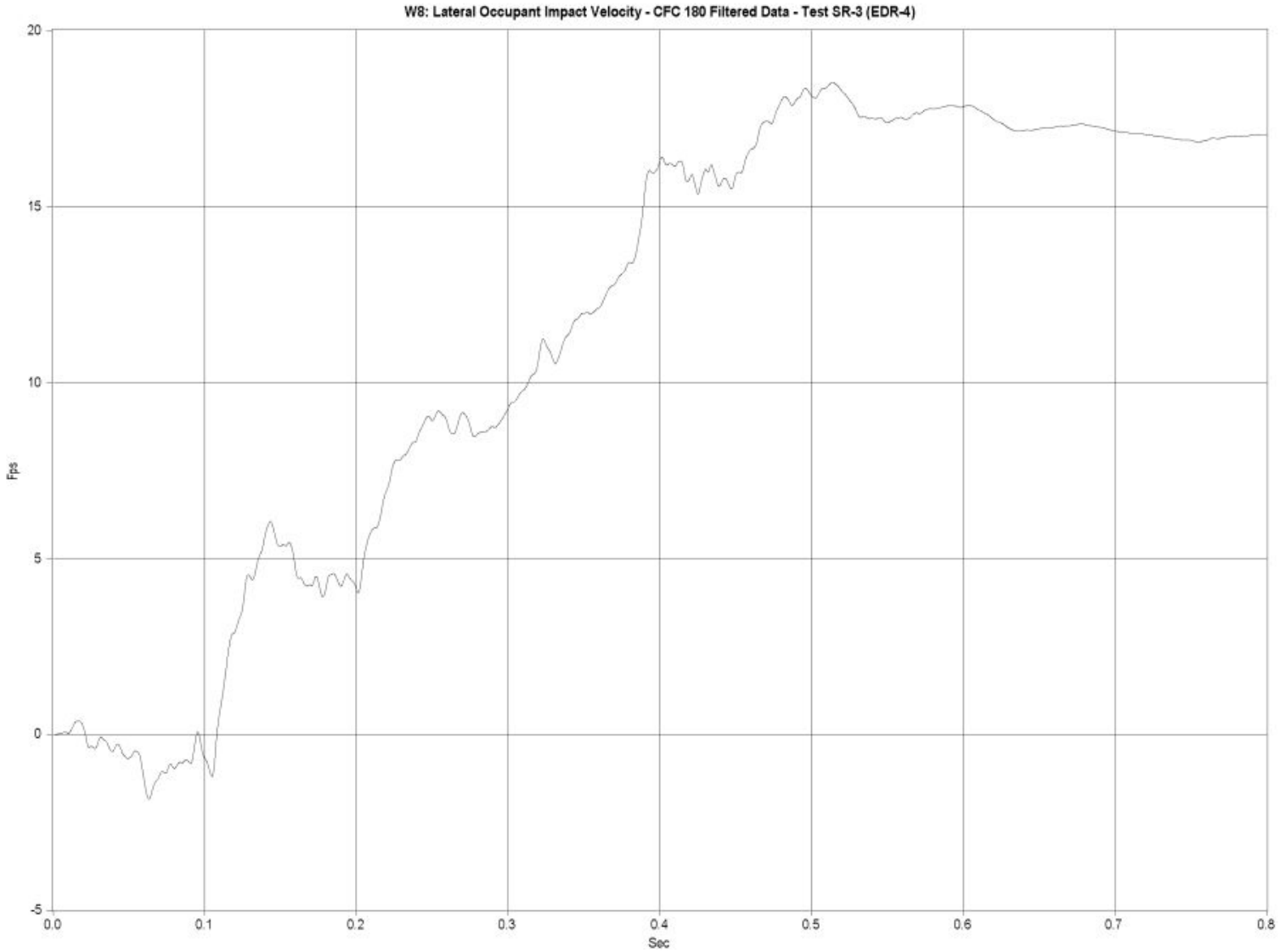

Figure D-5. Graph of Lateral Occupant Impact Velocity - Filtered Data, Test SR-3

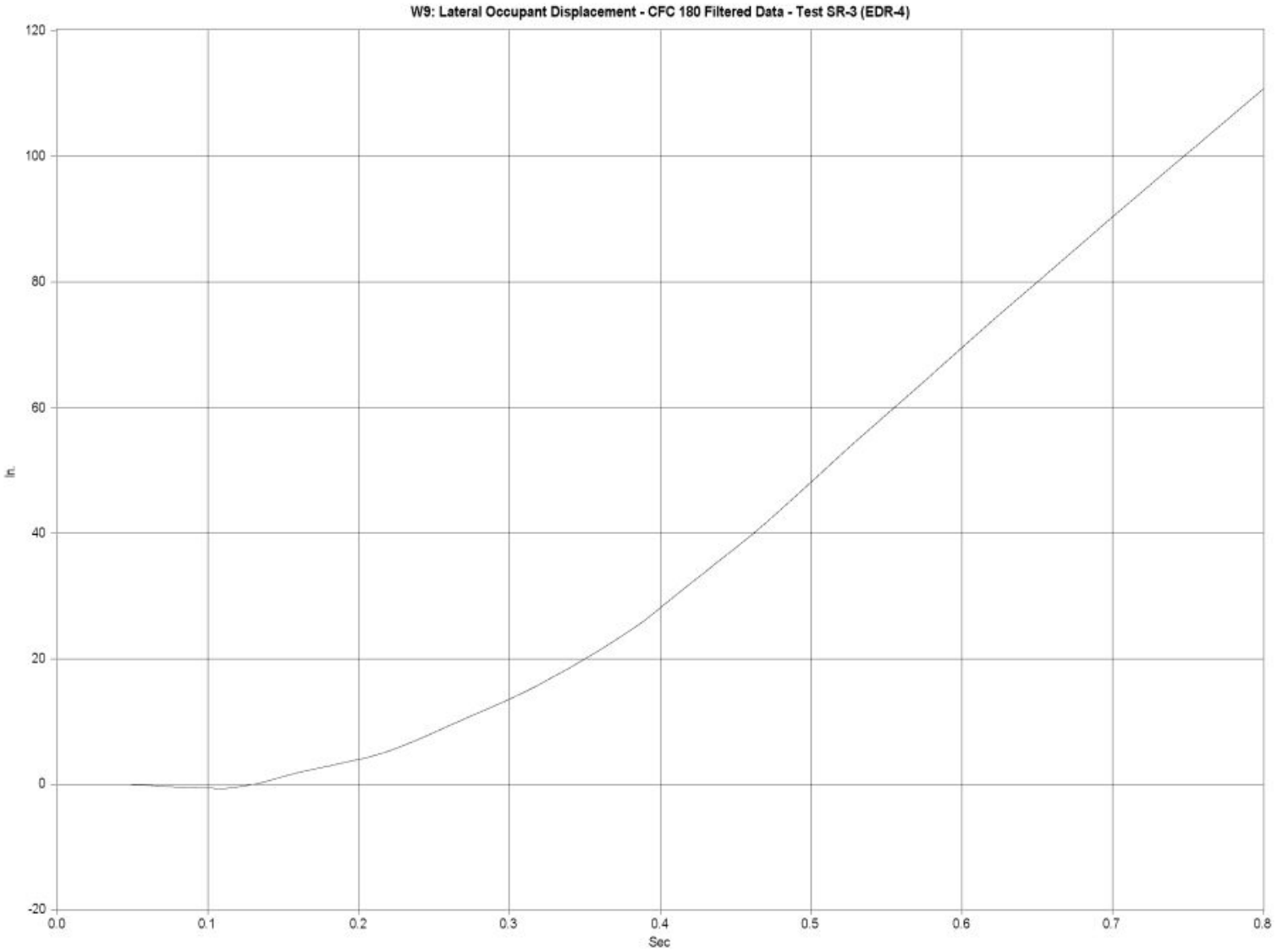

Figure D-6. Graph of Lateral Occupant Displacement - Filtered Data, Test SR-3

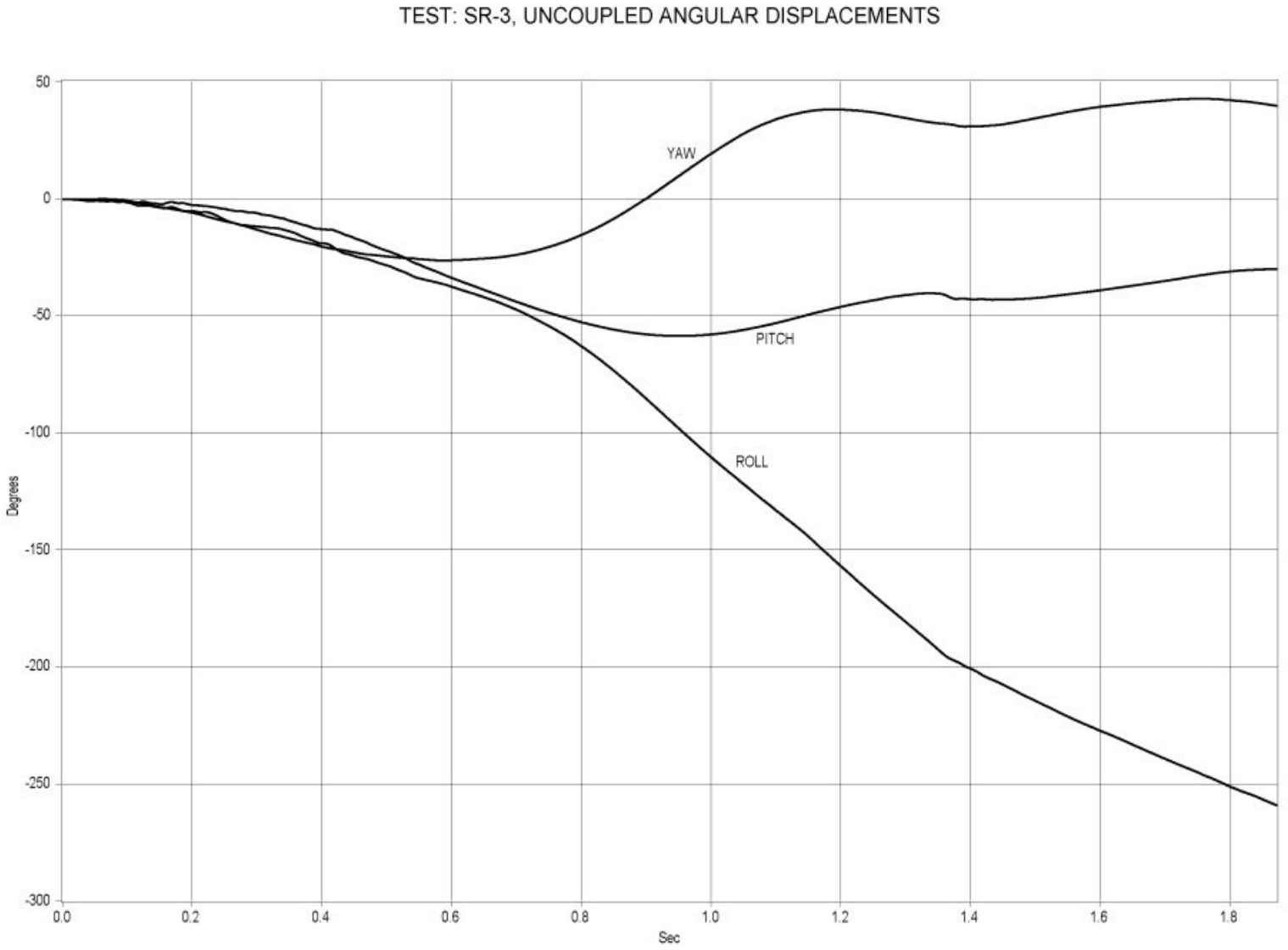

Figure D-7. Rate Transducer Data, Test SR-3

APPENDIX E

OCCUPANT COMPARTMENT DEFORMATION, TEST SR-4

Figure E-1. Occupant Compartment Deformation, Test SR-4

VEHICLE PRE/POST CRUSH INFO

TEST: SR-4
VEHICLE: 1997/GMC/WHITE

POINT	X	Y	Z	X'	Y'	Z'	DEL X	DEL Y	DEL Z
1	56.75	-27.5	2.75	NA	NA	NA	-56.75	27.5	-2.75
2	57	-22	3.5	50.25	-20	4.5	-6.75	2	1
3	57	-13.5	3.5	54	-12.75	6	-3	0.75	2.5
4	53	-4.75	-1	52.25	-4	1.25	-0.75	0.75	2.25
5	53	0.5	-1.25	52.25	0	0.75	-0.75	-0.5	2
6	51.25	-28.25	6.25	48	-26.75	10.5	-3.25	1.5	4.25
7	54.5	-21.5	5	49.25	-19.25	6.25	-5.25	2.25	1.25
8	51.25	-11.5	5.75	50.25	-11.5	8.5	-1	0	2.75
9	47.25	-4.75	1	46.5	-4.5	2.25	-0.75	0.25	1.25
10	44.5	-29	7	45	-27.5	12.75	0.5	1.5	5.75
11	49.5	-20	6.75	45.75	-19.25	9	-3.75	0.75	2.25
12	47	-12	6.75	45.75	-11.5	9	-1.25	0.5	2.25
13	44.5	0	0.5	43.5	0	2.5	-1		2
14	39.5	-27	6.5	39.5	-26.5	10	0	0.5	3.5
15	40.5	-20.25	6.5	39.75	-20	8.5	-0.75	0.25	2
16	41	-12	6.75	40	-11.75	8.25	-1	0.25	1.5
17	40	-3.5	1	39.25	-3.5	2	-0.75	0	1
18	33.25	-27.5	6.25	33	-27	8.75	-0.25	0.5	2.5
19	43.75	-17.25	6.5	33.5	-17	8	-10.25	0.25	1.5
20	43.75	-7.25	5	33.5	-8.25	3.75	-10.25	-1	-1.25
21	43.5	0.25	1.25	34	-0.25	3.75	-9.5	-0.5	2.5
22	26.5	-27.75	5.5	36.75	-28	7.5	10.25	-0.25	2
23	26.25	-18	4.75	25.75	-18.25	5.25	-0.5	-0.25	0.5
24	27	-1.5	1.25	26.75	-1.5	3	-0.25	0	1.75
25	17.5	-12.25	4.5	17	-12.75	4.75	-0.5	-0.5	0.25
26	31	-32	-7.5	28	-31.5	-6	-3	0.5	1.5
27	43.25	-24.75	-25	42.5	-25	-22	-0.75	-0.25	3
28	44.25	0	-25	43.75	0	-23	-0.5		2
29									
30									

ORIENTATION AND REFERENCE INFO

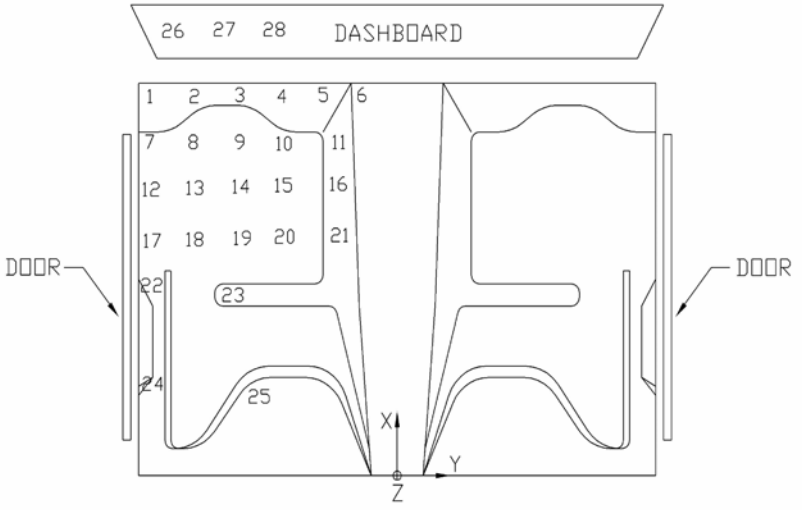

Figure E-1. Occupant Compartment Deformation, Test SR-4

APPENDIX F

ACCELEROMETER DATA ANALYSIS, TEST SR-4

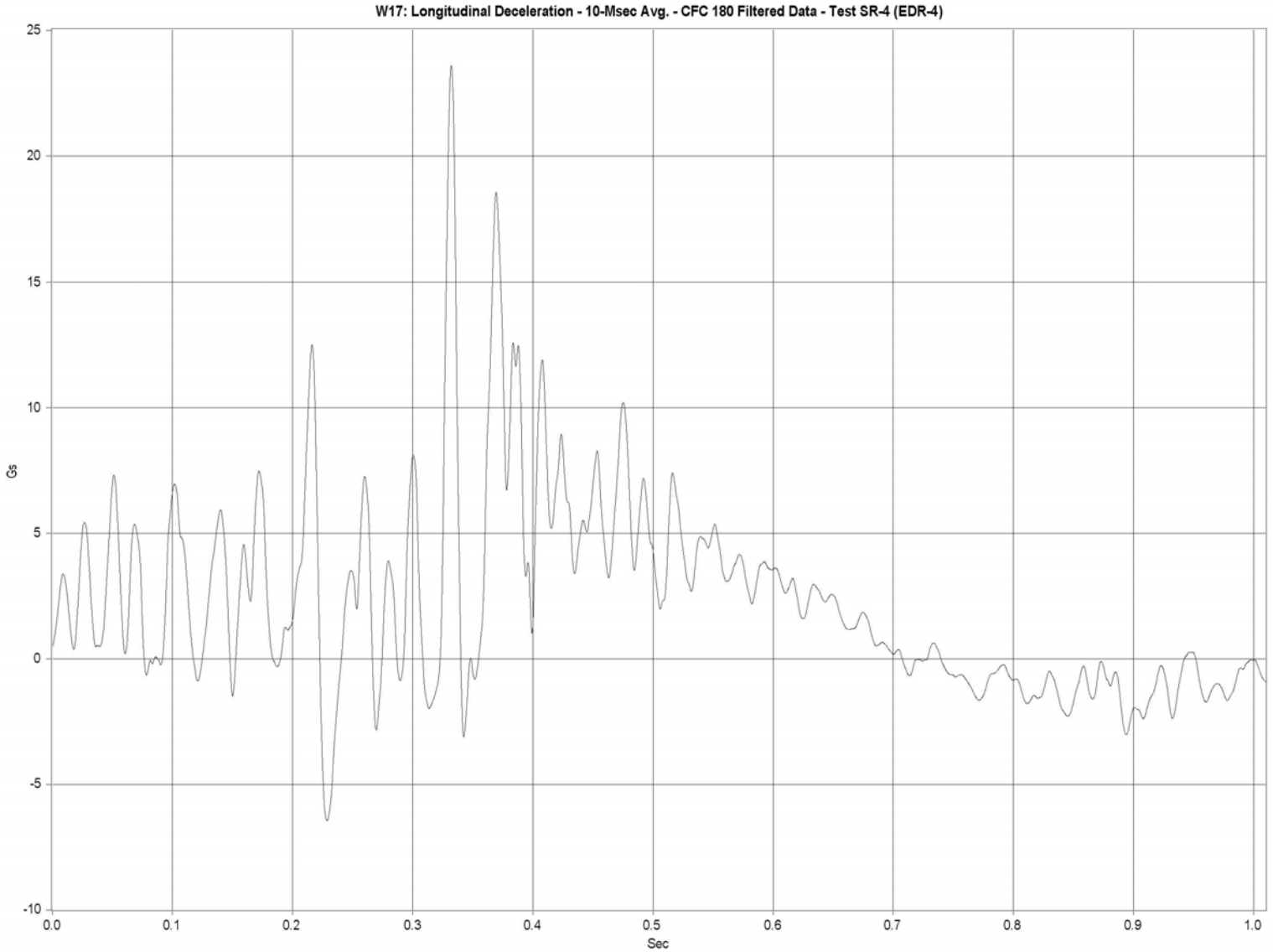

Figure F-1. Graph of Longitudinal Deceleration - Filtered Data, Test SR-4

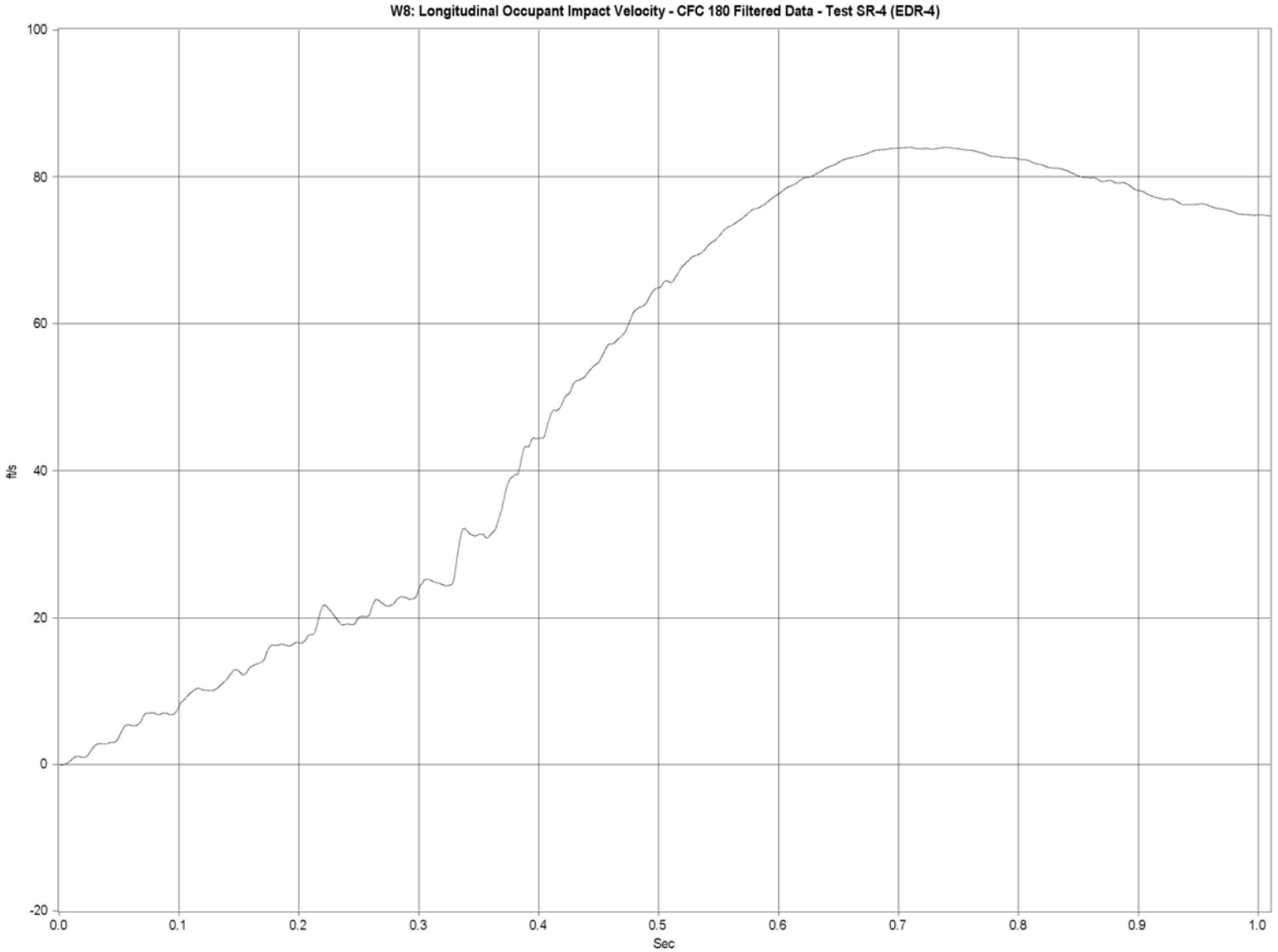

Figure F-2. Graph of Longitudinal Occupant Impact Velocity - Filtered Data, Test SR-4

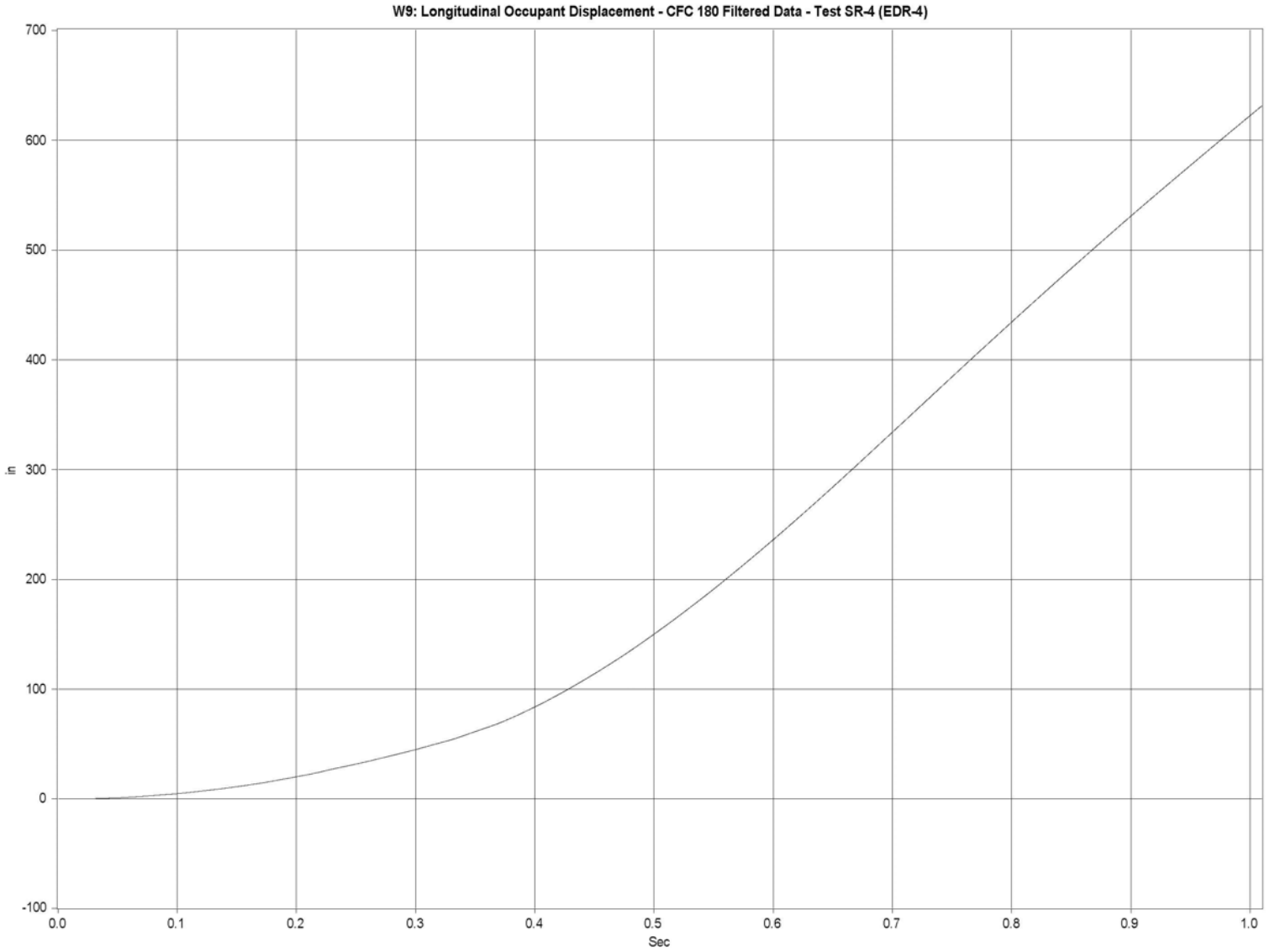

Figure F-3. Graph of Longitudinal Occupant Displacement - Filtered Data, Test SR-4

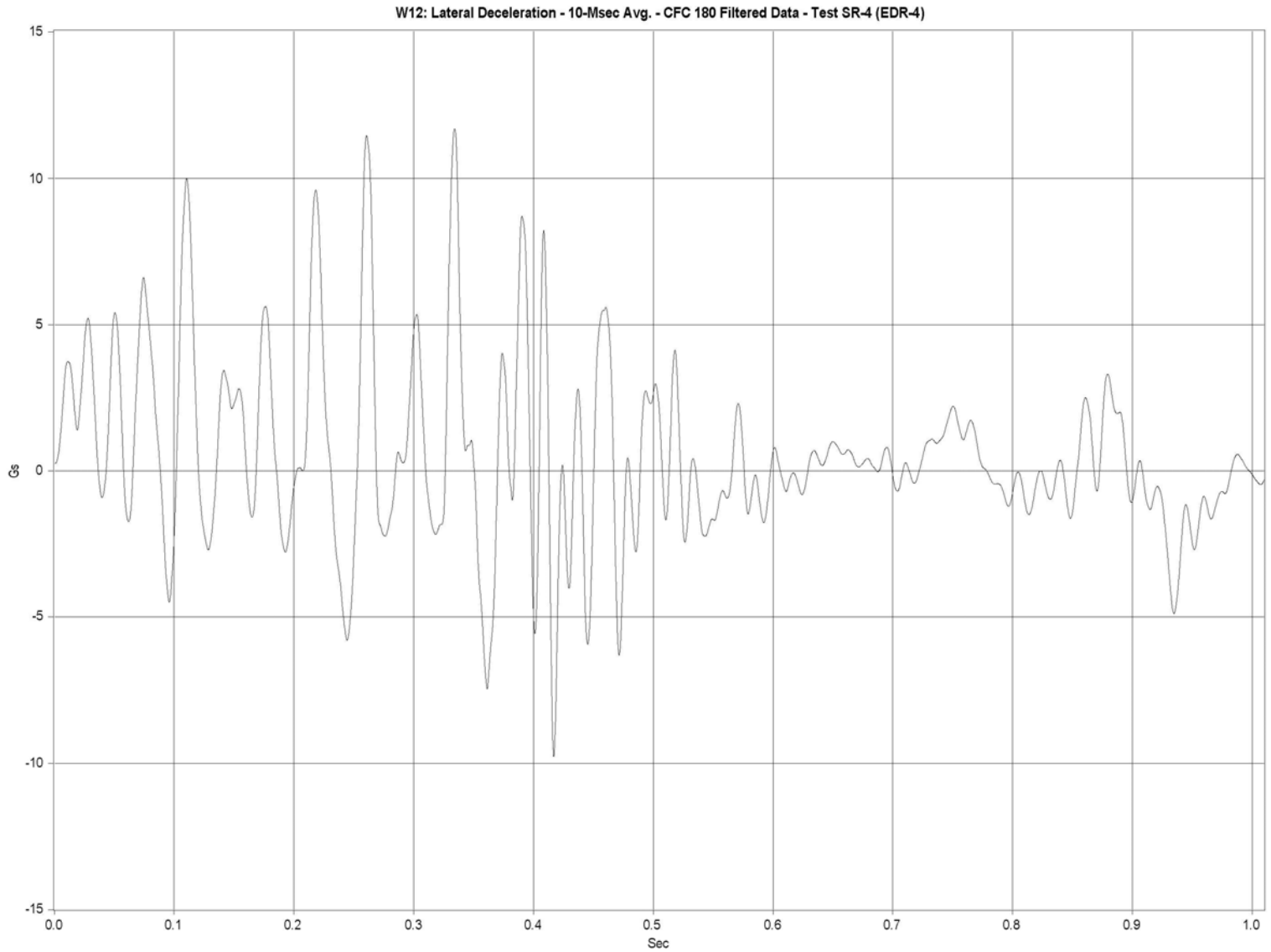

Figure F-4. Graph of Lateral Deceleration - Filtered Data, Test SR-4

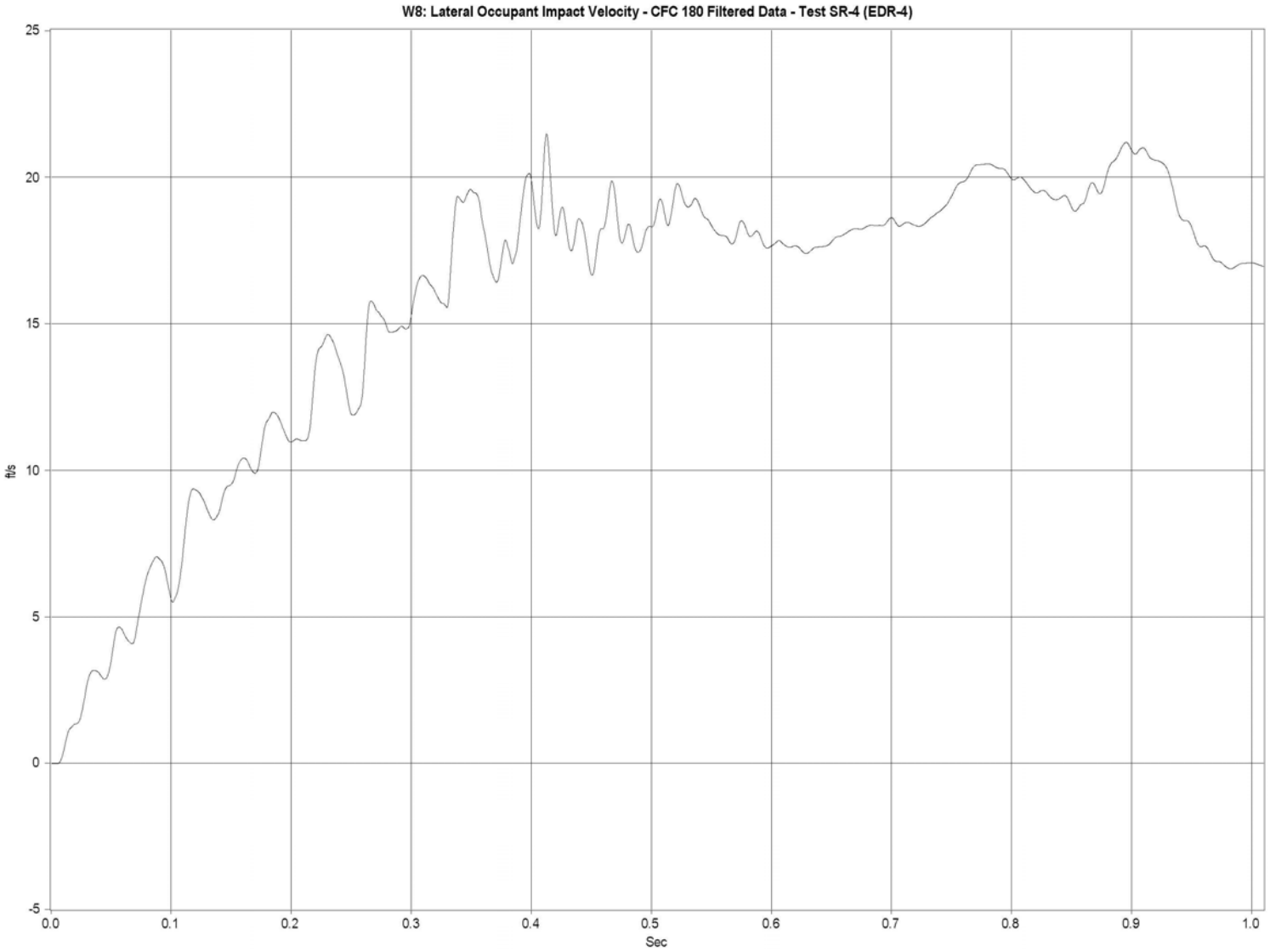

Figure F-5. Graph of Lateral Occupant Impact Velocity - Filtered Data, Test SR-4

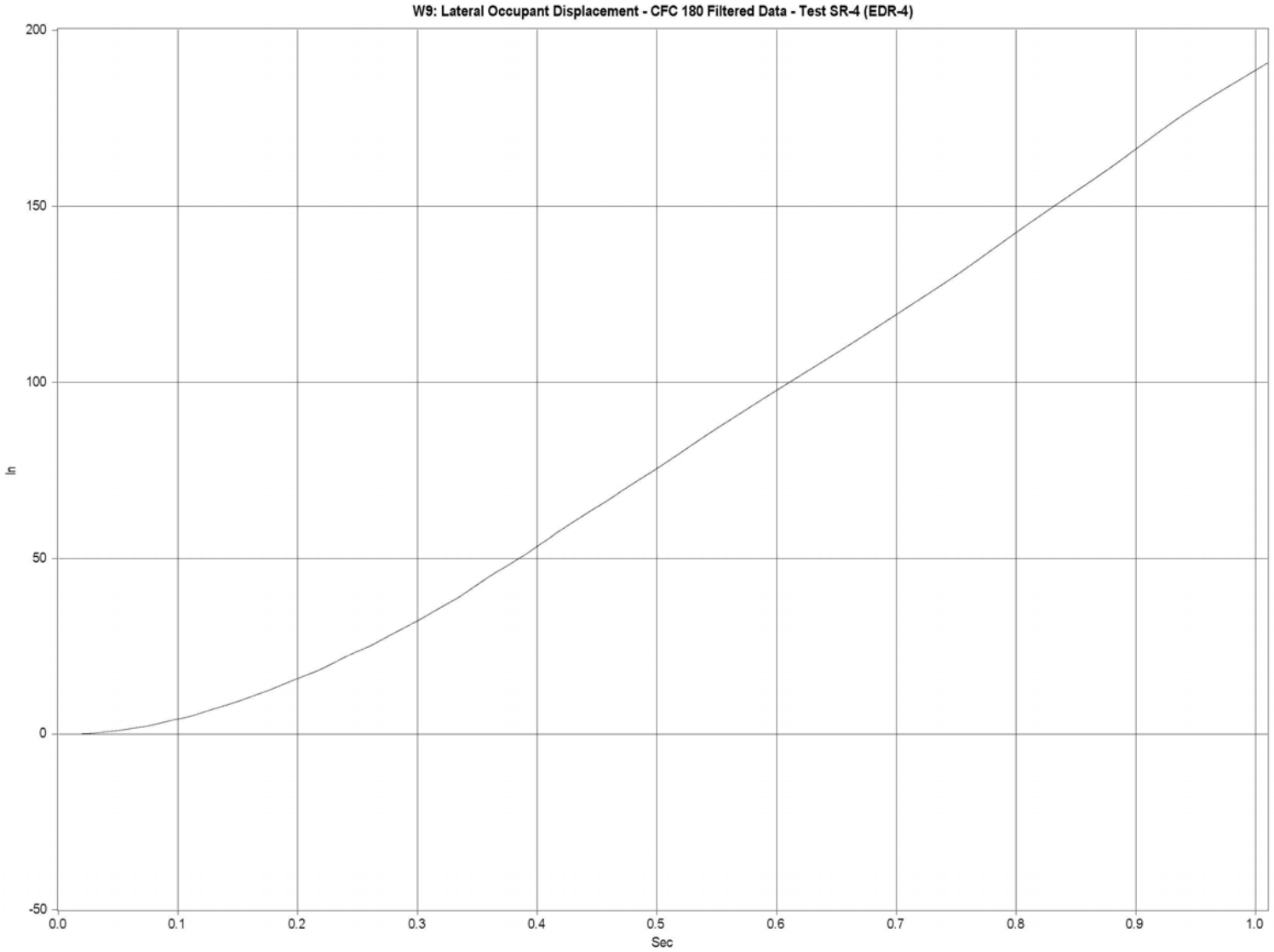

Figure F-6. Graph of Lateral Occupant Displacement - Filtered Data, Test SR-4